TURUN YLIOPISTO

From Wood Industry Side Streams to Drug Candidates: Semisynthesis of Novel Polyphenolic Compounds from Pine Bark Proanthocyanidins

Nea Tammi
Pro Gradu thesis
Natural Chemistry Research Group
University of Turku
Department of Chemistry
April 2025

The originality of this thesis has been checked in accordance with the University of Turku quality assurance system using the Turnitin Originality Check service.

TURUN YLIOPISTO
Kemian laitos

TAMMI, NEA: Puuteollisuuden sivuvirroista lääkeaihioiksi: Uusien polyfenoliyhdisteiden semisynteesi männynkuoren proantosyanidiineista

Pro Gradu-tutkielma, 58 s, 20 liitettä

Kemia

Huhtikuu 2025

Proantosyanidiinit (PA:t, eng. proanthocyanidins) ovat flavan-3-olien oligomeereja tai polymeereja. Pääte- ja jatkoyksiköt voivat olla linkittyneet B-tyypin PA:ssa C4–C8- tai C4–C6-sidoksella tai A-tyypin PA:ssa lisäksi C2–O–C7- tai C2–O–C5-eetterisidoksella. Männynkuoresta uutetut ja erotetut luonnolliset PA:t voidaan muokata happokatalysoidun aldehydien kondensaatioreaktion avulla uusiksi, semisynteettisiksi metyleenisiltaisiksi (C–CH_2–C) yhdisteiksi. Tässä tutkielmassa formaldehydia käytettiin linkitysreaktion elektrofiilina. Tutkimusten mukaan semisynteettiset flavan-3-olien väliset linkitykset parantavat PA-dimeerin proteiinisaostuskapasiteettia (PPC, eng. protein precipitation capacity) verrattuna vastaavaan luonnolliseen C–C-linkitykseen.

Suomen puuteollisuus tuottaa vuosittain sivutuotteena kolme miljoonaa tonnia männynkuorta, jonka tyypillisin hyödyntämistapa on polttaminen energiaksi. Männynkuori sisältää kuitenkin paljon prosyanidiinia (PC, eng. procyanidin), PA:n alaluokkaa, jolla on vapaiden radikaalien pelkistysaktiivisuutta ja muita antioksidanttiaktiivisuuksia. Kuoren sisältämiä luonnollisia polyfenoleja voitaisiin helposti muokata aldehydien kondensaatioreaktion avulla uusiksi, mahdollisesti paremman bioaktiivisuuden omaaviksi yhdisteiksi.

Tässä tutkielmassa PC:t uutettiin, erotettiin kromatografisesti ja yhdistettiin niiden retentioaikojen ja polymerisaatioasteiden perusteella. Näitä toisistaan kemiallisesti eroavia fraktioita käytettiin aldehydien kondensaatioreaktioiden lähtömateriaaleina ja tutkittiin fraktioiden eroja reaktioissa. Uusien metyleenisiltaisten linkitysten muodostumista havaittiin jokaisessa polymerisaatioasteessa. Toiset fraktiot muodostivat enemmän sakkaa reagoidessaan, ja myös muodostuneiden metyleenisiltaisten linkitysten määrä vaihteli polymerisaatioasteiden välillä fraktion sisällä. Korkeamman polymerisaatioasteen PC:t ovat hankalasti analysoitavissa, ja tämä ongelma ilmeni nopeasti myös semisynteettisten PC:iden kohdalla niiden muodostamien sakkojen liukoisuusongelmien kautta.

Uusien semisynteettisten PC:iden PPC:t määritettiin ja merkittäviä PPC-tuloksiin vaikuttavia tekijöitä huomattiin olevan fraktion retentioaika ja keskimääräinen polymerisaatioaste sekä metyleenisiltojen lukumäärä. PC:iden eluoituminen käänteisfaasikromatografiassa yhdisteseoksien kromatografisena kumpuna aiheutti haasteita myös PPC-mittauksissa tulosten heijastaessa monimutkaisten seoksien yhteisvaikutuksellisia aktiivisuuksia. Tutkielma tarjoaa tärkeää tietoa semisynteettisistä PC:ista, mutta niiden bioaktiivisuuksien ymmärtämiseksi ja potentiaalin kartoittamiseksi lääketieteellisissä sovelluksissa tarvitaan lisää tutkimusta tulevaisuudessa.

Avainsanat: kiertotalous, kestävä kemia, männynkuori, proantosyanidiinit, prosyanidiinit, polymeerit, semisynteesi

UNIVERSITY OF TURKU
Department of Chemistry

TAMMI, NEA: From Wood Industry Side Streams to Drug Candidates: Semisynthesis of Novel Polyphenolic Compounds from Pine Bark Proanthocyanidins

Pro Gradu-thesis, 58 p., 20 appendices

Chemistry

April 2025

Proanthocyanidins (PAs) are oligomers or polymers of flavan-3-ols, consisting of one terminal unit and one or more extension units. In B-type PAs, these units are linked via C4–C8 or C4–C6 bonds. A-type PAs, in contrast, feature at least one additional ether bond, such as C2–O–C7 or C2–O–C5. Flavan-3-ols are part of the flavonoid family and are naturally widespread, for example, in pine bark. Natural PAs can be extracted and chromatographically separated from pine bark, then modified into semisynthetic PAs through an acid-catalyzed aldehyde condensation reaction. The semisynthetic PAs feature one or more methylene-bridged (C–CH_2–C) linkages between the monomer units. In this thesis, formaldehyde was used as an electrophile in this bridging reaction. With dimers, these semisynthetic interflavan-3-ol linkages demonstrate superior protein precipitation capacities (PPCs) compared to their corresponding natural counterparts according to studies.

Each year, the Finnish forest industry generates three million tons of bark as a byproduct, much of which is currently used for energy production through burning. However, pine bark is a rich source of procyanidins (PCs), a subclass of PAs known, e.g., free-radical scavenging activity and other antioxidant activities. These natural polyphenols can be readily modified with aldehyde condensation reactions, creating novel compounds with potentially enhanced bioactivity.

In this thesis, pine bark PCs were extracted, chromatographically fractionated, and combined based on their retention times and mean degrees of polymerization (mDPs). These chemically different fractions were modified using aldehyde condensation reactions. Additionally, differences among these fractions in the reactions were studied. The formation of methylene-bridged linkages was observed in every DP. The fractions varied from one another in terms of precipitate formation and the number of methylene-bridged linkages formed at each DP. However, higher DP PAs are notoriously challenging to analyze, and this challenge became particularly evident with semisynthetic PAs due to solubility issues of the formed precipitates.

To assess the impact of semisynthetic modifications, the PPCs of methylene-bridged PCs were measured. Key factors influencing PPCs included retention time, mDP of the starting material, and number of methylene-bridged linkages in the product. PCs eluting in the reversed-phase chromatography as a chromatographic hump consisting of mixtures of PC oligomers and polymers caused challenges throughout the thesis, especially at this point since the results presented the combined effects of the PC mixture. While this study provides valuable insights into semisynthetic PCs, further research is needed to fully elucidate their bioactivities and potential in pharmaceutical applications.

Keywords: circular economy, pine bark, proanthocyanidins, procyanidins, polymers, semisynthesis, sustainable chemistry

Contents

1 Abbreviations

BSA	bovine serum albumin
DAD	diode array detector
DMSO	dimethyl sulfoxide
DP	degree of polymerization
ESI	electrospray ionization
HESI	heated electrospray ionization
HRF	heterocyclic ring fission
LC-MS	liquid chromatography-mass spectrometry
MALDI	matrix-assisted laser desorption ionization
mDP	mean degree of polymerization
MS/MS	tandem mass spectrometry
PA	proanthocyanidin
PC	procyanidin
PD	prodelphinidin
PGG	pentagalloylglucose
PPC	protein precipitation capacity

PRP	proline-rich protein
PTFE	polytetrafluoroethylene
QM	quinone methide
RDA	Retro-Diels-Alder
RT	retention time
SDHB	Super 2,5-Dihydroxybenzoic acid
SPE	solid phase extraction
TOF	time-of-flight
UHPLC	ultrahigh-performance liquid chromatography
UV	ultraviolet
QQQ	triple quadrupole

2 Introduction

Proanthocyanidins (PAs, Figure 1), also known as condensed tannins, are oligomers and polymers of flavan-3-ols consisting of one terminal and one or more extension units.[1,2] Flavan-3-ols belong to flavonoids and are naturally widespread, especially in plants, fruits, and vegetables.[2] Plant polyphenols, such as PAs, play a role in defending against herbivores, ultraviolet (UV) radiation, and pathogens[3], given their natural functions and widespread presence in plants. Consequently, PAs are also found in many plant-based foods and beverages, such as wine and beer[4], which has created interest in the potential health benefits of PAs. The biological and pharmacological effects of PA polymers are reported be more beneficial in preventing diseases related to their antioxidant actions compared to monomers.[5]

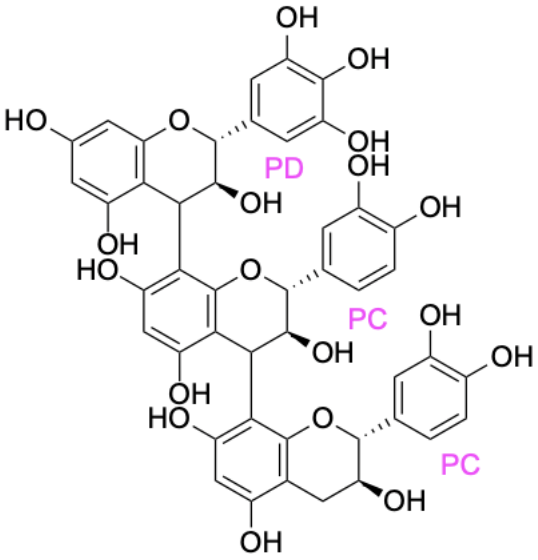

Figure 1. An example structure of trimeric proanthocyanidin, which consists of two catechin (PC) units and one gallocatechin (PD) unit.

2.1 Flavan-3-ols and proanthocyanidins

Oligomeric or polymeric PA structures are made up of similar building blocks, flavan-3-ols. Flavan-3-ols consist of two stereocenters, the C2 and C3 carbons. Afzelechin, catechin, and gallocatechin (structures **1**, **2**, and **3** in Figure 2**)** display a *trans* (2*R*, 3*S*) orientation, while epiafzelechin, epicatechin, and epigallocatechin (structures **4**, **5**, and **6** in Figure 2**)** exhibit a *cis* (2*R*, 3*R*) orientation with C2 and C3 carbons.[6,7] Structures **1** and **4** differ only in the stereochemistry of the hydroxyl group at the C3 carbon. Similarly, structures **2** and **5** and

structures **3** and **6** also differ in this way. These structure pairs (**1** and **4**, **2** and **5,** and **3** and **6**) are diastereomers of each other, differing only in their spatial orientation.[8,9]

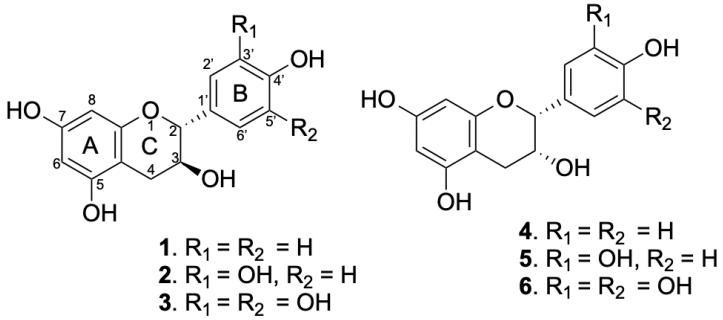

Figure 2. Structures of the most common monomeric flavan-3-ol building blocks of (epi)afzelechins (**1**, **4**), (epi)catechins (**2**, **5**), and (epi)gallocatechins (**3**, **6**).

Within PA structures, monohydroxylated (epi)afzelechins are called propelargonidin units, dehydroxylated (epi)catechins are called procyanidin (PC) units, and trihydroxylated (epi)gallocatechins are called prodelphinidin (PD) units.[8] This classification is made based on the stereochemistry at the C2 and C3 carbons in the C-ring as well as the hydroxylation pattern of the B-ring.[1] In B-type PAs, the monomeric units are linked via C4–C8 or C4–C6 bonds (Figure 3A), while A-type PAs include an additional ether bond either C2–O–C7 or C2–O–C5 (Figure 3B).[10,11] The oligomeric or polymeric PA structures consist of one terminal unit and one or more extension units (Figure 3C). PAs containing PC and PD units (Figure 1) are commonly found in plants. Due to differences in PC/PD composition, relative stereochemistry, and degree of polymerization (DP), PAs represent a complex and diverse group of compounds.[1] Mixtures of PAs can be called either PC- or PD-rich based on the PC/PD composition of the complete mixture.

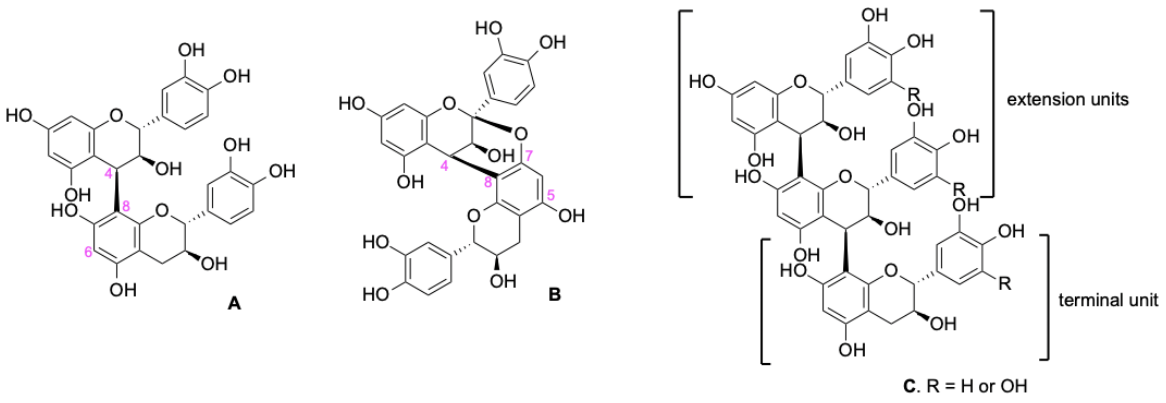

Figure 3. Structures of B-type procyanidin dimer (**A**) with C4–C8 linkage and A-type procyanidin dimer (**B**) with C4–C8 and C2–O–C7 linkages. Example structure of a proanthocyanidin trimer (**C**) with one terminal unit and two extension units linked via C4–C8 bonds is also presented.

In plants, PAs exist as mixtures of varying polymeric sizes. Therefore, the mean degree of polymerization (mDP) is commonly used to represent their average size.[1] However, PA composition is far more complex than a single mDP value suggests as their molecular sizes can range from dimers to large polymers containing more than ten monomer units.

2.2 Bioactivity of proanthocyanidins

PAs exhibit a range of bioactivities, including antioxidant activity and anti-tumor-promoting effects[12], as well as antimicrobial and anti-allergy activities[13]. PA-rich plants are linked to protein binding capacity and bioactivities related to ruminants. Interest in the potential use of PAs as nutraceuticals has grown, highlighting their role in addressing environmental and parasitic issues related to ruminant production.[14] PAs are of significant interest in medicine due to their numerous biological and pharmacological activities.[11] The number of hydroxyl groups in the B-ring of the upper unit of dimeric PAs is reportedly related to their antimicrobial activity.[15] Studies indicate that PAs provide beneficial effects on obesity, inflammatory bowel disease, and other inflammatory and metabolic disorders.[16,17]

PCs display potential antioxidant properties *in vitro*, but *in vivo*, this depends on the absorption and metabolism of PCs post-digestion, and their reducing properties and conjugation.[18] Following perfusion with dimers, monomers have been shown to enter the portal vein *in vivo* and conjugate with glucuronides, for instance, in the liver.[19,20] However, dimers are likely to be bioavailable as monomers, although they are not fully absorbed across the rat's small intestine.[18] Indeed, it is widely acknowledged that PA molecules remain stable in the stomach, and only monomers are absorbed in the small intestine.[21,22] Thus, the majority of ingested PA reaches the colon, where it may be metabolized by gut microflora[23,24] and exert its biological activities independently[25].

PCs represent a significant portion of the total flavonoids consumed in Western diets. Foods high in PCs are believed to lower LDL cholesterol levels and blood pressure. Additionally, PCs provide other health benefits for humans, making them a topic of great interest in the field of nutrition.[25]

PAs exhibit a strong affinity for proline-rich proteins (PRPs), which comprise 70% of human parotid saliva. Studies indicate that larger and more hydrophobic PAs bind more strongly to PRPs due to multidentate interactions.[26] Hydrophobic interaction[27], hydrogen bonding[28], and aromatic stacking play significant roles in the complex protein precipitation between PAs and proteins. Hydrophobic interaction is proposed to be the dominant mode of

interaction, with hydrogen bonding serving as the secondary mode.[27,28] The size of the PAs is related to the formation of cross-linking, promoting protein aggregation, and encouraging precipitation of the PA-protein complex. However, variations in PC/PD ratio, stereochemistry, and the interflavan-3-ol linkage types impact the precipitation activity, and therefore, all features, in addition to the size, should be considered.[6]

Considering the interest of PAs in medicine, particularly the protein binding is a key factor considering the potential in medical applications, due to the drug's mechanism of action in the human body. Protein binding activity enables the compound's potential to be used as a treatment for diseases that cause an increase in the albumin concentrations in the body.[29,30]

2.3 Characterization of proanthocyanidins

To gain deeper insights into the structure-bioactivity relationships of PAs, it is essential to obtain pure compounds or chemically well-characterized mixtures of a select few PAs. Various chromatographic methods have been employed in the isolation and purification of PAs, typically leading to the purification of small oligomers or mixtures of polymers.[14] In reversed-phase liquid chromatography, PAs elute simultaneously as mixtures of compounds of differing sizes, resulting in a distinctive hump in the UV chromatogram. This presents a significant challenge for the further purification of polymeric PAs. Additionally, there are concerns that polymeric compounds may not ionize effectively in the ion source, complicating specific analyses.[31] Therefore, the primary challenge in characterizing PAs is related to larger, polymeric PAs.

The highly polymerized PAs are reported to have molecular weights reaching up to 30 kDa.[32] Matrix-assisted laser desorption ionization–time-of-flight-mass spectrometry (MALDI-TOF-MS) has been used to determine the interflavan-3-ol linkage types and DP values of the PAs.[33] Electrospray ionization mass spectrometry (ESI-MS^n) has also been utilized to identify PA molecular ions and their fragments. Unfortunately, neither of these methods can differentiate the PA isomers.[7]

Often, ESI-MS^n is conducted in negative ionization mode as PCs are more effectively detected due to the acidity of the phenolic protons.[34,35] B-type PCs, ranging from dimers to heptamers, form a distinct series of $[M-H]^-$ ions separated by 288 Da, spanning from 577 Da to 2017 Da. The characteristic fragmentation patterns of PCs can be utilized for structural characterization. The fragmentation pattern for dimeric PCs (Figure 4A) is shown as an example. PC sequence ions of 287 Da and 289 Da (Figure 4B, C) result from a direct cleavage

or a quinone methide (QM) cleavage of the interflavan-3-ol bonds. Retro Diels-Alder (RDA) and heterocyclic ring fission (HRF) product ions are typical fragments of PC dimers. The RDA product ion of 425 Da (Figure 4D) and the HRF product ion of 451 Da (Figure 4E) can be systematically detected within the samples. Additionally, a sequential loss of H_2O from the RDA fragment, resulting in product ion of 407 Da, is detected. Higher DP oligomeric and polymeric PCs fragmentate the same way. The RDA product ions result from a cleavage of 152 Da, and HRF product ions from a cleavage of 126 Da. The oxidation of the catechol B-ring of PCs generates *o*-quinones with a mass difference of 2 Da compared to the original PCs. Such oxidation has been noted in mass spectrometric analyses.[36] A thorough investigation of mass peak intensities and patterns is essential to confirm A-type PCs rather than an oxidation or fragmentation product of B-type PCs[37] as the A-type PCs and the oxidation products of B-type PCs exhibit the same *m/z* values.

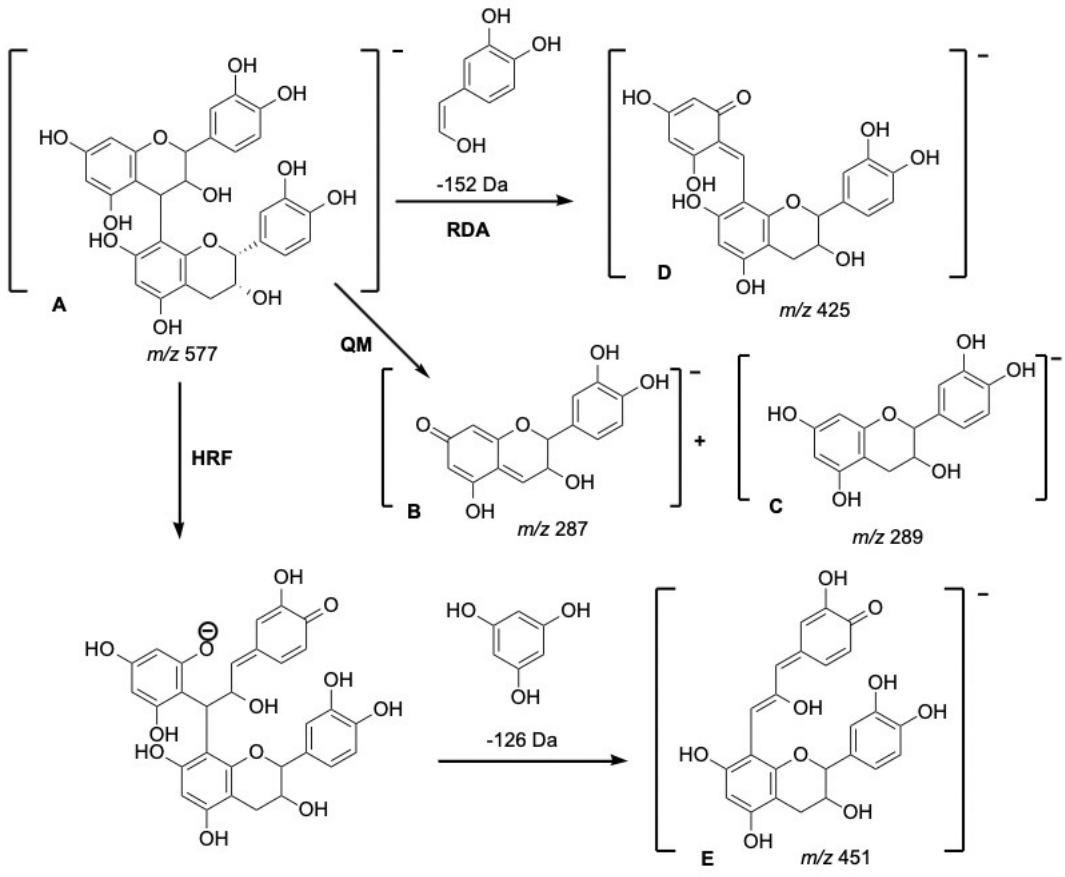

Figure 4. Typical fragmentation pattern in a negative electrospray ionization for dimeric procyanidin (PC) ion, 577 Da (**A**). PC fragments (**B**, **C**) are obtained by quinone methide (QM) cleavage of the interflavan-3-ol bonds. Retro Diels-Alder (RDA) product ion (**D**) is formed by the loss of 152 Da. Heterocyclic ring fission (HRF) product ion (**E**) is formed by the loss of 126 Da. The figure is adapted from Karonen et al. (2021).

2.4 From natural to synthetic proanthocyanidins

PAs are found in many plants, but their content is usually rather low.[38] However, industrial waste and byproducts contain significant amounts of PCs that could be more effectively utilized. Natural PCs can be easily extracted from industrial waste, such as bark or smashed apples from the beverage industry. Particularly low mDP PCs can be successfully extracted using non-heavy solvents, such as EtOH. PCs exhibit low to moderate bioactivities that could be enhanced through semisynthesis to create novel compounds for pharmaceutical applications. Utilizing the industrial byproducts is cost-effective and makes great use of accessible raw material sources.

Based on wine-making and aging mechanisms in wines, PAs derived from various sources can be enzymatically or chemically modified, leading to new semisynthetic interflavan-3-ol linkages. Modification can occur through a condensation reaction following the acid-catalyzed cleavage of the natural interflavan-3-ol bond. An alternative modification involves an electrophilic substitution reaction at the C6 or C8 carbon of the A-ring of flavan-3-ol units. In this bridging reaction, aldehydes serve as the most significant electrophiles. Depending on the structure of the aldehyde used, either methylene (C–CH_2–C) or ethylene-bridged (C–[CH_2–CH_3]–C) products can result from these modification reactions.[39] The acid-catalyzed cleavage is observed to happen during wine aging, which indicates that it takes time.[40] However, substitution reactions are prone to occur with lower energies, thus faster, making them more likely to occur under these conditions.[10]

The expected modification reaction for PAs is an oligomerization mechanism of catechins (Figure 5A) via an aldehyde (Figure 5B) through two subsequent electrophilic aromatic substitutions (Figure 5C, D), resulting in the methylene-bridged dimer (Figure 5E), utilizing the exact mechanism that forms adducts in red wine.[41] The optimized conditions for the substitution reaction include acidic conditions (pH 2.5) with a molar ratio of 10 mM catechin to 20 mM aldehyde at 40 °C.[42,43] In the electrophilic substitution, the aldehyde acts as an electrophile and positively charged ion, which replaces the hydrogen as a leaving group in the C8 carbon of the aromatic A-ring. This forms the methylene-bridged linkage base (Figure 5C), which undergoes another electrophilic substitution (Figure 5D), resulting in a PC dimer with a methylene-bridged linkage between the monomer units. However, only one electrophilic substitution reaction may occur, resulting in a PC oligomer with a methyl group linked to the farthest extension unit, a similar structure to what is seen in Figure 5D. Nevertheless, the

reaction through two subsequent electrophilic substitutions is still the most likely alternative in this case.

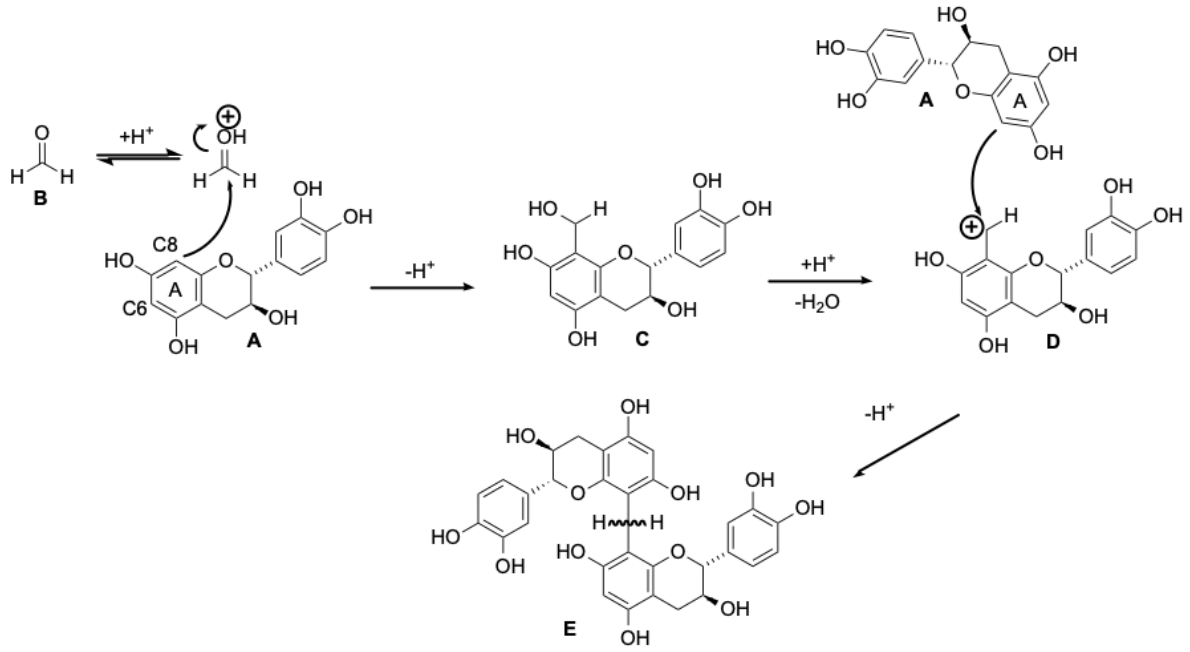

Figure 5. Oligomerization mechanism of catechin (**A**) with formaldehyde (**B**) through two subsequent electrophilic substitutions (**C** and **D)**. The product of the condensation reaction (**E**) is methylene-bridged procyanidin dimer. The figure is adapted from Laitila et al. (2023).

2.5 Pine bark as raw material and its potential as a source of bioactive compounds

Each year, about three million tons of bark from coniferous wood is generated as byproducts of the forest industry in Finland. To date, the most common use of bark is for energy production through burning. Approximately 10 percent of the wood consists of bark. Coniferous wood bark contains antimicrobial and antioxidant compounds that enhance storage life. Antioxidants are particularly abundant in the barks of trees cultivated under extreme conditions in Northern Finland.[44]

PAs are found in wood and bark, primarily as PCs in the pine bark.[13] Crucial information was found about the bark of *Pinus pinaster* and *P. radiata* but not of *P. sylvestris*. *P. pinaster* exhibited mDP of 2.1 and 6.04 mg PCs, responding to 65% PCs of the total phenolic content. *P. radiata* exhibited mDP of 2.7 and 10.79 mg PCs, responding to 84% PCs of the total phenolic content. Additionally, both species exhibited more catechins as terminal units than epicatechins.[45] Overall, PCs were predominant in the bark of all pine species, as found in the literature.

2.6 Purpose of this work

PA-rich plant species are associated with a range of bioactivities, but the efficacy of PCs depends heavily on their size and structure. Previous work (Engström et al., unpublished) indicated that PCs from pine bark can undergo efficient aldehyde condensation, offering a route to structurally modify and potentially enhance their bioactivity. This study aimed to semisynthesize methylene-bridged PC analogs from pine bark – a renewable byproduct of the Finnish forest industry – through aldehyde condensation reactions. PCs were fractionated by size and polymerization degree, reacted with formaldehyde, purified, and evaluated for protein precipitation capacity (PPC), a proxy for bioactivity. By exploring how structural modification affects PPC across different oligomer sizes, this work provides insight into the design of new, potentially more bioactive PC derivatives. If these show significantly improved bioactivity (e.g., protein precipitation or other disease-relevant effects) and have drug-like properties, they could be considered early-stage drug candidates worth further study for potential pharmaceutical use.

3 Materials and Methods

Materials

High-performance liquid chromatography (HPLC) grade MeOH for preparative LC, reagent grade dimethyl sulfoxide (DMSO) for precipitate dissolution tests, and super 2,5-dihydroxybenzoic acid (SDHB) for the matrix of precipitate analyses were purchased from Sigma-Aldrich (Steinheim, Germany). Reagent grade MeOH for solvent and solid phase extraction (SPE) use, HPLC grade acetonitrile (ACN) for precipitate dissolution tests, HPLC grade acetone for the matrix of precipitate analyses, and LC-MS grade ACN for analysis equipment were purchased from Honeywell (France). Analytical reagent grade 37–41% formaldehyde solution for the condensation reactions and analytical reagent grade acetone for solvent and extraction use were purchased from Fisher Chemical (Finland). LC-MS grade formic acid for the condensation reactions and analytical reagent grade euro-denatured EtOH for solvent and extraction use were purchased from VWR (Fontenay-soys-Bois, France). All water used was ultra-pure, produced by Merck Millipore Synergy UV water purification system (Darmstadt, Germany).

150 mg SPE cartridges (Oasis PRIME HLB 3 cc) were purchased from Waters. The 1 mL syringes (HSW HENKE–JECT) and 0.22 μm polytetrafluoroethylene (PTFE) filters (Clarify) were used to filter each sample prior to analyses. Sephadex LH-20 gel was prepared on 6.11.2021, and the gel was stored in a MeOH/water (50/50, v/v) solution. The pine tree bark used was sourced from Metsä Group and had been macerating since 2017. The pine bark was previously extracted and freeze-dried, making it ready for use as an extract.

Methods

3.1 Sephadex LH-20 fractionation in a beaker

Sephadex LH-20 gel was initially washed with an acetone/water solvent (90/10, v/v) and stabilized with water to remove possible acetone residues. 28 g of freeze-dried pine bark extract was dissolved in an adequate amount of water (50–100 ml), filtered with 0.22 μm PTFE filter, and mixed with the fluffy Sephadex LH-20 gel overnight. Excess water was collected as a zero fraction before eluting the sample with 5 x 300 mL of water, 5 x 300 mL of pure MeOH, and 5 x 300 mL of acetone/water (80/20, v/v) solvent using a Büchner funnel. 1 mL of each fraction was transferred into 2 mL Eppendorf tubes and evaporated with an Eppendorf concentrator to

the aqueous phase and analyzed with ultrahigh-performance liquid chromatography coupled with diode array detection (UHPLC-DAD) as 10-fold dilutions. All fractions were then evaporated with a rotary evaporator to the aqueous phase, combined based on the UHPLC-DAD results, and frozen and freeze-dried using a concentrator (Savant SC210A SpeedVac) coupled with a vapor trap (Savant RVT5105 Refrigerated Vapor Trap). Combined Sephadex fractions gathered with acetone as a solvent are later referred to as acetone material, and Sephadex fractions with MeOH as a solvent MeOH material.

3.2 Preparative liquid chromatography purification

The HPLC system consisted of a Waters Delta 600 LC, a Waters 600 Controller, a Waters 2998 photodiode array Detector, and a Waters Fraction Collector III. The preparative column (327 x 33 mm) was packed with LiChroprep RP-18 (40–63 μm) material (Merck KGaA, Darmstadt, Germany). MeOH (A) and 1% aqueous formic acid (B) were used as eluents. Before elution, the column was thoroughly stabilized for 30 min with 0% A in B. Two different gradients (Tables 1 and 2) were tested with 10 mg of pine bark extract dissolved in 2 mL of MeOH/water (15/85, v/v) to optimize the gradient for the actual runs. 500 mg of freeze-dried acetone or MeOH material was dissolved in 750 μl MeOH and 4250 μl water and filtered before the elution.

The preparative LC gradient is described in Table 2. A constant flow rate of 8.0 mL min^{-1} was used. Fractions were collected into 10 mL test tubes from 40 to 190 min for acetone material runs and from 30 to 180 min for MeOH material runs, resulting in a total of 120 individual fractions per run, with each fraction containing the PAs eluting during an 85 s retention time (RT) window. Three preparative LC runs were done for the MeOH material, and two for the acetone material. Every third collected fraction from both runs was selected and analyzed by UHPLC-DAD-ESI-triple quadrupole (QQQ)-tandem mass spectrometry (MS/MS) and UHPLC-DAD-heated electrospray ionization (HESI)-Orbitrap-MS/MS.

The MeOH or acetone material fractions gathered from the preparative LC runs were pooled according to the analysis results, and new combined, purified fractions were obtained. These combined and purified fractions are referred to as prep fractions in general or prepMeOH 1, prepAce 1, and so on for the rest of this thesis. The prep fractions were then evaporated to the water phase, frozen, and freeze-dried. Altogether, 16 prep fractions were produced.

Table 1. The initial gradient for preparative liquid chromatography.

Time (min)	Flow (mL/min)	Methanol (A, %)	1% aqueous formic acid (B, %)
0	8.0	100	0
5	8.0	100	0
180	8.0	60.0	40.0
220	8.0	40.0	60.0
240	8.0	20.0	80.0
260	8.0	20.0	80.0
270	8.0	100	0
300	8.0	100	0

Table 2. The final gradient in preparative liquid chromatography.

Time (min)	Flow (mL/min)	Methanol (A, %)	1% aqueous formic acid (B, %)
0	8.0	100	0
240	8.0	20.0	80.0
260	8.0	20.0	80.0
270	8.0	100	0
300	8.0	100	0

3.3 Condensation reactions

Before the large-scale condensation reaction, the reaction was tested on a smaller scale using five MeOH and five acetone material fractions from preparative LC runs. 300 µl of MeOH and 1700 µl of HCOOH/water (0.1/ 99.9, v/v) were added to each tube, and zero samples were collected. The tubes were incubated at 45 °C, and 10 µl of formaldehyde was added once the solution temperature reached 45 °C. Reaction subsamples were collected at 30 min, 4 h, and 24 h and analyzed as 10-fold dilutions by UHPLC-DAD-ESI-QQQ-MS/MS.

The 16 PC fractions were collected from the preparative LC. The condensation reaction, also called semisynthesis, was performed in a three-necked boiling flask, along with the other components shown in Figure 6. The reaction solution of each semisynthesis was prepared by adding 750 µl of MeOH and 4250 µl of HCOOH/water (0.1/ 99.9, v/v) into the freeze-dried PC fraction. 200 µl of the zero sample was collected before transferring the solution to the three-necked boiling flask. Formaldehyde was added to the solution after the temperature reached 45 °C, and the reaction time was started. The masses of each prep fraction and the volumes of formaldehyde used in the condensation reactions are shown in Table 3.

The reaction was stopped after 3.5 h by putting the boiling flask into an ice bath. A subsample of 150 µl was collected and placed on ice. Both the zero and 3.5 h samples were immediately analyzed by UHPLC-DAD-ESI-QQQ-MS/MS as 10-fold dilutions. The reaction solution was divided into three 2 mL Eppendorf tubes, centrifuged, and then decanted. For the liquid phases, SPE followed. After the SPE, liquid phase products, later referred to as final products, were evaporated to the water phase, frozen, and freeze-dried. The precipitates remaining at the bottom of the Eppendorf tubes were washed with 500 µl of cold water, shaken with a vortex for 10 min, centrifuged, and decanted. This process was repeated three times. Finally, the precipitates were frozen and freeze-dried.

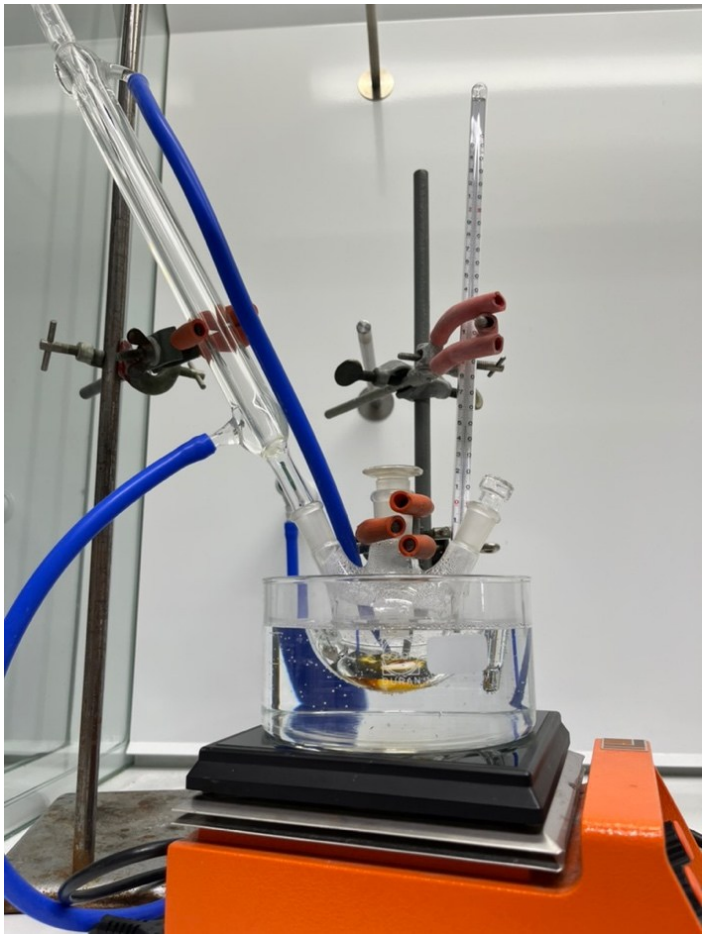

Figure 6. The condensation reaction equipment included a water cycle, heater, thermometer, magnet, magnetic stirrer, three-necked boiling flask, and reflux condenser.

Table 3. Masses of prepMeOH and prepAce fractions and volumes of formaldehyde used in the condensation reactions. Fr = fraction.

Combined preparative LC fractions	Names of the fractions	Mass of freeze-dried purified fraction (mg)	Volume of formaldehyde (μl)
MeOH fr. 2–19	prepMeOH 1	9.5	10
MeOH fr. 20–35	prepMeOH 2	100	48
MeOH fr. 36–46	prepMeOH 3	100	48
MeOH fr. 47–53	prepMeOH 4	100	48
MeOH fr. 54–68	prepMeOH 5	100	48
MeOH fr. 69–76	prepMeOH 6	71	34
MeOH fr. 77–89	prepMeOH 7	90	44
MeOH fr. 90–99	prepMeOH 8	43	21
MeOH fr. 100–112	prepMeOH 9	23	11
Ace fr. 18–29	prepAce 1	22	11
Ace fr. 30–40	prepAce 2	72	35
Ace fr. 41–51	prepAce 3	100	48
Ace fr. 52–59	prepAce 4	75	36
Ace fr. 60–70	prepAce 5	91	44
Ace fr. 71–82	prepAce 6	54	26
Ace fr. 83–89	prepAce 7	17	10

Before the final analyses, the solubility of the semisynthesis precipitates was tested in water, ACN, MeOH, DMSO, DMSO/MeOH (50/50, v/v), DMSO/water (50/50, v/v), and DMSO/acetone (85/15, v/v). The prepMeOH and prepAce semisynthesis precipitates with different RTs were assessed at 1 mg/mL concentrations. All samples were shaken with a vortex for 2 h, placed in an ultrasonic bath for 10 min, filtered, and analyzed using UHPLC-DAD-ESI-QQQ-MS/MS to determine if any dissolution occurred with any of the solvents. MALDI-TOF-MS was also employed to analyze the precipitates.

After completing 16 condensation reactions, the zero samples and final products were analyzed using UHPLC-DAD-ESI-QQQ-MS/MS and UHPLC-DAD-HESI-Orbitrap-MS/MS. Zero samples from each reaction were analyzed as 10-fold dilutions, and products were prepared at a concentration of 1 mg/mL in MeOH/water (15/85, v/v). Zero samples were diluted with MeOH/water (15/85, v/v) solvent.

3.4 Solid phase extraction of reaction product

SPE was performed under a vacuum using cartridges with a loading capacity of 150 mg. One cartridge was utilized if the mass of the prep fraction was 20 mg or less, while two cartridges

were utilized for fractions weighing between 30 and 50 mg or more. Initially, the cartridges were conditioned with 5 x 1 mL pure MeOH followed by 5 x 1 mL water. Next, a liquid phase product was loaded into the cartridge, and the solvent was filtered into 2 mL Eppendorf tubes as a zero fraction. The washing/elution solvents included 5 x 1 mL of water, 3 x 1 mL of MeOH/water (10/90, v/v), 3 x 1 mL of MeOH/water (50/50, v/v), and 5 x 1 mL of pure MeOH, all collected into 2 mL Eppendorf tubes. SPE fractions of prepMeOH 2–5 products were studied in more detail as their starting materials were the most abundant ones. The MeOH/water (50/50, v/v) and pure MeOH SPE fractions of prepMeOH 2–5 products were first evaporated to approximately 15% MeOH content and adjusted to a volume of 1 mL using MeOH/water (15/85, v/v) solvent before being analyzed using UHPLC-DAD-ESI-QQQ-MS/MS. Finally, MeOH was evaporated from the fractions, which were then combined, frozen, and freeze-dried. SPE fractions of prepMeOH 1 and 6–9 products and prepAce 1 and 9 products were promptly evaporated to the water phase and combined, frozen, and freeze-dried, all on their own.

3.5 UHPLC-DAD-ESI-QQQ-MS/MS

The UHPLC-DAD-ESI-QQQ-MS/MS system consisted of Acquity ultraperformance liquid chromatography (UPLC) system (Waters Corp., Milford, MA, USA) coupled to a Xevo TQ QQQ-MS with ESI (Waters Corp., Milford, MA, USA). The Acquity UPLC system consisted of a binary solvent manager, sample manager, column oven, and DAD. The column was an Acquity BEH Phenyl column (100 mm x 2.1 mm i.d; 1.7 μm particle size; Water Corp, Wexford, Ireland).

The mobile phase consisted of ACN (A) and 0.1 % aqueous formic acid (B), and the elution profile was as in Table 4. UV data at 190–500 nm and mass data were collected from 0 to 10 min. A different elution profile was used with the same solvents for the analyses other than semisynthesis (Table 5), in which UV data at 190–500 nm and mass data were collected from 0 to 7 min. The flow rate of the mobile phase was 0.5 mL min^{-1}. The electrospray ion source was operated in negative mode with the following parameters: capillary voltage 1.8 kV, ion extraction voltage 3V, source temperature 150 °C, desolvation temperature 650 °C, desolvation gas (N_2) flow rate 1000 L h^{-1} and cone gas (N_2) flow rate 100 L h^{-1}. Argon was used as the collision gas in the collision chamber. All the samples were filtered with 0.22 μm PTFE filters before analyses, and the injection volume was 5 μl via full loop injection. MassLynx

software (Waters Corp., Milford, MA, USA) was used to analyze all the samples. Main polyphenol sub-groups were quantified with the Engström et al. method.[1,46]

Table 4. The UPLC gradient in UHPLC-DAD-ESI-QQQ-MS/MS analyses.

Time (min)	acetonitrile (A, %)	0.1% aqueous formic acid (B, %)
0	0.1	99.9
0.5	0.1	99.9
5.0	30.0	70.0
8.0	50.0	50.0
9.0	57.0	43.0
9.1	90.0	10.0
11.1	90.0	10.0
11.2	0.1	99.9
12.5	0.1	99.9

Table 5. The UPLC gradient in UHPLC-DAD-ESI-QQQ-MS/MS analysis for other than semisynthesis analyses.

Time (min)	acetonitrile (A, %)	0.1% aqueous formic acid (B, %)
0	0.1	99.9
0.5	0.1	99.9
5.0	30.0	70.0
6.0	35.0	65.0
6.1	90.0	10.0
8.1	90.0	10.0
8.2	0.1	99.9
9.5	0.1	99.9

3.6 UHPLC-DAD

The UHPLC-DAD system consisted of Waters UPLC system (Waters Corp., Milford, MA, USA) including a sample manager, a binary solvent manager, a column, and a DAD. The column used was a 100 x 2.1 mm inner diameter, 1.7 µm Acquity UPLC BEH Phenyl column (Waters Corp., Wexford, Ireland). The flow rate of the eluent was 0.5 mL min^{-1}. The elution profile is presented in Table 5. UV data was collected at 190–500 nm from 0 to 7 min. MassLynx software (Waters Corp., Milford, MA, USA) was used to analyze all the samples.

3.7 UHPLC-DAD-HESI-Orbitrap-MS/MS

The UHPLC-DAD-HESI-Orbitrap-MS/MS system consisted of Waters UPLC system (Waters Corp., Milford, MA, USA) linked to a Q Exactive Orbitrap MS (Thermo Fisher Scientific GmbH, Bremen, Germany). The Acquity UPLC system included a binary solvent manager, sample manager, column oven, and DAD. The column used was an Acquity BEH Phenyl column (100 mm x 2.1 mm i.d.; 1.7 µm particle size; Waters Corp., Wexford, Ireland).

The mobile phase was composed of ACN (A) and 0.1% aqueous formic acid (B), with the elution profile detailed in Table 6 for the preparative LC fraction analyses. The elution profile in Table 4 was utilized for the final analyses of the condensation reaction zero samples and final products. The flow rate was set at 0.5 ml min^{-1}. The ion source, heated electrospray ionization (HESI), was operated in negative ion mode, with the capillary voltage set to -3 kV. The capillary temperature was maintained at 380 °C, and the flow rates for the sheath and auxiliary gas heater (N_2) were 60 and 20 arbitrary units, respectively. The full scan mass range extended from 150 to 2250 Da, with an automatic gain control of 3 x 10^6 and a resolution of 70,000. UV and mass data were collected from 0 to 9 min (Table 6) or from 0 to 11 min (Table 4). N_2 served as the collision gas. Xcalibur software (Thermo Fisher Scientific) was employed to analyze all the data.

Table 6. The UPLC gradient in UHPLC-DAD-HESI-Orbitrap-MS/MS analysis for the preparative liquid chromatographdy fractions.

Time (min)	acetonitrile (A, %)	0.1% aqueous formic acid (B, %)
0	0.1	99.9
0.5	0.1	99.9
5.0	30.0	70.0
7.0	44.0	56.0
7.1	90.0	10.0
9.1	90.0	10.0
9.2	0.1	99.9
10.5	0.1	99.9

3.8 MALDI-TOF-MS

MALDI-TOF-MS was used for the analyses of aldehyde condensation reaction precipitates. The measurements were performed using a Bruker timsTOF fleX MALDI-2 equipped with a post-ionization laser. The laser power was set to 70%, and for a spectrum, 1000 shots were

collected with 1000 Hz frequency. Red phosphorus was utilized as a reference. The matrix used was comprised of 40 mg/mL SDHB in acetone. This matrix was mixed with a 3 mg/mL solution of the analyzed mixtures in a 1:1 (v/v) ratio. Additionally, 5- and 25-fold dilutions were done, resulting in three samples total. 0.5 µl of the mixture was applied onto the MALDI target plate (Bruker) and dried with nitrogen before analysis. The spectra were obtained in positive mode with a mass range of 250-1500 Da. Data processing and peak analysis were carried out using DataAnalysis.

3.9 Protein precipitation capacity

PPC was measured using a 96-well plate reader (Multiscan Ascent, Labsystems) at room temperature. Standard solutions of pentagalloylglucose (PGG) at concentrations of 0.2, 0.3, 0.4, and 0.6 mg/mL were prepared in EtOH/water (10/90, v/v) from a stock solution of 1 mg/mL PGG. The pH 5 buffer was prepared by adding 10.6 mg of L-ascorbic acid to 800 mL of water in a 1000 mL beaker. 2.85 mL of acetic acid was added to the solution and mixed with a magnetic stirrer. 2 M NaOH was used to adjust pH to 5. The solution was transferred to a 1000 mL volumetric flask, and the final volume was adjusted to 1000 mL with water and stirred. Bovine Serum Albumin (BSA) solution (200 µM) was prepared in pH 5 buffer by weighing 2.66 g of BSA and mixing it with the buffer.[47]

First, tests were conducted to determine the appropriate solvent and concentration for the samples. Concentrations for the tests included 5, 2.5, and 1 mg/mL, along with the solvents water and MeOH/water (15/85, v/v) solution. In addition to absorbance results, visual inspection was done to evaluate the precipitation reaction. The final test was performed on all prepMeOH and prepAce fractions, including all prepMeOH products and one prepAce product. Three parallel samples or fewer per sample, depending on the sample volume, were processed, along with one control per sample.

Three replicate samples of each PGG standard solution were pipetted into the first row, placing 100 µl of the sample in each well. Three replicate samples of prepMeOH products and prepMeOH fractions were then pipetted into the next five rows of plate one (rows B–F) in order of increasing fraction number. One control sample for each prepMeOH fraction and product was added to the last two rows of plate one (rows G–H). Three or fewer replicate samples of prepAce fractions and prepAce 1 product were pipetted into the first two rows of plate two (rows A–B). One control sample for each prepAce fraction and prepAce 1 product was added

to the third row (row C) of plate two. 100 µl of BSA solution was pipetted into the sample rows, and 100 µl of pH 5 buffer was added to the control sample rows of each plate. The plate reader method was then started with a 1 min mixing period, after which absorbance was measured in 30 s intervals for 30 min at 340 and 414 nm, including a 10 s mixing period before each measurement.

4 Results and Discussion

4.1 Sephadex LH-20 fractionation in a beaker

Based on the shape similarity on UV chromatograms at 280 nm from UHPLC-DAD, MeOH eluted fractions 1–5 (Figure 7A–E), acetone eluted fractions 1–4 (Figure 7F–I), and water eluted fractions 1–4 (Appendix 1A–D) were combined and freeze-dried resulting in three fractions in total. The acetone eluted fraction 5 (Figure 7J) and the water eluted fraction 5 (Appendix 1E) were freeze-dried on their own.

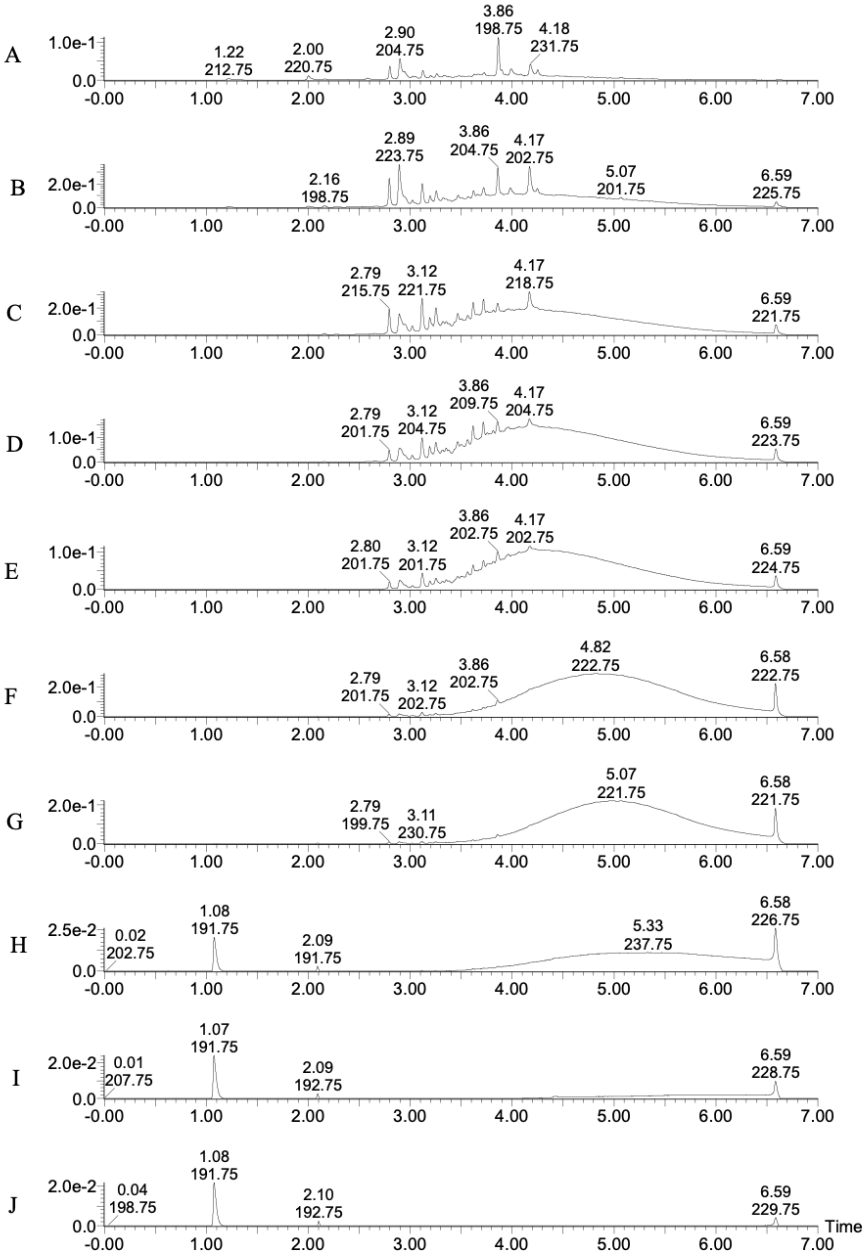

Figure 7. UV chromatograms (280 nm) of the MeOH eluted fractions 1–5 (A–E) and acetone eluted fractions 1–5 (F–J) from the Sephadex LH-20 fractionation of the pine bark procyanidins.

The masses of the freeze-dried fractions were 3.25 g for the MeOH material, 1.29 g for the acetone material, and 6.42 g for the water fractions 1–4. Due to the high PC contents, the MeOH and acetone materials were chosen for preparative LC purification.

4.2 Preparative liquid chromatography purification

Every third acetone and MeOH material fraction from preparative LC runs was analyzed using UHPLC-DAD-ESI-QQQ-MS/MS. The mDP was calculated for every analyzed preparative LC fraction (Appendix 2). The fractions were then combined based on their mDPs and similarities in the UV chromatograms at 280 nm, resulting in prepMeOH and prepAce fractions with the same RT widths within the prep fractions. The RT shifts in UV chromatograms at 280 nm are illustrated and presented for MeOH (Appendix 3) and acetone material (Appendix 4) fractions from preparative LC. The mDPs of prepMeOH fractions 2–35 were the same, but to maintain consistent areas across the prep fractions, prepMeOH fractions 2–19 and 20–35 were combined separately. This was done based on the different RTs and shapes of the chromatographic areas of prepMeOH fraction 17 (Figure 8A) and fraction 20 (Figure 8B). PrepMeOH fractions 20–35 and 36–46 were also combined separately based on the RTs and shape differences of prepMeOH fraction 20 (Figure 8B) and fraction 38 (Figure 8C).

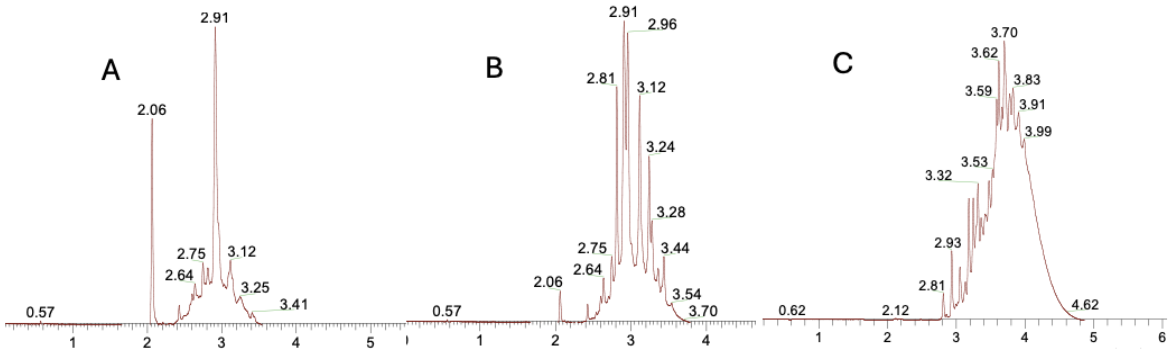

Figure 8. UV chromatograms at 280 nm of prepMeOH fractions 17 (A), 20 (B), and 38 (C) from the preparative liquid chromatography of pine bark procyanidins.

Additionally, prep fractions were combined by increasing RTs to investigate differences in fractions caused by RTs and mDPs. As a result, prepMeOH fractions 51 (Figure 9A) and 69–72 (Figure 9G–H) could not be combined. PrepMeOH fractions 54–66 (Figure 9B–F) were positioned between those with differing mDPs and RTs. Lastly, prepMeOH fraction 51 (Figure 9A) is part of prepMeOH 4, while fractions 54–66 (Figure 9B–F) are a part of prepMeOH 5,

and fractions 69–72 (Figure 9G–H) belong to prepMeOH 6, based on their similarities and differences in shapes and RTs in the UV chromatograms. The same method was applied to combine the prepAce fractions based on increasing RTs and similarities in mDPs. All 120 MeOH or acetone material fractions from preparative LC runs could not be utilized due to low intensities in UV chromatograms and, therefore, were not combined or freeze-dried.

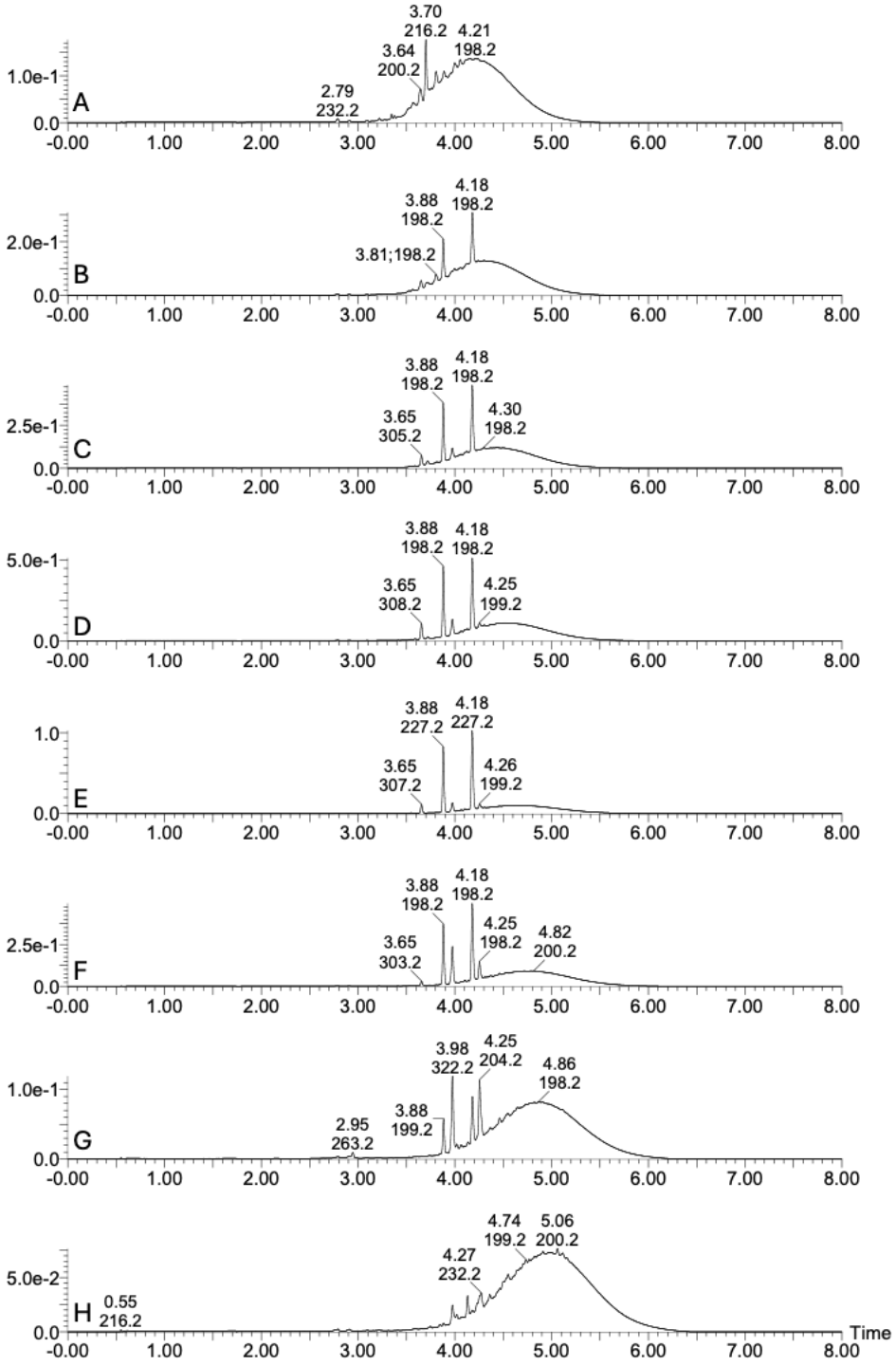

Figure 9. UV chromatograms at 280 nm of every third prepMeOH fraction 51–72 (A–H) from the preparative liquid chromatography of pine bark procyanidins.

Altogether, 16 prep fractions were produced from the preparative LC: nine prepMeOH fractions (Figure 10A) and seven prepAce fractions (Figure 10B). The UV chromatograms of the prepMeOH (Appendix 5) and prepAce fractions (Appendix 6) varied in shapes and RTs. The masses of the prep fractions to be used as the starting materials in the condensation reactions ranged from 10 to 100 mg. The mDPs of the prepMeOH and prepAce fractions (Figure 11) increased from early elution to the middle. Towards the end, mDPs decreased near the starting mDPs, most likely due to the analytical features such as ionization problems and a low fragmentation efficiency caused by the higher DP PCs.

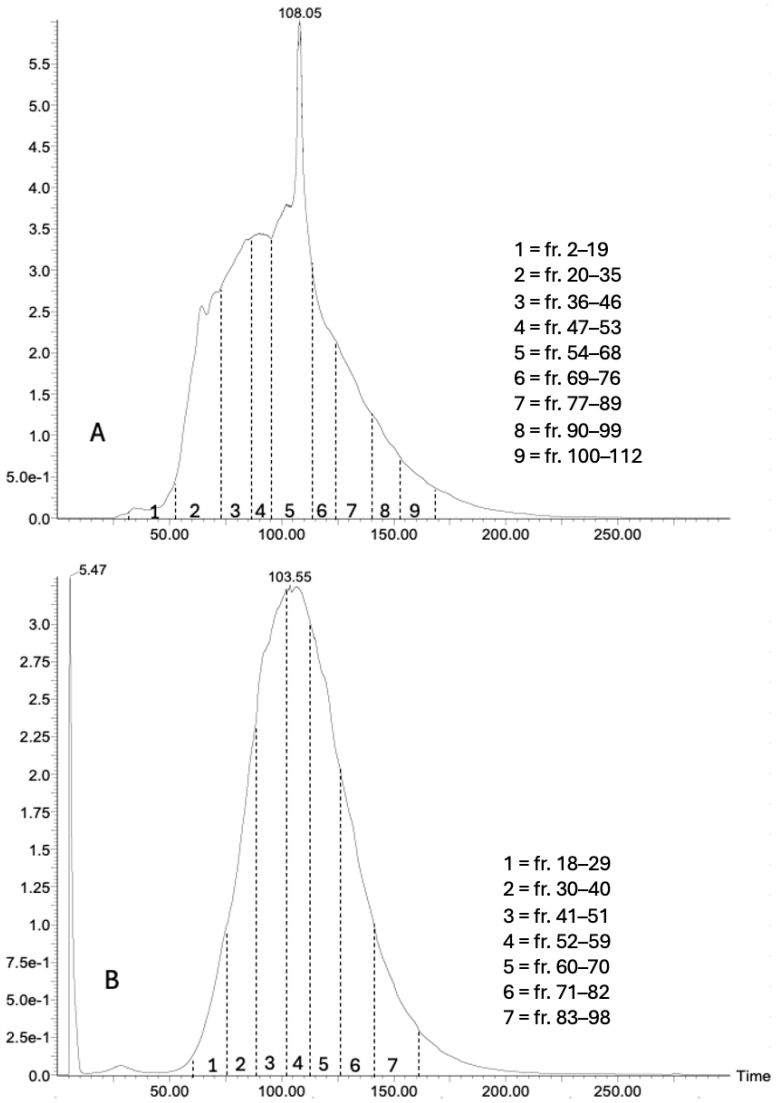

Figure 10. UV chromatograms at 280 nm of MeOH (A) and acetone material (B) obtained from the preparative liquid chromatography runs of pine bark procyanidins. The numbers within the UV chromatograms refer to the combined prepMeOH and prepAce fractions. Fr = fraction, Ace = acetone.

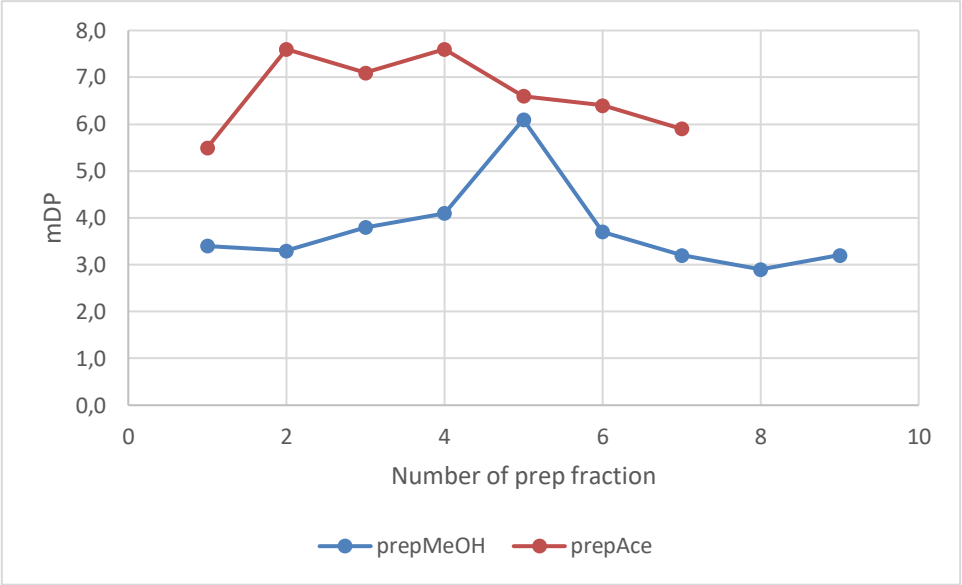

Figure 11. Mean degrees of polymerization (mDPs) of the 16 prep fractions obtained from the preparative liquid chromatography of pine bark procyanidins. The blue graph corresponds to the prepMeOH fractions and red graph corresponds to the prepAce fractions from Sephadex LH-20 fractionation. Ace = acetone.

4.3 Condensation reactions

The small-scale condensation reactions of five prepMeOH fractions 24, 39, 57, 71, and 104, and five prepAce fractions 34, 53, 70, 84, and 92 indicated that the reaction conditions were successful. The formation of new compounds was evidenced by the UV chromatograms and mass spectra before and after the reaction (Appendices 7 and 8). Furthermore, different reaction behaviors were already noted at this stage, predicting similar but more complex outcomes on larger-scale reactions due to the broader fraction profiles in these reactions. Most importantly, the small-scale reaction tests suggested that applying these reaction conditions to the larger-scale condensation reactions aimed at semisynthesizing something new was likely to be successful.

Already the starting materials (prepMeOH fractions) of the reactions exhibited different UV chromatogram profiles and full scan MS spectra. The reaction kinetics and the final products varied greatly between fractions. However, as anticipated based on the analytical behavior of the natural PCs, all final products were mixtures of various PC analog oligomers and polymers rather than individual compounds. The mDPs were calculated for zero and 3.5 h samples, and final products (Figure 12). The condensation reactions of the prepMeOH fractions resulted in unaltered or decreased mDPs, except for the prepMeOH 1, 5, 7, and 9 (Figure 12), for which the mDPs increased. On the other hand, the condensation reactions of the prepAce

fractions resulted in decreased or unknown mDPs because of the precipitation in the reactions, except that of prepAce 1 (Appendix 9), for which the mDP increased.

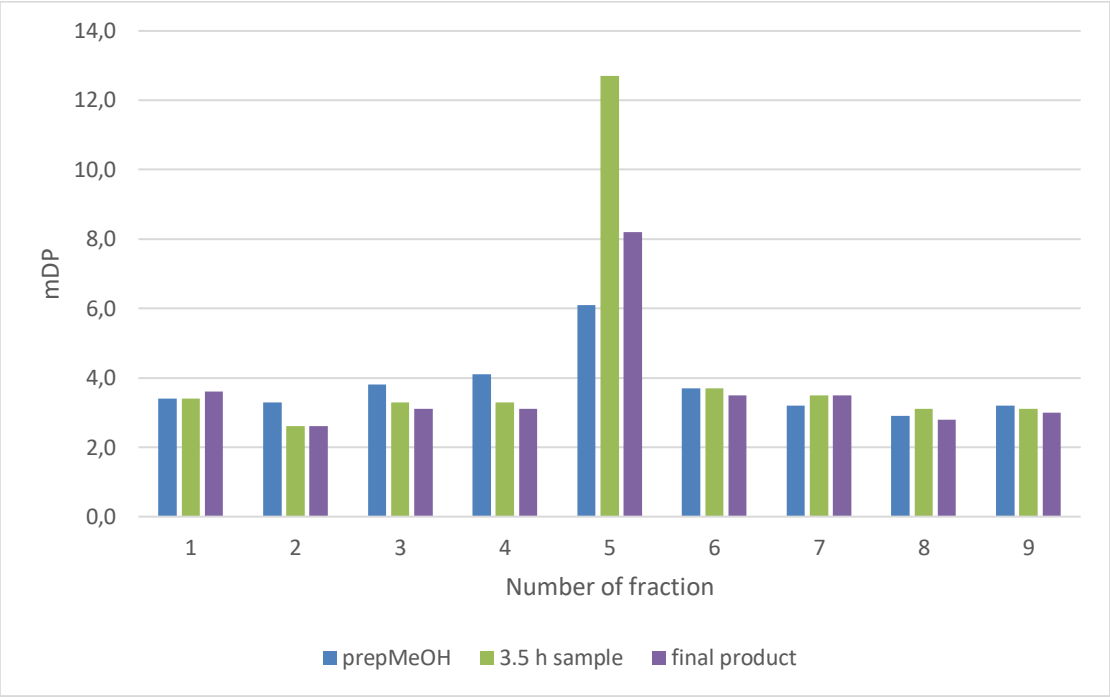

Figure 12. Changes in the mean degrees of polymerization (mDPs) of the prepMeOH fractions in the semisynthesis of pine bark procyanidins. The mDPs of the prepMeOH fractions, their 3.5 h samples, and the final products are presented.

The zero and 3.5 h samples were prepared as 10-fold dilutions (ie. 0.5–2 mg/ml), resulting in different concentrations as the final products were analyzed at 1 mg/mL concentration. Therefore, the concentrations were not congruent, and this might slightly affect the comparability of the results. The increase in mDPs from before to after the condensation reactions of prepMeOH 1, 5, 7, and 9, as well as prepAce 1, is somewhat questionable. It is worth considering whether the reactions continue before the final products are obtained since the reaction solutions are centrifuged etc. before freezing.

To assess the PA content and composition before and after the condensation reaction, the integrated PC peak areas of group-specific responses were calculated as PC-% of the total PA content (Table 7) for the prep fractions, 3.5 h samples, and final products. While the PC percentages were consistent initially, they began to differ in the 3.5 h samples and the final products. However, the PC-% of other prepMeOH fractions remained above 90%, except for prepMeOH 5 product, where the percentage dropped to 60–70%. The PC percentages are presented for all prep fractions, even though the prepAce 2–6 products fully precipitated. Structural changes, such as the formation of methylene-bridged or other new linkages, affect the ionization and the fragmentation efficiency of the PCs to monomers, which likely impact

the group-specific responses of the 3.5 h samples and final products. Additionally, the group-specific method does not necessarily recognize the fragments of methylene-bridged PCs, which affects the responses and consequently the mDP decreasingly. Therefore, these results are not one-sided or straightforward, as the obtained PC responses may be considerably lower than reality.

Table 7. Procyanidin (PC) content (%) out of the total proanthocyanidin content. The group-specific method's integrated PC peak area responses were used to determine the PC-% for prepMeOH and prepAce fractions, their 3.5 h samples, and final products obtained from pine bark PCs.

Prep fractions	PC (%) of prepMeOH / Ace	PC (%) of 3.5 h sample	PC (%) of final product
prepMeOH 1	99	99	99
prepMeOH 2	99	98	98
prepMeOH 3	99	97	96
prepMeOH 4	98	97	96
prepMeOH 5	90	57	67
prepMeOH 6	97	93	93
prepMeOH 7	98	94	93
prepMeOH 8	97	92	93
prepMeOH 9	97	94	95
prepAce 1	99	99	99
prepAce 2	99	96	–
prepAce 3	99	97	–
prepAce 4	98	76	–
prepAce 5	99	86	–
prepAce 6	99	94	–
prepAce 7	99	99	98

Identification and characterization of the original PAs and the condensation reaction products

Mass peaks from B-type PCs, ranging from monomer to hexamer, were observed in the full scan MS spectra of prepMeOH 1 and 2 (Figure 13A, C) in a negative ionization mode. Characteristic HRF and RDA fragments (Appendix 10) were detected in the full scan MS spectra, confirming the presence of B-type PCs. The PC-pure fractions reacted with formaldehyde in the condensation reactions, resulting in methylene-bridged PCs that displayed a mass difference of 14 Da compared to the natural PCs. The addition of 14 Da can result from the methylene-bridged linkage between the monomers or from the linkage of a methyl group to the farthest extension unit. The methyl group linked to the farthest extension unit could result

from the electrophilic attack of formaldehyde without the reaction continuing that would eventually lead to the formation of the methylene-bridged linkage. However, the structures formed are expected to be the methylene-bridged PCs as these structures are reportedly formed under these conditions.

The full scan MS spectra of the prepMeOH 1 and 2 (Figure 13A, C) and their products (Figure 13B, D) resembled each other. However, the full scan MS spectrum of the prepMeOH 2 product (Figure 13D) exhibited more intense mass peaks of methylene-bridged PCs than that of prepMeOH 1 product (Figure 13B), indicating a more vigorous reaction of prepMeOH 2 (Figure 13C), resulting in methylene-bridged PCs. PrepMeOH 1 (Figure 13A) exhibited mass peaks of PC oligomer + 14 Da that got more intense in the product (Figure 13B). However, these mass peaks refer to the methylene-bridged PCs, which cannot exist in the starting materials. The tentative identification of these mass peaks turned out quite difficult. The first proposed identification for the mass peaks were PC oligomer + taxifolin compounds, which most likely could be products of a long maceration. Another tentative identification of these mass peaks could be A-type PC oligomer + PD structures which would be contaminations from Sephadex LH-20 gel or preparative LC, since A-type PAs or PDs are not commonly met in pine bark. However, nothing could be confirmed based on the data available. Therefore, the mass peaks corresponding to these maceration products or contaminations are later referred to as unidentified compounds. However, the mass peaks of PC oligomer + 14 Da in the prepMeOH 2 product were tentatively identified as methylene-bridged PCs instead of some unidentified compounds based on the molecular formulas. The increase in the peak intensities of unidentified compounds was observed, and the PC mass peaks remained unchanged during the condensation reaction of prepMeOH 1. Therefore, the formation of methylene-bridged PCs was also expected. The unidentified compounds coeluted with methylene-bridged PCs, and unidentified compounds predominated based on the molecular formulas not corresponding to methylene-bridged PCs.

The tentative identification of the most abundant compounds in the prepMeOH 1 and 2 and their products is presented in Table 8. Based on the mass peak comparison, desired methylene-bridged PCs were formed during the condensation reactions of these two fractions and, more importantly, were detectable in their products as they did not precipitate out from the reaction solution. However, in the prepMeOH 1 product, the methylene-bridged PCs and unidentified compounds supposedly coeluted, and the latter ones predominated based on the molecular formulas. The formation of methylene-bridged PCs from dimer to pentamer was

observed in the prepMeOH 2 product (Table 8). Additionally, two methylene-bridged linkages in PC pentamer were observed in the prepMeOH 2 product.

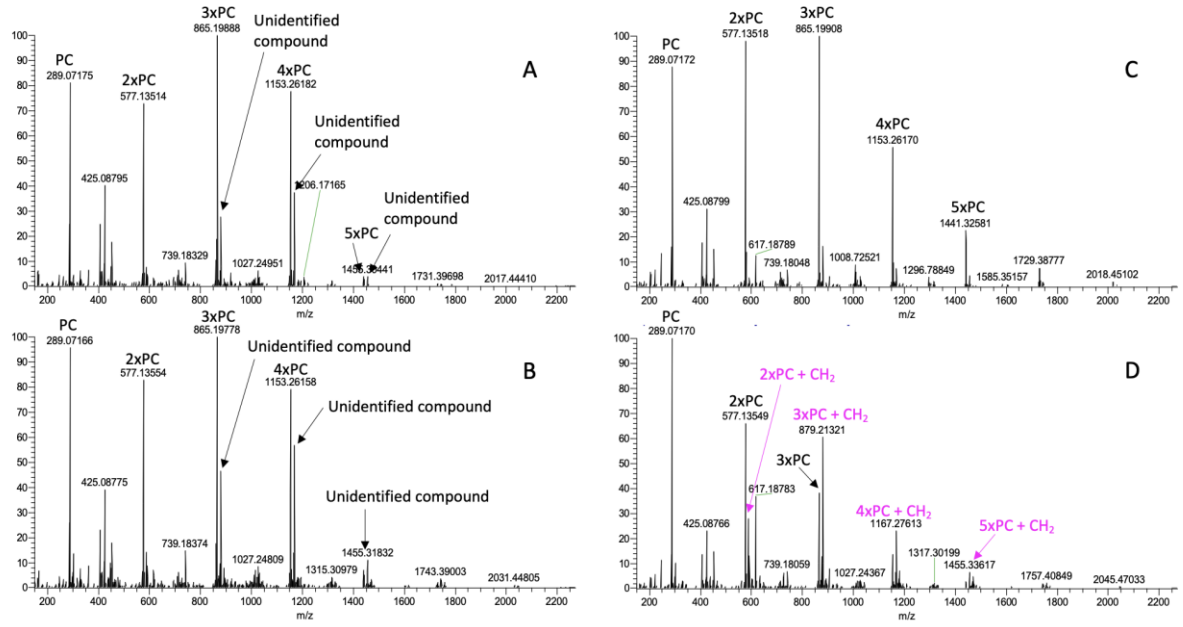

Figure 13. Full scan MS spectra in negative electrospray ionization of the prepMeOH 1 (A) and its product (B) and of the prepMeOH 2 (C) and its product (D) from the semisynthesis of pine bark procyanidins (PCs). Tentative identifications of the most abundant compounds are presented in the spectra.

Table 8. Tentative identification of the most abundant compounds of prepMeOH 1 and 2 and their products resulting from the semisynthesis of pine bark procyanidins (PCs). The final products also contain the underlined $[M-H]^-$ values. DP = the degree of polymerization.

Original PAs

prepMeOH	DP	Bond type	Molecular formula	Mcalculated	Monomeric composition	$[M-H]^-$
1	1	–	$C_{15}H_{14}O_6$	290.07904	PC	289.07175
	2	B	$C_{30}H_{26}O_{12}$	578.14243	2xPC	577.13514
	3	B	$C_{45}H_{38}O_{18}$	866.20582	3×PC	865.19888
	4	B	$C_{60}H_{50}O_{24}$	1154.26921	4×PC	1153.26182
	5	B	$C_{75}H_{62}O_{30}$	1442.33260	5×PC	1441.32358
2	1	–	$C_{15}H_{14}O_6$	290.07904	PC	289.07172
	2	B	$C_{30}H_{26}O_{12}$	578.14243	2xPC	577.13518
	3	B	$C_{45}H_{38}O_{18}$	866.20582	3×PC	865.19908
	4	B	$C_{60}H_{50}O_{24}$	1154.26921	4×PC	1153.26170
	5	B	$C_{75}H_{62}O_{30}$	1442.33260	5×PC	1441.32581
	6	B	$C_{90}H_{74}O_{36}$	1730.39599	6xPC	1729.38777

Final products

prepMeOH	DP	Bond type	Molecular formula	Mcalculated	Monomeric composition	$[M-H]^-$
1	3	B	$C_{45}H_{36}O_{19}$	880.18509	unidentified compound	879.17771

	4	B	$C_{60}H_{48}O_{25}$	1168.24848	unidentified compound	1167.24134
	5	B	$C_{76}H_{64}O_{30}$	1456.34825	unidentified compound	1455.31832
2	2	B	$C_{31}H_{28}O_{12}$	592.15808	2xPC+CH_2	591.15194
	3	B	$C_{46}H_{40}O_{18}$	880.22147	3xPC+CH_2	879.21321
	4	B	$C_{61}H_{52}O_{24}$	1168.28486	4xPC+CH_2	1167.27613
	5	B	$C_{76}H_{64}O_{30}$	1456.23825	5xPC+CH_2	1455.33617
	5	B	$C_{77}H_{66}O_{30}$	1470.36390	5xPC+2xCH_2	1469.34939

The only prepAce fractions that did not fully precipitate were prepAce 1 and 7. However, the yield of the prepAce 7 was not sufficient to obtain clear results from the analyses. Therefore, the only prepAce fraction that could be studied in further detail was prepAce 1 (Figure 14A). The SPE zero fraction of prepAce 1 (Figure 14B) allowed the passage of natural PCs. The SPE is discussed in more detail in section 4.4. However, natural PCs and their corresponding methylene-bridged PCs remained in the product (Figure 14C). PrepAce 1 and 2 showed minimal differences in UV chromatograms and full scan MS spectra as all the full scan MS spectra of prepAce fractions resembled each other. However, due to its higher mDP, prepAce 2 produced a significant amount of precipitate in the condensation reaction compared to prepAce 1. In conclusion, the high mDPs of prep fractions appear to greatly increase the yield of the precipitate due to the formation of high DP polymeric methylene-bridged PCs, which most likely are hydrophobic and insoluble in common organic solvents.

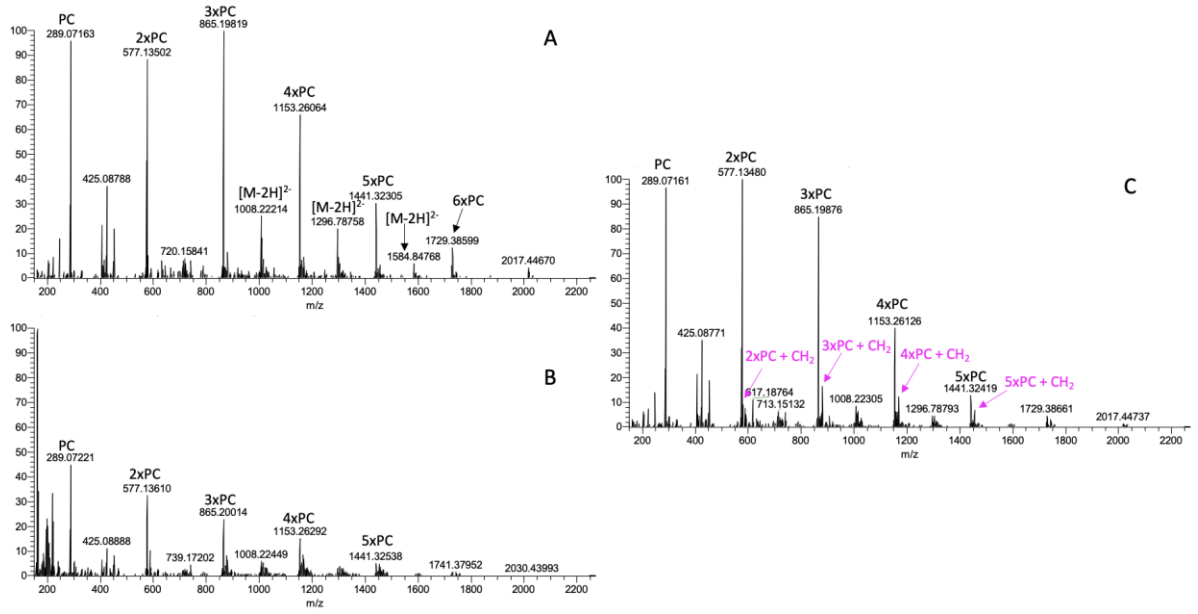

Figure 14. Full scan MS spectra in negative electrospray ionization of prepAce 1 (A), its solid phase extraction zero fraction (B), and the final product (C) from the semisynthesis of pine bark procyanidins (PCs). Tentative identifications of the most abundant compounds are presented in the spectra.

The tentative identification of the most abundant compounds of the prepAce 1–7 and the prepAce 1 product is presented in Table 9. Based on the mass peak comparison, desired methylene-bridged PCs were formed during the condensation reaction of prepAce 1 and, more importantly, were detectable as they did not precipitate out from the reaction solution. Additionally, the formation of the methylene-bridged linkages in every DP PCs was observed in prepAce 1 product (Table 9).

Table 9. Tentative identification of the most abundant compounds of prepAce 1–7 and their products from the aldehyde condensation reactions of pine bark procyanidins (PCs). DP = degree of polymerization.

Original PAs

prepAce	DP	Bond type	Molecular formula	Mcalculated	Monomeric composition	$[M-H]^-$
all	1	–	$C_{15}H_{14}O_6$	290.07904	PC	289.07163
all	2	B	$C_{30}H_{26}O_{12}$	578.14243	2xPC	577.13502
all	3	B	$C_{45}H_{38}O_{18}$	866.20582	3×PC	865.19819
all	4	B	$C_{60}H_{50}O_{24}$	1154.26921	4×PC	1153.26064
all	5	B	$C_{75}H_{62}O_{30}$	1442.33260	5×PC	1441.32305
1–6	6	B	$C_{90}H_{74}O_{36}$	1730.39599	6xPC	1729.38599
1–4	7	B	$C_{105}H_{86}O_{42}$	2018.45959	7xPC	2017.44670
7	-	-	$C_{15}H_{10}O_7$	302.04269	quercetin	301.03552
7	-	-	$C_{21}H_{20}O_{11}$	448.10062	quercitrin	447.09359

Final products

prepAce	DP	Bond type	Molecular formula	Mcalculated	Monomeric composition	$[M-H]^-$
1	2	B	$C_{31}H_{28}O_{12}$	592.15808	2xPC+CH_2	591.15202
	3	B	$C_{46}H_{40}O_{18}$	880.22147	3xPC+CH_2	879.21688
	4	B	$C_{61}H_{52}O_{24}$	1168.28486	4xPC+CH_2	1167.27167
	5	B	$C_{76}H_{64}O_{30}$	1456.23825	5xPC+CH_2	1455.33281
	6	B	$C_{91}H_{76}O_{36}$	1744.41164	6xPC+CH_2	1743.39686

Primarily, B-type natural PCs ranging from dimer to heptamer with every DP most likely underwent two subsequent electrophilic substitution reactions, as suggested in the literature. The acid-catalyzed cleavage of the interflavan-3-ol bond is theoretically possible but not likely to happen under these conditions as easily or quickly as substitution reactions. The reaction pathway of two subsequent electrophilic substitutions was also supported by the reaction kinetics.

Oligomeric PCs with one methylene-bridged linkage were tentatively identified and characterized from the products. B-type methylene-bridged PC dimers (Figure 15A) were

tentatively identified from prepMeOH 2 and prepAce 1 products. B-type natural (Figure 15B) and methylene-bridged (Figure 15C) PC trimers were tentatively identified in the prepMeOH 2 and prepAce 1 products. Additionally, B-type methylene-bridged PC tetramers (Figure 16A) and pentamers (Figure 16B) were tentatively identified in these two products. The higher the DP of the original PC, the more methylene-bridged linkages between the monomer units may exist in the formed semisynthetic PCs. In the present study, two methylene-bridged linkages in B-type PC pentamer (Figure 16C) were tentatively identified in the prepMeOH 2 product. Otherwise, two or more methylene-bridged linkage PCs were not observed in this data. The structures are tentative since there is no certainty of the place of the linkage. More thorough structural analyses are needed to confirm the actual structures.

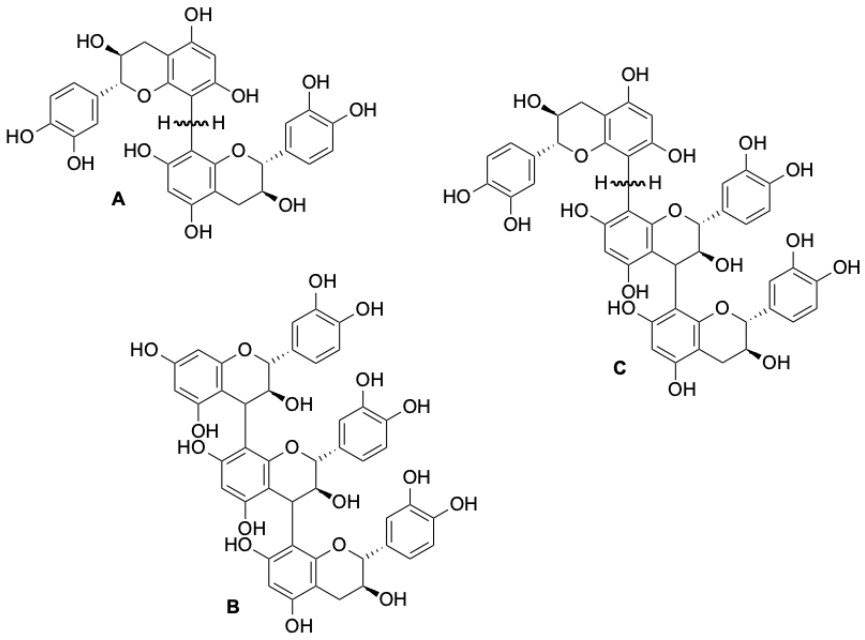

Figure 15. Tentative structures of B-type methylene-bridged procyanidin (PC) dimer (**A**), B-type C–C-bridged PC trimer (**B**), and methylene-bridged PC trimer (**C**).

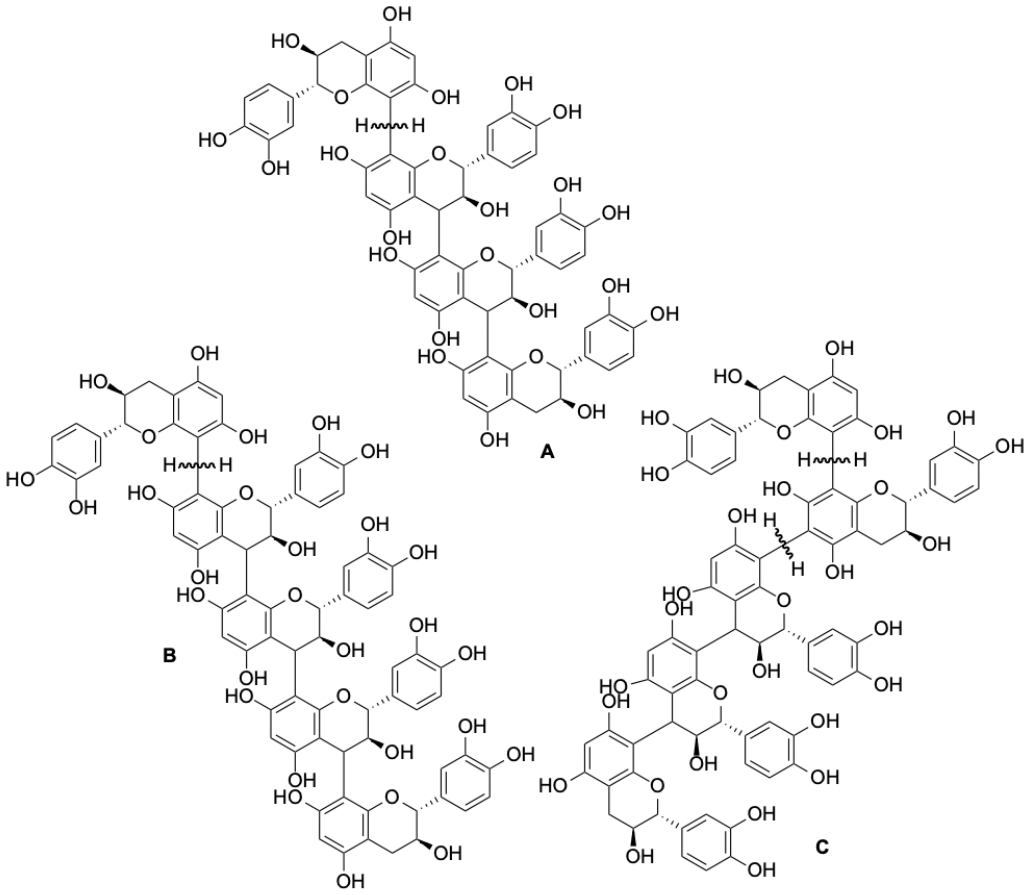

Figure 16. Tentative structures of B-type methylene-bridged procyanidin tetramer (**A**), pentamer (**B**), and pentamer with two methylene-bridged linkages (**C**).

Apart from prepMeOH 1 and 2 and prepAce 1 products, other products did not contain any soluble methylene-bridged PCs, although their starting materials contained PCs. Additionally, the unidentified compounds that were present in the prepMeOH 1 and its product were not present in other prepMeOH fractions or their products. PrepMeOH 3 was abundant in PC (Appendix 11A) but exhibited some additional mass peaks in the full scan MS spectrum. PC peaks vanished, while other mass peaks intensified in the full scan MS spectrum of the prepMeOH 3 product (Appendix 11B). The full scan MS spectrum of the prepMeOH 4 (Appendix 11C) resembled those of prepMeOH 1 and 2. However, no methylene-bridged PCs were observed in the most intense peaks of the full scan MS spectrum of the prepMeOH 4 product (Appendix 11D), indicating the precipitation of the formed methylene-bridged PCs.

The full scan MS spectrum of prepMeOH 5 displayed an intense peak at *m/z* 465 (Figure 17A), indicating the presence of taxifolin and taxifolin hexoside, which are found in pine bark[48]. In contrast, only minor PC mass peaks were present. PC mass peaks were absent in the full scan MS spectrum of prepMeOH 5 product, while the mass peaks corresponding to taxifolin and taxifolin hexoside were still present (Figure 17B). However, these results did not support the

observations: an exceptional increase in the mDPs and a decrease in the PC-% during the condensation reaction. The presence of taxifolin and its derivatives in the reaction solution explains the somehow strange mDPs and PC-% results due to the false detection of taxifolin mass peak at *m/z* 303 since the group-specific method recognizes the *m/z* 303 as the PD extension unit.

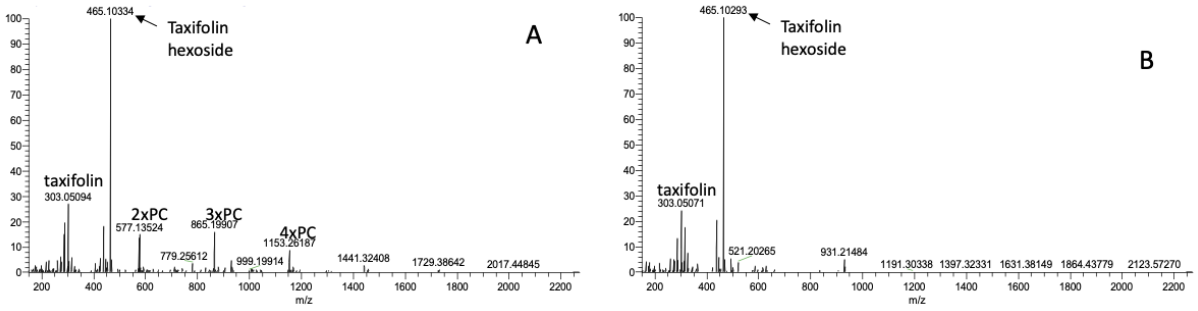

Figure 17. Full scan MS spectra in negative ionization of prepMeOH 5 (A) and its product (B) from the semisynthesis of pine bark procyanidins (PCs). Tentative identifications of the most abundant compounds are presented in the spectra.

The full scan MS spectra of prepMeOH 6–9 exhibited some PC mass peaks but were richer in quercetin derivatives (Appendices 12A, C and 13A, C). Moreover, all the full scan MS spectra of prepMeOH 6–9 products lacked the methylene-bridged PCs, as these likely precipitated as with prepMeOH 4 product, and were abundant in quercetin derivatives (Appendices 12B, D and 13B, D).

UV chromatograms at 280 nm of the prepMeOH products are shown in Appendix 14. A shift in RTs was observed as the fraction numbers increased, similar to previous observations with prepMeOH fractions. A distinct polymeric hump, formed during the condensation reaction, was evident in prepMeOH 1–4 products (Appendix 14A–D). The polymeric hump was absent in prepMeOH 5–7 products (Appendix 14E–G), with no significant formations compared to the starting materials, apart from a slight broadening of the hump. Meanwhile, prepMeOH 8–9 products (Appendix 14H–I) closely resembled the starting materials of those, indicating they remained chemically stable. These different behaviors of the prepMeOH fractions can be explained by the different PC compositions due to the chemically different PCs eluting at different RTs. The differences in PC concentrations might also impact the reaction behaviors as some fractions are rich in PC and others exhibit high concentrations of other flavonoids instead, such as taxifolin and quercetin derivatives. However, the disappearance of PC mass peaks could be a result of the precipitation of PCs or plainly the low concentration of PCs particularly in the prepMeOH 6–9.

Tentative identification and characterization of the most abundant compounds in prepMeOH 3–9 and their products are provided in Appendices 15 and 16. B-type natural PCs ranging from dimer to heptamer were present, similar to in prepMeOH 1 and 2, along with low molecular weight flavonoids such as taxifolin and quercetin derivatives. However, methylene-bridged PCs were absent in the prepMeOH 3–9 products. Instead, numerous tentatively identified low molecular weight flavonoids were detected. The most intense mass peaks of prepMeOH 5–8 were tentatively identified as low molecular weight flavonoids. There was no evidence of these low molecular weight flavonoids reacting with formaldehyde in the condensation reactions.

In addition to the detailed differences, a distinct pattern emerged in the series of mass peaks that follow one another (Figure 18). The first peak represents the natural B-type PC trimer. Following this is the B-type methylene-bridged PC trimer, which can coelute with the unidentified compound. A possible PC trimer with two methylene-bridged linkages continues the series. Additional $[M-2H]^{2-}$ ion mass peaks emerge among the mass peaks, corresponding to the higher DP PC oligomers and polymers. This situation becomes more complex as the DP increases, leading to significant overlap and considerable background noise in the full scan MS spectrum, complicating interpretation.

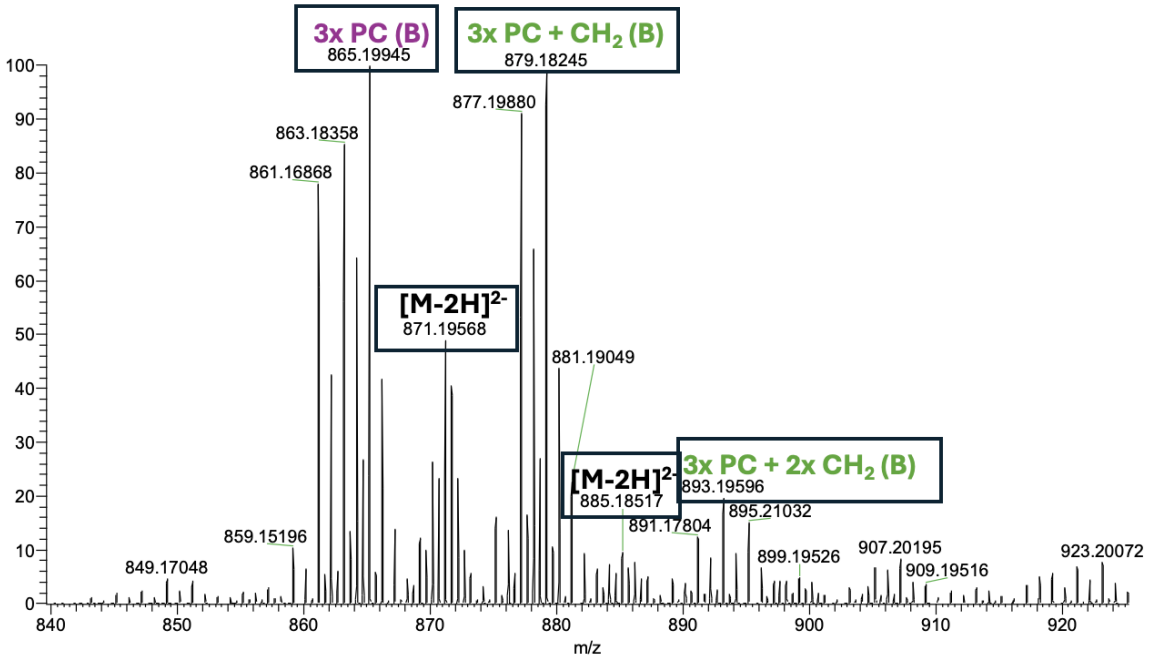

Figure 18. An illustration of the mass peak hump pattern of pine bark procyanidins (PC) in the full scan MS spectrum in negative electrospray ionization. Full scan MS spectrum of prepMeOH 1 illustrates the theoretical products of aldehyde condensation reactions. The natural B-type PC trimer initiates the series, followed by its methylene-bridged ($-CH_2-$) trimer. Next comes the B-type PC trimer with two methylene-bridged linkages. Additional $[M-2H]^{2-}$

ions corresponding to higher oligomers or polymers emerge amidst these mass peaks. This continues and becomes more complex as the degree of polymerization increases.

These identifications and characterizations focus on PCs and their products. However, several other compounds were found in the starting materials and later products that were not studied in more detail. These may result from the unknown reactions that occurred during the maceration time of many years of the pine bark before active extraction. It was also considered whether some of these compounds could be a result of contamination from the Sephadex LH-20 gel or the column used in preparative LC. However, there is no certainty what the actual originality of these compounds is.

Precipitation of the prep products in the condensation reactions

As mentioned earlier, prepMeOH 3–9 products lacked the PC mass peaks in the full scan MS spectra (Appendices 11–13, Figure 14). Suggested explanations were the precipitation of the formed high DP methylene-bridged PCs or the low concentration of PCs in the prepMeOH 3–9 in the beginning.

Thus, the absence of the PC peaks in the full scan MS spectra of prepMeOH 3–9 products could be attributed to precipitation during the condensation reaction. The precipitates were likely higher DP methylene-bridged PC oligomers and polymers. These higher DP methylene-bridged PC oligomers and polymers likely precipitated because they were not soluble in the MeOH/water (15/85, v/v) reaction solution as those would need more concentrated organic solvent to stay in liquid form. However, as observed with the precipitates, even the most common pure organic solvents could not dissolve the precipitates. Therefore, even more rough conditions are needed to dissolve the precipitates due to their high DP polymeric features. Instead, primarily quercetin derivatives, which concentrated during the reactions, were abundant in the reaction solutions at 3.5 h time points.

A similar phenomenon was observed with prepAce fractions. In five of the seven samples, the reaction products completely precipitated out of the reaction solution. The full scan MS spectra of prepAce 1 (Figure 14A) and 2–7 (Appendix 17) resembled those of prepMeOH 1 and 2, except for the presence of additional doubly charged ions positioned among the PC oligomers, from trimer to hexamer. These doubly charged ions indicated the presence of higher DP polymeric PCs compared to the prepMeOH fractions. The higher DP polymeric PCs likely formed methylene-bridged PC polymers during the reaction. The strong

hydrophobicity and need for pure organic solvents or even rougher conditions for these formed products to remain in the reaction solutions are expected to explain the strong precipitation.

The masses of the soluble prepMeOH and prepAce products and the precipitated products are shown in Figure 19. Only prepMeOH 1 and prepAce 1 products did not form any precipitate, while prepAce 2–6 products completely precipitated out of the reaction solutions. PrepAce 7 product yielded so little product that it could be included in the fractions that completely precipitated. PrepMeOH 2–9 products formed more precipitates than final products, but the yields of the final products were still sufficient for analyses. The yield of the precipitates compared to final products for prepMeOH 3 to 7 exceeded 90%. For the other fractions, this yield was significantly lower. The fractions that produced over 90% precipitate were those with the highest mDPs. Additionally, precipitation was more pronounced in prepAce fractions compared to prepMeOH fractions, possibly due to the higher mDPs.

In conclusion, high mDP prep fractions tend to yield more precipitates than final products, possibly due to the formation and precipitation of the high DP methylene-bridged PCs. At the same time, lower mDP prep fractions tend to form methylene-bridged PCs that remain soluble in the reaction solutions. Additionally, the PC purity and the abundance of other flavonoids in the prep fractions have an impact on the compound compositions of the products. However, it cannot be confirmed whether the precipitation or the overall low concentration of PCs caused the disappearance of the PC mass peaks in some products. Still, as the prepAce fractions were almost entirely composed of PCs and most of them fully precipitated in the reactions, it proves that PCs react and form precipitates that are composed of methylene-bridged PC oligomers and polymers. Therefore, it can be said that also, in the case of prepMeOH fractions, the precipitates are composed of methylene-bridged PCs that are formed in the reactions.

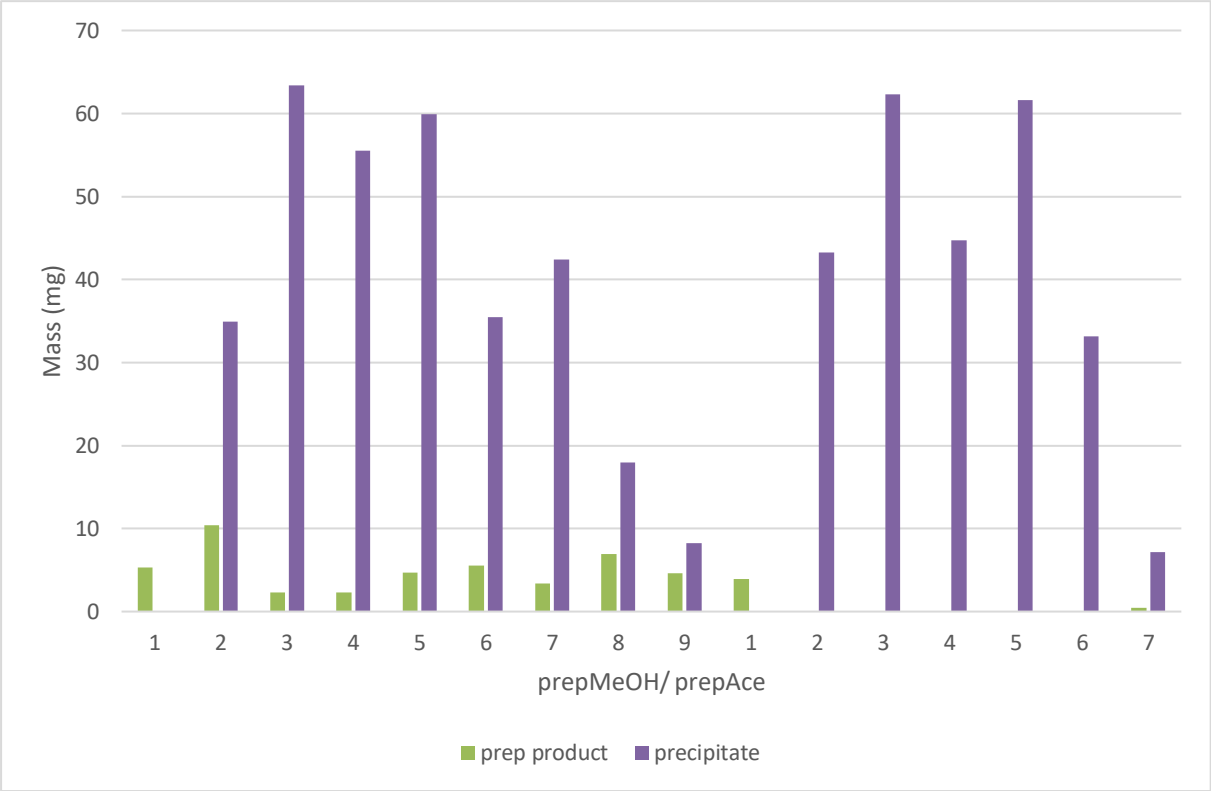

Figure 19. Masses (mg) of the freeze-dried prepMeOH and prepAce liquid phase products and the precipitated products from the semisynthesis of pine bark procyanidins.

Analyzing the precipitates was challenging since they were insoluble in all tested solvents (DMSO, MeOH, ACN, and acetone). The precipitates were also analyzed using MALDI-TOF-MS, but these results did not yield any better results. MALDI results did not provide additional information about the compounds in the precipitates or their DPs even though the precipitates dissolved partly to the solvent used but not enough to obtain clear spectra. This also indicated that the expectedly high DP products in the precipitates are unlikely to serve as potential drug candidates due to their expected polymeric structure and insolubility in common solvents. Furthermore, as the DP rises, a greater number of isomers are present, making the data more intricate and the mass peaks less clear for analysis. On the other hand, lower mDP PCs can be extracted with EtOH or EtOH/water solvent which makes them good candidates for industrial use. It is unnecessary to use rough solvents to extract high DP PCs due to their final products not applying to pharmaceutical applications well.

Overall, after evaluating the semisynthesis reactions and results, high mDP prep fractions may not be ideal starting materials due to the formation of insoluble precipitates. Additionally, high mDP prep fractions seem to react quite vigorously. The reaction time for particularly prepAce fractions was too long, resulting in the precipitation of all the compounds, with no further information obtained about the final products. However, the lower mDP prep

fractions offered promising results. Optimizing the reaction time and conditions for the lower mDP prep fractions, guided by a thorough understanding of the raw material extracted from pine bark and its chemical properties, pine bark could serve as a potential starting material for new drugs.

4.4 Solid phase extraction of reaction product

The main purpose of SPE was to eliminate formaldehyde while also obtaining more information about the elution profiles of formed products with different organic solvent compositions. It was proposed that formaldehyde would elute in the water fractions. This was necessary to prevent the reaction from continuing and forming a precipitate due to the presence of formaldehyde, which would interfere with the analysis equipment. The hypothesis was validated by adding epicatechin to the SPE zero and water fractions and maintaining them at 45 °C for an hour. The results indicated that a reaction occurred in the initial water fractions as the SPE zero fraction displayed the epicatechin peak (Appendix 18A), while the hour reaction sample exhibited four additional peaks following the epicatechin peak (Appendix 18B). This confirmed that SPE could effectively be utilized to eliminate formaldehyde in the SPE zero and first water fractions. The latest SPE water fractions did not react with epicatechin, which indicated the absence of formaldehyde.

The SPE fractions of prepMeOH 2–5 products were analyzed individually. A clear pattern emerged with all four products. Nothing significant eluted in the SPE zero or water fractions, while some low molecular weight compounds eluted in the MeOH/water (10/90, v/v) fractions (Figure 20A–C). The chromatographic hump formed by the products (Figure 20D), consistently eluted with the first fraction of MeOH/water (50/50, v/v). With prepMeOH 2, this hump also eluted with the pure MeOH fraction 1 (Figure 20G), and remnants of it remained with pure MeOH fractions 2–4 (Figure 20H–J). Distinct mass peaks from monomer to heptamer were observed in the full scan MS spectra of each SPE MeOH fraction within.

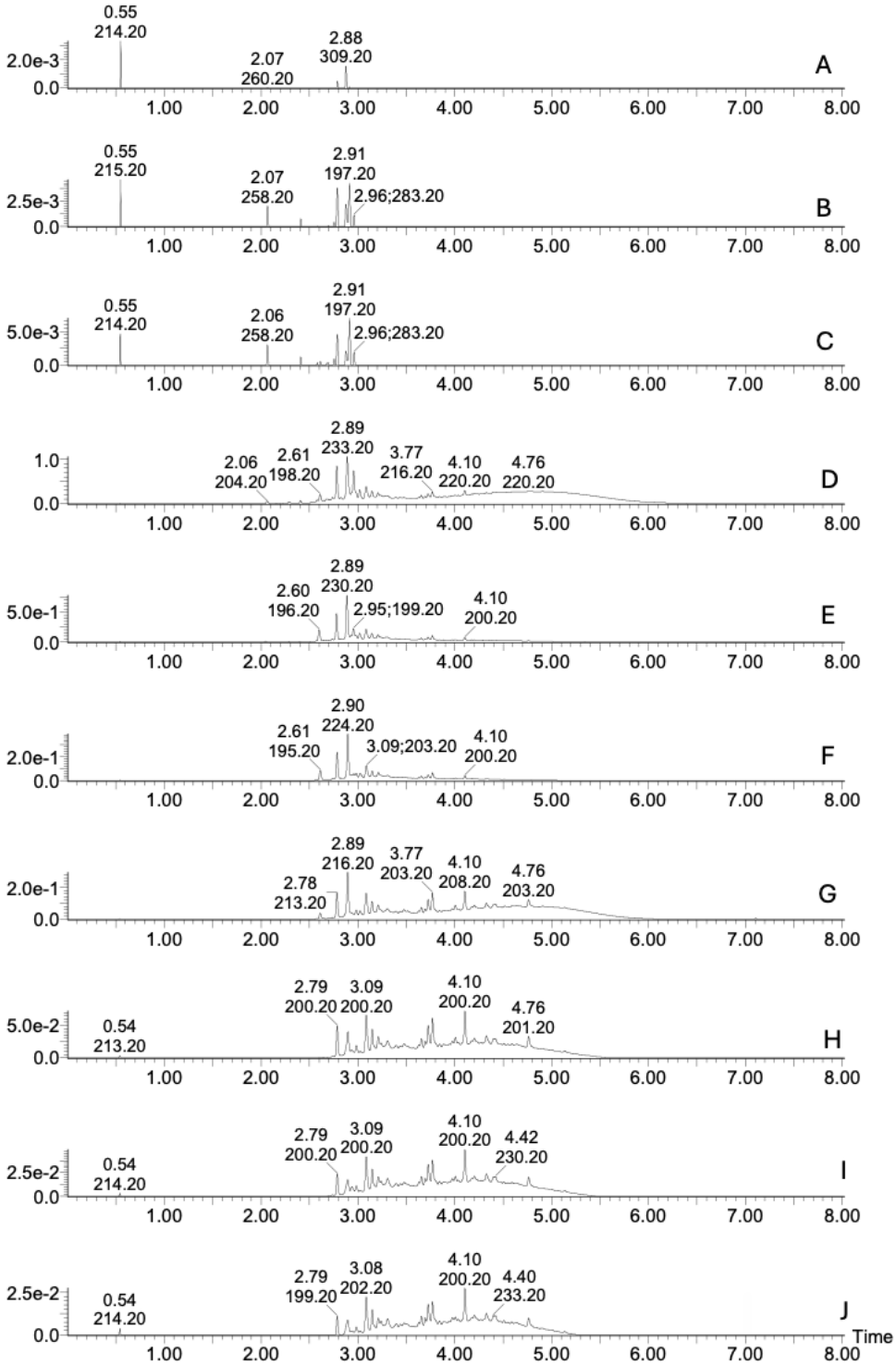

Figure 20. UV chromatograms at 280 nm of solid phase extraction (SPE) fractions from prepMeOH 2 product. The solvents used for SPE were MeOH/water (10/90, v/v) (A–C), MeOH/water (50/50, v/v) (D–F), and pure MeOH (G–J).

The hump formed during the condensation reactions of prepMeOH 3–5 eluted only with the first fraction of MeOH/water (50/50, v/v). Based on the UV chromatogram responses, the SPE fractions of prepMeOH 3–4 products contained more myricetin and quercetin derivatives than

PC. This was confirmed by the full scan MS spectra (Appendices 19 and 20). A minor PC response was observed with the hump formed in prepMeOH 5 product. Otherwise, only mass peaks tentatively identified as taxifolin and taxifolin hexoside were present in the full scan MS spectra of all the SPE fractions. This observation further confirmed the false increasing effect on mDP and decreasing effect on PC-% of taxifolin to the results of prepMeOH 5 product.

The PC-% of the total PA content and mDPs for all SPE fractions of prepMeOH 2–5 products are presented in Table 10. The PC-% of MeOH fractions of the prepMeOH 2–4 products were quite stable, but considerable variation in the percentages was observed in the MeOH fractions of prepMeOH 5 product, in which a decrease was noted compared to the others. The mDPs of the SPE fractions remained consistent with prepMeOH 2–4 products, while those increased with the pure MeOH fractions 1–2 of prepMeOH 5 product.

Table 10. Procyanidin (PC) percentages and mean degrees of polymerization (mDPs) for various solid phase extraction (SPE) fractions of prepMeOH 2–5 products obtained from semisynthesis of pine bark PCs. Fr = fraction.

	MeOH fr. 2		MeOH fr. 3		MeOH fr. 4		MeOH fr. 5	
SPE fractions	PC (%)	mDP	PC (%)	mDP	PC (%)	mDP	PC (%)	mDP
50% MeOH fr.1	98	3.1	97	3.8	98	3.6	92	4.5
50% MeOH fr. 2	98	2.5	92	2.8	96	2.5	65	5.8
50% MeOH fr. 3	99	2.3	94	2.5	95	2.6	53	8.1
100% MeOH fr. 1	99	2.8	98	2.8	95	3.3	47	13.8
100% MeOH fr. 2	99	2.8	98	2.4	95	2.6	50	12.2
100% MeOH fr. 3	99	2.8	99	2.4	98	2.4	71	6.6
100% MeOH fr. 4	99	2.8	98	2.4	98	2.4	84	4.4
100% MeOH fr. 5	–	–	99	2.4	99	2.4	87	4.0

The decrease in the PC-% of prepMeOH 5 product suggested strong precipitation of PCs in the sample with increasing mDP. The increase in mDPs and decrease in PC-% occurred in the same SPE fractions of prepMeOH 5 product. However, considering the false effects of taxifolin on mDPs and PC-%, the drop in PC-% in SPE fractions of prepMeOH 5 product should not be considered. The effect of low PC concentration and high concentration of other flavonoids remains unknown in the case of the reaction behavior. However, it can be said that the presence of taxifolin is problematic, considering the use of a group-specific method to determine mDPs and PC-%. Additionally, the possible precipitation of PCs and concentration of taxifolin or its derivatives decreases the PC-% and increases the mDPs dramatically due to the false positives in the group-specific method.

The SPE fractions of prepMeOH 1 and 6–9 products and prepAce 1–7 products were pooled immediately after the fractionation and removal of the formaldehyde. The 500 mg cartridge effectively contained all the compounds of the prepMeOH products. However, two prepAce products that remained in the liquid phase caused some problems. The SPE zero fractions of prepMeOH products were clear in color. In contrast, the SPE zero fractions of prepAce products were very yellow, suggesting that the cartridge might not have effectively retained potentially high DP PCs. Nevertheless, something remained attached to the cartridge material, as indicated by the color of the MeOH/water (50/50, v/v) and pure MeOH fractions. These SPE zero fractions were freeze-dried for further investigation.

The color indication of the SPE zero fraction of prepAce 1 product was confirmed accurate based on the analysis results (Figure 21D). The UV chromatograms of prepAce 1 (Figure 21A), 3.5 h sample (Figure 21B), and its final product (Figure 21C) showed similar UV peaks before the chromatographic hump. However, the shapes and RTs of the humps varied among these three samples. The UV chromatogram of the SPE zero fraction (Figure 21D) differed from the others (Figure 21A–C), presenting a more even chromatographic hump that indicated the presence of higher DP polymers. Additionally, according to the group-specific responses, the SPE zero fraction was pure in PC. This also supported the notion that the cartridge could only retain lower DP oligomers, not higher DP polymers. The issue was that formaldehyde was still present in the SPE zero fraction, which made the fraction unstable at room temperature and able to react forward. However, the final product may come out in two parts: the SPE zero fraction (Figure 21D) lets the hydrophilic PCs out, and the cartridge holds the rest (Figure 21C) that are hydrophobic and need the organic solvent to be extracted. This idea was supported by the combination of the UV chromatogram shapes of the product (Figure 21C) and the SPE zero fraction (Figure 21D) corresponding to the UV chromatogram shape of the 3.5 h sample (Figure 21B).

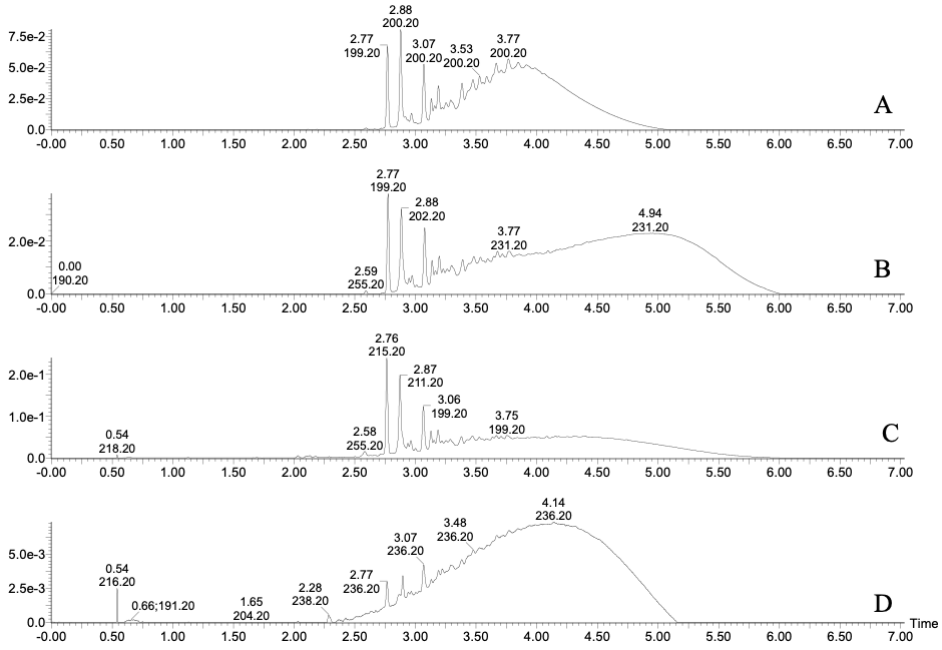

Figure 21. UV chromatograms at 280 nm of the prepAce 1 (A), its 3.5 h sample (B), final product (C), and SPE zero fraction (D) obtained from the semisynthesis of pine bark procyanidins.

4.5 Protein precipitation capacity

PPCs of prepMeOH and prepAce fractions along the prepMeOH products and prepAce 1 product were determined. The lower mDP prepMeOH fractions showed systematical results with enough replicates per sample, but the results of their products were quite surprising even though the number of replicates was sufficient as well. The higher mDP prepAce fractions showed systematical results except the prepAce 7. Only the PPC of prepAce 1 product was successfully determined. The PPCs varied greatly due to different factors to be discussed in more detail.

First, it was noted from the test runs that MeOH interfered with the precipitation reactions, even at low concentrations. Based on the absorbances and visual evaluation, the final concentration was determined to be 2.5 mg/mL, and the solvent water.

The change in the PPCs of prepMeOH fractions was characteristic of PCs.[49] Initially, the PPCs increased as the mDPs increased and decreased as the mDPs decreased, as reported in the literature. However, while the PPCs decreased as the mDPs decreased, they also decreased with increasing RTs. There is, however, no systematic connection established between RTs and PPCs, according to Leppä et al. (2020)[49]. Generally, the increasing RT means the elution of

higher DP polymers that at the certain point lose the PPCs due to the non-flexible larger structures. The PPCs for prepMeOH 3 to 5 were the highest, corresponding with the high mDPs of those fractions. However, the PPC of late RT prepMeOH 9 was lower than that of prepMeOH 1, even though they shared the same mDP. The PPC of prepMeOH 9 with decreasing mDP can be explained by the overall low concentration of PCs or the introduction of higher DP PC polymers, which cause a decrease in the mDP, due to the ionization and fragmentation challenges in MS, and PPC, due to the loss of structure's flexibility.

Figure 22 illustrates the differences between the prep fractions and their respective products. Only the prepMeOH 1 product showed increased PPC compared to the starting material. Other prepMeOH products exhibited lower PPCs than their corresponding starting materials. Nevertheless, prepMeOH 1 and 2 were very similar in their mass spectra and mDPs. They differed from each other by the mass peak intensity ratio of natural and methylene-bridged PCs. Additionally, unidentified compounds predominating in the prepMeOH 1 product instead of methylene-bridged PCs differentiated it from the prepMeOH 2 product. Methylene-bridged PCs were still expected to be present in the prepMeOH 1 product, as discussed earlier. This expectation was supported by the similar PPCs of prepMeOH 1 and 2 products (Figure 22).

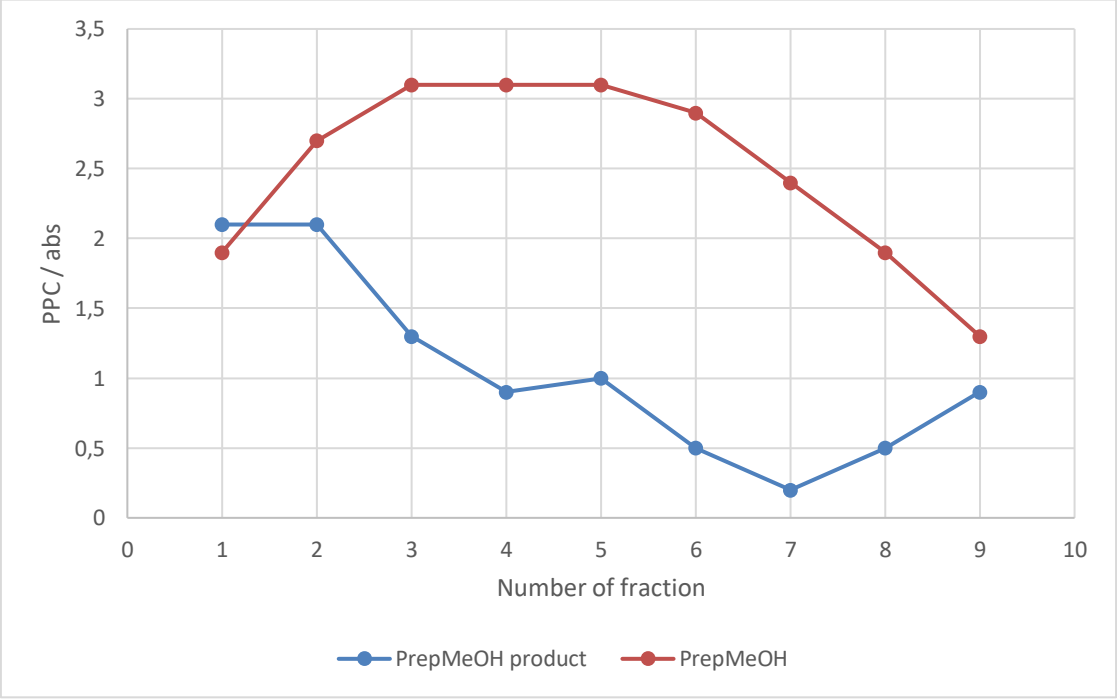

Figure 22. Protein precipitation capacity (PPC) results of prepMeOH fractions and their products from the semisynthesis of pine bark procyanidins.

The reported observation about the superior PPC of PC trimer compared to methylene-bridged PC dimer[38] can be noted from this data as prepMeOH 1 product exhibits only lower DP

methylene-bridged PCs or low DP unidentified compounds, and prepMeOH 2 exhibits slightly higher DP PCs compared to prepMeOH 1 (Figure 22). The PC-% stability, formation of no precipitate during the semisynthesis, and a low mDP of the prepMeOH 1 could be attributed to the increased PPC of its product compared to other fractions (Table 7). The slightly increased PPC of the prepMeOH 1 product also supported the assumption that methylene-bridged PCs were present in the product along with the unidentified compounds. On the other hand, the PPCs of prepMeOH 1 and 2 products were similar, but only the PPC of prepMeOH 2 was superior to those due to the expected presence of slightly higher DP PCs in the reaction solution. Therefore, the prepMeOH 1 and 2 products have a similar impact on the PPC.

The PPCs of prepMeOH 3–9 products were quite low, likely due to the high concentration of taxifolin and quercetin derivatives in these products. The only plausible explanation was the precipitation of methylene-bridged PCs coupled with the increased concentrations of taxifolin and quercetin derivatives in the reaction solutions. The colors of the prepMeOH fractions became progressively more yellow with the increasing fraction number. Specifically, the colors of the prepMeOH 6–9 were significantly yellower than those of their products (Figure 23). This also affected the PPCs, as yellow light is absorbed at a wavelength of 414 nm, even though the impact of that was partly fixed by the control samples. However, the effect of the yellow color was not so substantial that the prepMeOH products would be preferable to the prepMeOH fractions, for example, approximately 0.5 versus 3.0. The PPCs of prepMeOH 1–5 were reliable because the colors of the products and prepMeOH fractions were nearly identical compared to the differences observed in prepMeOH 6–9.

There was a decrease in PC-% of other prep fractions and their products, all of which formed precipitates during the condensation reactions. As a result, the PPCs of the prepMeOH 3–9 products were inferior to those of the prepMeOH 1 and 2 products due to the loss of PCs in the precipitates and the concentration of taxifolin and quercetin derivatives in the product. However, the increase in PPCs observed for the prepMeOH 8 and 9 products – following a consistent decline in PPCs for the earlier products – could not be explained by their PC content alone. These two products had higher overall yields in a liquid phase and produced less precipitate compared to prepMeOH 2–7 products. This lower precipitate yield may account for the increased PPCs, as it suggests that a greater proportion of PCs remained in the final liquid reaction product. Overall, it is highly likely that the compounds exhibiting good PPC precipitated, while the less reactive PCs stayed soluble in the final products, which partly explains the decreasing PPCs of the products.

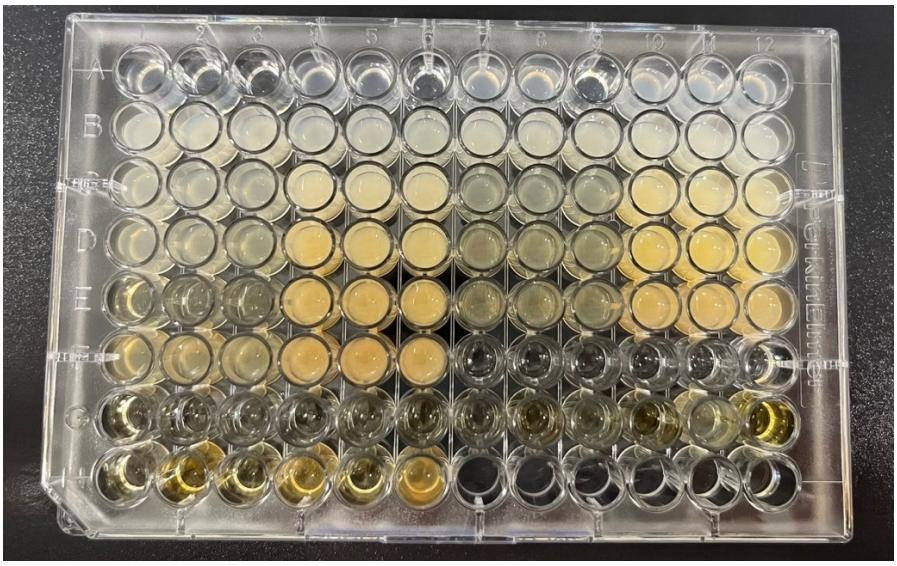

Figure 23. Image of a plate I from protein precipitation capacity measurements. Rows B–F include three parallel prepMeOH products from the semisynthesis of pine bark procyanidins and their three parallel corresponding prepMeOH fractions by increasing fraction number. Rows G–H contain one control sample for each product or prepMeOH fraction, arranged by increasing fraction number.

The change in PPCs of prepAce fractions was characteristic of PCs[49] (Figure 24) but did not follow the pattern as systematically as prepMeOH fractions. The PPCs for prepAce 2 and 3 were the highest, corresponding with the high mDPs of those fractions. Initially, the PPCs increased as the mDPs increased until prepAce 3 but decreased non-systemically as the mDPs did not decrease much. This could be explained by the solubility problems and the lack of parallel samples to confirm the results. However, the decrease in PPCs starting from prepAce 4 may be caused by the higher DP PCs eluting by the increasing RT. This could affect the PPCs as high DP PCs may not dissolve properly to water and their large structures lose the flexibility that is a key factor of binding to proteins. Additionally, the PPC of prepAce 7 did not fit the systematical results and, therefore, might be a result of the lack of parallel samples or a measurement error. However, a similar pattern was observed with the yellow colors of prepAce fractions. The color became more yellow as the fraction number increased (Figure 25).

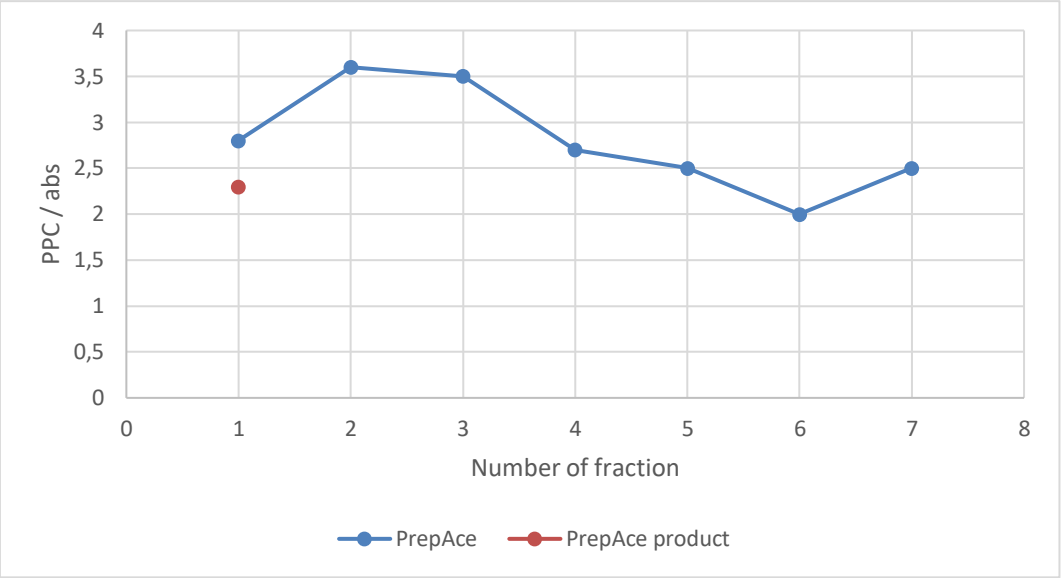

Figure 24. Protein precipitation capacity (PPC) results of prepAce fractions and product from the semisynthesis of pine bark procyanidins.

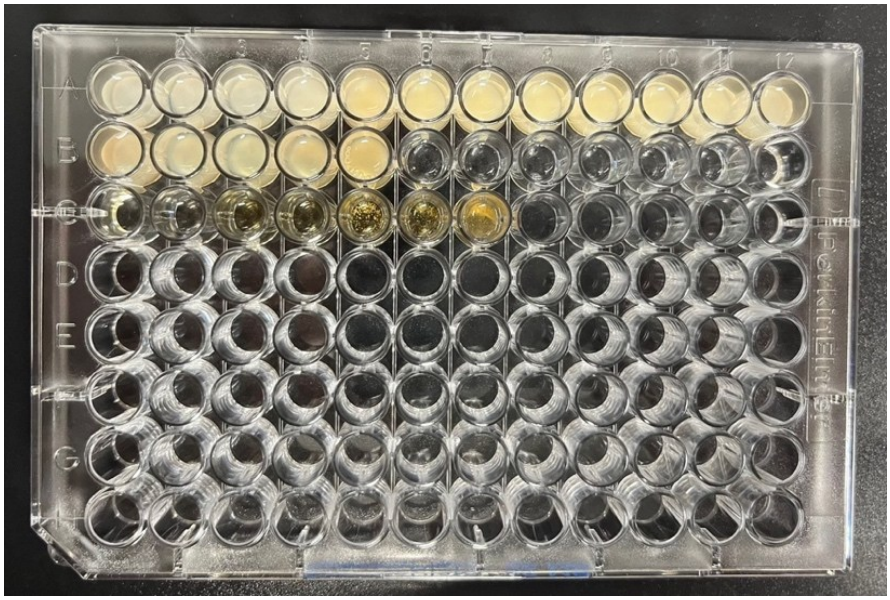

Figure 25. Image of a plate II from protein precipitation capacity measurements. Rows A–B include three or fewer parallel prepAce fractions and one prepAce product from the semisynthesis of pine bark procyanidins by the increasing fraction number. Row C contains one control sample for prepAce fraction or product, arranged by increasing fraction number.

The significant precipitation in the prepAce products presented challenges, and less information was available compared to the prepMeOH products. PrepAce 1 product did not fully precipitate, but the PPC decreased during the condensation reaction (Figure 24). Additionally, the PPCs of prepMeOH 2 (2.7) and prepAce 1 (2.8) were quite close; however, the PPC of prepAce 1 product (2.4) was slightly better than that of prepMeOH 2 product (2.1). This discrepancy could be attributed to the mDP differences (3 and 7). However, the presence of higher DP PCs in the

prepAce 1 product might cause solubility issues that impact the PPC decreasingly. Additionally, some of the PCs present in the 3.5 h sample of prepAce 1 product were lost in the SPE zero fraction. Therefore, the PPC of the prepAce 1 product is supposedly much better than the one presented since the PCs lost in the SPE zero fractions most likely would impact the PPC increasingly. Otherwise, no further conclusions could be drawn about the PPCs of the prepAce products.

These results defied all expectations as the products were anticipated to exhibit better PPCs compared to the prep fractions. However, the possibility of the products not being fully dissolvable to water is good to keep in mind when evaluating the PPCs. The main reason behind the worse PPCs of the products was the precipitation of PCs and the lack of understanding regarding the compounds in the precipitates and their PPCs. The cumulative effect of combining various oligomer and polymer compositions, along with their numerous isomers, instead of focusing on pure individual or well-characterized compounds, complicated the ability to identify the impact of specific structural features. Particularly, when features not studied in this thesis – for example, the *cis*/*trans* ratio of the monomer units or other features[49] – can influence the PPCs. Additionally, the other flavonoids remaining in the products played a role in the decreased PPCs, resulting in outcomes that were poorer than expected. All this complicated interpretation and made concluding challenging, as the PPCs are a result of the cumulative effect of all the compounds in the mixture.

Additionally, there was no previous study on the PPC of methylene-bridged higher DP oligomers or polymers. Good PPC is a desirable feature of a potential drug candidate considering its mechanism of action in the human body. Therefore, the PPCs of these products were studied. Methylene-bridged linkages have been shown to enhance the PPC with dimeric PCs, and the higher DP should also contribute to an increase in PPC up to a certain point. Based on these results, this expectation cannot be verified as the higher DP products most likely suffer from precipitation and dissolvability to water and therefore the PPCs cannot be fully trusted as such. Furthermore, the most abundant compounds are reported to be reliable for the PPCs[49], which in this case are complex mixtures of PC oligomers and polymers or other flavonoids. Nevertheless, an increase in PPC during the semisynthesis was observed with the low mDP and RT prepMeOH fraction as a starting material. Therefore, considering the potential for semisynthesizing more bioactive compounds to be used as potential drug candidates, low mDP and PC-pure fractions with low RT appear to be the most favorable options.

5 Conclusions

The reaction behavior of prepMeOH and prepAce fractions varied due to differences in RTs, mDPs, and PC purity. PrepMeOH 1 and 2 were almost entirely composed of PCs, whereas other fractions had additionally varying amounts of taxifolin and quercetin derivatives. PrepAce fractions were PC-rich and exhibited higher mDPs than prepMeOH fractions. Additionally, all the prep fractions contained lots of maceration products or contaminations, most of which were not identified or characterized in this study.

Elevated mDPs resulted in significant precipitation during the condensation reactions of the prepAce fractions, whereas the lowest mDP prepAce fraction did not completely precipitate. However, all the flavonoid-rich and PC-poor prepMeOH fractions caused precipitation of methylene-bridged PCs, concentrating the flavonoid derivatives in the reaction solution. In total, only three products contained methylene-bridged PCs.

The condensation reactions resulted in the coelution of natural and methylene-bridged PCs with different DPs, which increased the number of isomers, especially with high mDP prep fractions. This resulted in complex mixtures of PC oligomers and polymers in the products, which made the interpretation and the accurate characterization difficult.

High mDP prepAce fractions were unsuitable as starting materials for aldehyde condensation reactions under these conditions due to the quick formation of precipitates that could not be analytically studied due to the solubility issues. However, lower mDP prepMeOH fractions could benefit from optimizing reaction time and conditions to prevent the strong precipitation of the methylene-bridged PCs. Moreover, further separation of the prepMeOH fractions could assist in obtaining simpler and chemically well-characterized compounds for use as starting materials. Furthermore, recognizing that some fractions contain more flavonoids than PCs, a more detailed combination of the preparative LC fractions of the MeOH material would be advantageous for gathering only the pure, PC-rich fractions for use in the condensation reactions.

The PPC results represented a combination of various DP PCs and all their isomers that were present in the products. Although the increase in PPCs from PC dimer to methylene-bridged PC dimer has been documented, the impact of high DP methylene-bridged PCs on PPC remains unstudied and unpublished. Based on the results, the products of low mDP prep fractions showed an increase in PPC by introducing low mDP methylene-bridged PCs with the presence of natural PCs. While products of higher mDP prep fractions contain methylene-bridged PCs, the PPCs diminish compared to natural PCs which in this study can be explained

by the insolubility of higher DP PCs in water. Elevated DP leads to significant precipitation of methylene-bridged PCs and concentration of flavonoids, which also reduce the PPCs due to the decrease in the number of hydroxyl groups capable of hydrogen bonding. However, strong conclusions about the PPCs of the products cannot be drawn due to the solubility issues and the challenges in analyzing the precipitates. Furthermore, there is a lack of information on the precipitates, but it does not suggest a positive indication of the precipitates that dissolve poorly in common solvents.

Altogether, the study demonstrated that the valorization of industrial side streams for pharmaceutical applications holds promise and warrants further investigation. High DP PCs are unlikely to be effective or promising drug candidates due to their poor solubility in common solvents. Therefore, the use of harsh solvents to extract high DP PCs is unnecessary, as the resulting products are not suitable for pharmaceutical applications. In contrast, low DP PCs show promise as potential drug candidates, owing to their good solubility in EtOH or even EtOH/water mixtures, enabling cost-effective and environmentally friendly extraction processes. Furthermore, these compounds may exhibit improved PPC compared to natural PCs, which could also be beneficial for the drug's mechanism of action. Moreover, such industrial approaches align with the principles of the circular economy and contribute to sustainable development – both of which are key global priorities.

A more detailed chromatographic separation of the products is required to clarify the PPCs of specific DP methylene-bridged PCs. Addressing the challenges related to the solubility of precipitates would also help in understanding the reasons behind the significant precipitation, which currently remains speculative regarding the formation of higher DP polymeric PCs due to difficulties in properly analyzing the precipitates. For compounds with multiple methylene-bridged linkages, a more thorough structural analysis is necessary to confirm the places of the linkages.

6 References

1. Engström, M. T. *et al.* Rapid Qualitative and Quantitative Analyses of Proanthocyanidin Oligomers and Polymers by UPLC-MS/MS. *J Agric Food Chem* **62**, 3390–3399 (2014).
2. Chung, J. E., Kurisawa, M., Kim, Y. J., Uyama, H. & Kobayashi, S. Amplification of Antioxidant Activity of Catechin by Polycondensation with Acetaldehyde. *Biomacromolecules* vol. 5 113–118 Preprint at https://doi.org/10.1021/bm0342436 (2004).
3. Quideau, S., Deffieux, D., Douat-Casassus, C. & Pouységu, L. Plant Polyphenols: Chemical Properties, Biological Activities, and Synthesis. *Angewandte Chemie - International Edition* vol. 50 586–621 Preprint at https://doi.org/10.1002/anie.201000044 (2011).
4. Es-Safi, N. E., Fulcrand, H., Cheynier, V. & Moutounet, M. Competition between (+)-Catechin and (-)-Epicatechin in Acetaldehyde- Induced Polymerization of Flavanols. *J Agric Food Chem* **47**, 2088–2095 (1999).
5. Uyama, H. *Synthesis and Applications of Catechin-Aldehyde Polycondensates*. (2006).
6. Zeller, W. E. Activity, purification, and analysis of condensed tannins: Current state of affairs and future endeavors. *Crop Sci* **59**, 886–904 (2019).
7. Lin, L. Z., Sun, J., Chen, P., Monagas, M. J. & Harnly, J. M. UHPLC-PDA-ESI/HRMSn profiling method to identify and quantify oligomeric proanthocyanidins in plant products. *J Agric Food Chem* **62**, 9387–9400 (2014).
8. Aron, P. M. & Kennedy, J. A. Flavan-3-ols: Nature, occurrence and biological activity. *Molecular Nutrition and Food Research* vol. 52 79–104 Preprint at https://doi.org/10.1002/mnfr.200700137 (2008).
9. Czochanska, Z., Foo, L. Y., Newman, R. H. & Porter, L. J. *Polymeric Proanthocyanidins. Stereochemistry, Structural Units, and Molecular Weight*. vol. 9 (1980).
10. Eld, C. W. *et al. Kinetics of Polymerization of (+)-Catechin with Formaldehyde[1]. J. Chem. Soc., Perkin Trans. 1* vol. 47 https://pubs.acs.org/sharingguidelines (1982).
11. Levdanskiy, V. A., Korol'kova, I. V., Levdanskiy, A. V. & Kuznetsov, B. N. Isolation and Study of Proanthocyanidins from Bark of Pine *Pinus sylvestris* L. *Russ J Bioorg Chem* **47**, 1445–1450 (2021).
12. Saito, A., Nakajima, N., Tanaka, A. & Ubukata, M. *Synthetic Studies of Proanthocyanidins. Part 2: Stereoselective Gram-Scale Synthesis of Procyanidin-B3*. (2002).
13. Karonen, M., Loponen, J., Ossipov, V. & Pihlaja, K. Analysis of procyanidins in pine bark with reversed-phase and normal-phase high-performance liquid chromatography-electrospray ionization mass spectrometry. *Anal Chim Acta* **522**, 105–112 (2004).
14. Leppä, M. M., Karonen, M., Tähtinen, P., Engström, M. T. & Salminen, J. P. Isolation of chemically well-defined semipreparative liquid chromatography fractions from complex mixtures of proanthocyanidin oligomers and polymers. *J Chromatogr A* **1576**, 67–79 (2018).
15. Hamada, Y. *et al.* Structure-Activity Relationship of Oligomeric Flavan-3-ols: Importance of the Upper-Unit B-ring Hydroxyl Groups in the Dimeric Structure for Strong Activities. *Molecules* **20**, 18870–18885 (2015).
16. González-Quilen, C. *et al.* Grape-seed proanthocyanidins are able to reverse intestinal dysfunction and metabolic endotoxemia induced by a cafeteria diet in wistar rats. *Nutrients* **11**, (2019).

17. Liu, W. *et al.* Grape seed proanthocyanidin extract ameliorates inflammation and adiposity by modulating gut microbiota in high-fat diet mice. *Mol Nutr Food Res* **61**, (2017).
18. Spencer, J. P. E. *et al.* Epicatechin is the Primary Bioavailable Form of the Procyanidin Dimers B2 and B5 after Transfer across the Small Intestine. *Biochem Biophys Res Commun* **285**, 588–593 (2001).
19. Baba, S., Osakabe, N., Natsume, M. & Terao, J. *ABSORPTION AND URINARY EXCRETION OF PROCYANIDIN B2 [EPICATECHIN-(4-8)-EPICATECHIN] IN RATS*. (2002).
20. Donovan, J. L. *et al. Human Nutrition and Metabolism Catechin Is Present as Metabolites in Human Plasma after Consumption of Red Wine*. *J. Nutr* vol. 129 (1999).
21. Rios, L. Y. *et al. Cocoa Procyanidins Are Stable during Gastric Transit in Humans*. *Am J Clin Nutr* vol. 76 (2002).
22. Tsang, C. *et al.* The absorption, metabolism and excretion of flavan-3-ols and procyanidins following the ingestion of a grape seed extract by rats. *British Journal of Nutrition* **94**, 170–181 (2005).
23. Choy, Y. Y. *et al.* Phenolic metabolites and substantial microbiome changes in pig feces by ingesting grape seed proanthocyanidins. *Food Funct* **5**, 2298–2308 (2014).
24. Clifford, M. N. Diet-derived phenols in plasma and tissues and their implications for health. *Planta Medica* vol. 70 1103–1114 Preprint at https://doi.org/10.1055/s-2004-835835 (2004).
25. García-Ramírez, B. *et al.* Tetramethylated Dimeric Procyanidins Are Detected in Rat Plasma and Liver Early after Oral Administration of Synthetic Oligomeric Procyanidins. *J Agric Food Chem* **54**, 2543–2551 (2006).
26. Baxter, N. J., Lilley, T. H., Haslam, E. & Williamson, M. P. *Multiple Interactions between Polyphenols and a Salivary Proline-Rich Protein Repeat Result in Complexation and Precipitation †*. https://pubs.acs.org/sharingguidelines (1997).
27. Cala, O. *et al.* NMR and molecular modeling of wine tannins binding to saliva proteins: Revisiting astringency from molecular and colloidal prospects. *FASEB Journal* **24**, 4281–4290 (2010).
28. Hagerman, A. E., Rice, M. E. & Ritchard, N. T. *Mechanisms of Protein Precipitation for Two Tannins, Pentagalloyl Glucose and Epicatechin 16 (4f8) Catechin (Procyanidin)*. https://pubs.acs.org/sharingguidelines (1998).
29. Tesseromatis, C. & Alevizou, A. *The Role of the Protein-Binding on the Mode of Drug Action as Well the Interactions with Other Drugs*. *EUROPEAN JOURNAL OF DRUG METABOLISM AND PHARMACOKINETICS* vol. 33 (2008).
30. Schmidt, S. *et al.* Effect of protein binding on the pharmacological activity of highly bound antibiotics. *Antimicrob Agents Chemother* **52**, 3994–4000 (2008).
31. Fulcrand, H. *et al.* Direct mass spectrometry approaches to characterize polyphenol composition of complex samples. *Phytochemistry* **69**, 3131–3138 (2008).
32. Hümmer, W. & Schreier, P. Analysis of proanthocyanidins. *Molecular Nutrition and Food Research* vol. 52 1381–1398 Preprint at https://doi.org/10.1002/mnfr.200700463 (2008).
33. Chai, W. M. *et al.* NMR, HPLC-ESI-MS, and MALDI-TOF MS analysis of condensed tannins from *Delonix regia* (Bojer ex Hook.) Raf. and their bioactivities. *J Agric Food Chem* **60**, 5013–5022 (2012).
34. Hellström, J., Sinkkonen, J., Karonen, M. & Mattila, P. Isolation and structure elucidation of procyanidin oligomers from Saskatoon berries (*Amelanchier alnifolia*). *J Agric Food Chem* **55**, 157–164 (2007).

35. Gu, L. *et al.* Liquid chromatographic/electrospray ionization mass spectrometric studies of proanthocyanidins in foods. *Journal of Mass Spectrometry* **38**, 1272–1280 (2003).
36. Karonen, M., Imran, I. Bin, Engström, M. T. & Salminen, J. P. Characterization of natural and alkaline-oxidized proanthocyanidins in plant extracts by ultrahigh-resolution UHPLC-MS/MS. *Molecules* **26**, (2021).
37. Sillanpää, M. *et al.* Exploring the Interactions between Plant Proanthocyanidins and Thiabendazole: Insights from Isothermal Titration Calorimetry. *Molecules* **29**, (2024).
38. Sprygin, V. G. & Kushnerova, N. F. Cranberry: A new source of oligomeric proanthocyanidins. *Pharm Chem J* **38**, 100–104 (2004).
39. Drinkine, J., Lopes, P., Kennedy, J. A., Teissedre, P. L. & Saucier, C. Analysis of Ethylidene-Bridged Flavan-3-ols in Wine. *J Agric Food Chem* **55**, 1109–1116 (2007).
40. Sáez, V. *et al.* The presence of sulfonated oligomeric and polymeric procyanidins in red wines impacts the estimated mean degree of polymerisation of condensed tannins by phloroglucinolysis. *OENO One* **59**, (2025).
41. Laitila, J. E., Tähtinen, P. T., Karonen, M. & Salminen, J. P. Red Wine Inspired Chemistry: Hemisynthesis of Procyanidin Analogs and Determination of Their Protein Precipitation Capacity, Octanol-Water Partition, and Stability in Phosphate-Buffered Saline. *J Agric Food Chem* **71**, 19832–19844 (2023).
42. Weber, F. & Winterhalter, P. Synthesis and structure elucidation of ethyliden-linked anthocyanin - Flavan-3-ol oligomers. *Food Research International* **65**, 69–76 (2014).
43. Es-Safi, N. E., Fulcrand, H., Cheynier, V. & Moutounet, M. Studies on the Acetaldehyde-Induced Condensation of (-)-Epicatechin and Malvidin 3-O-Glucoside in a Model Solution System. *J Agric Food Chem* **47**, 2096–2102 (1999).
44. Ministry of Agriculture and Forestry of Finland. Green bioeconomy. https://mmm.fi/en/forests/use-of-wood/green-bioeconomy (2025). Accessed 23 Feb 2025.
45. Jerez, M., Sineiro, J. & Nuñez, M. J. Fractionation of pine bark extracts: Selecting procyanidins. *European Food Research and Technology* **229**, 651–659 (2009).
46. Engström, M. T., Pälijärvi, M. & Salminen, J. P. Rapid fingerprint analysis of plant extracts for ellagitannins, gallic acid, and quinic acid derivatives and quercetin-, kaempferol- and myricetin-based flavonol glycosides by UPLC-QqQ-MS/MS. *J Agric Food Chem* **63**, 4068–4079 (2015).
47. Engström, M. T. *et al.* Structural Features of Hydrolyzable Tannins Determine Their Ability to Form Insoluble Complexes with Bovine Serum Albumin. *J Agric Food Chem* **67**, 6798–6808 (2019).
48. Cretu, E. *et al. In vitro* study on the antioxidant activity of a polyphenol-rich extract from *pinus brutia* bark and its fractions. *J Med Food* **16**, 984–991 (2013).
49. Leppä, M. M., Laitila, J. E. & Salminen, J. P. Distribution of Protein Precipitation Capacity within Variable Proanthocyanidin Fingerprints. *Molecules* **25**, (2020).

7 Appendices

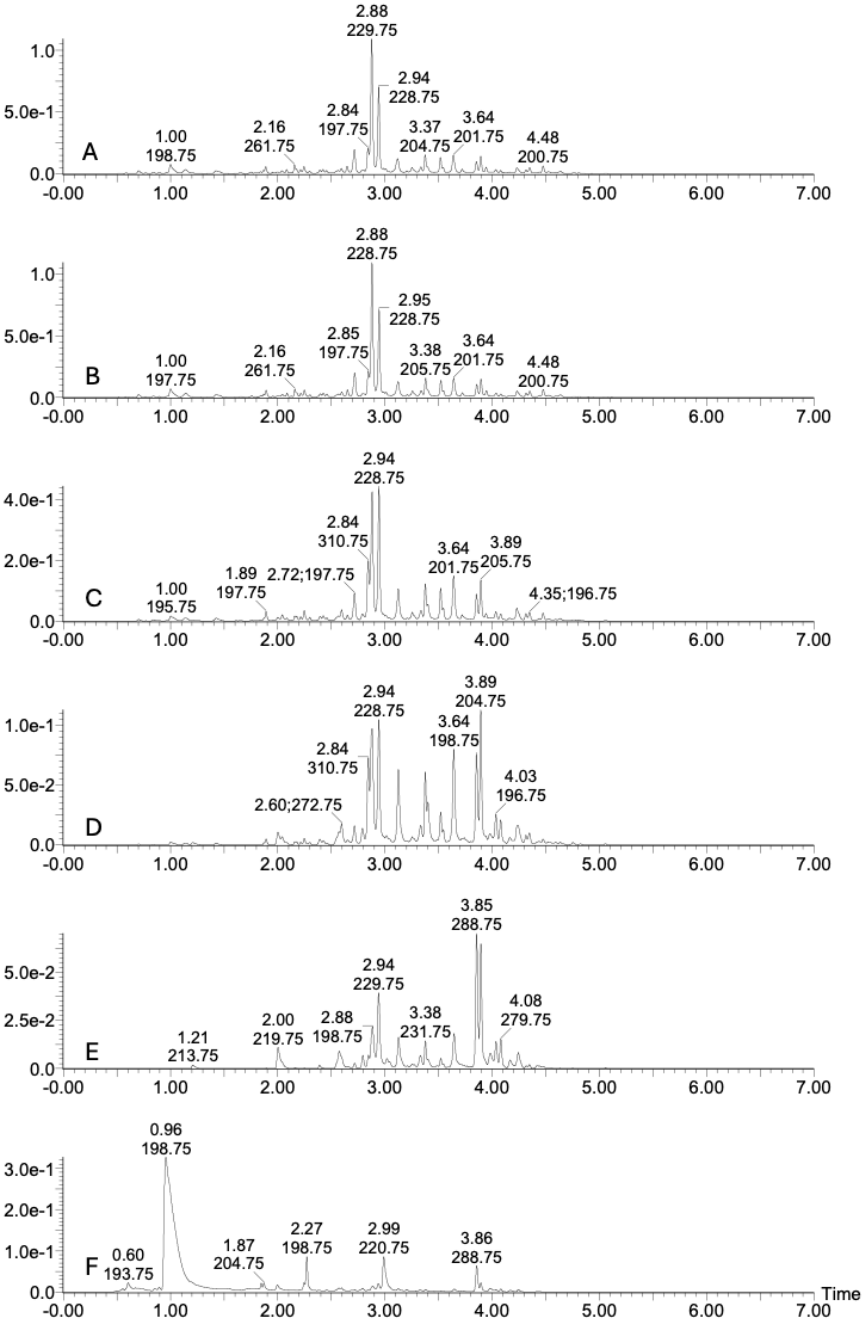

Appendix 1. UV chromatograms at 280 nm of Sephadex LH-20 zero (A) and water fractions 1–5 (B–F) of pine bark extract.

Appendix 2. Mean degrees of polymerization (mDPs) and procyanidin (PC) percentages of MeOH or acetone fractions from preparative (prep) liquid chromatography obtained from pine bark PCs.

Purified fraction of acetone prep	mDP	PC (%)	Purified fraction of MeOH prep	mDP	PC (%)
10	5.7	98.1	3	3.7	99.5
13	6.0	99.1	6	3.5	99.7
16	5.7	99.6	9	3.0	99.3
19	5.3	99.7	12	3.2	98.1
22	5.1	99.5	15	4.3	98.7
25	6.2	99.6	18	4.5	99.1
28	6.9	99.6	21	4.4	99.5
31	9.5	99.6	24	3.3	99.3
34	10.4	99.6	27	3.2	99.2
37	10.1	99.6	30	3.2	98.6
40	9.7	99.6	33	3.3	98.9
43	9.2	99.5	36	3.9	99.1
46	9.7	99.5	39	4.8	98.9
49	9.9	99.3	42	4.9	99.1
52	9.7	99.2	45	4.6	99.0
55	10.1	98.8	48	4.6	99.2
58	9.9	98.7	51	4.9	99.0
61	9.0	99.2	54	6.0	96.1
64	9.1	99.5	57	6.9	93.0
67	9.0	99.5	60	7.0	91.7
70	8.9	99.5	63	8.7	86.2
73	8.5	99.6	66	7.3	89.9
76	8.6	99.7	69	5.1	96.4
79	8.2	99.6	72	4.4	98.5
82	8.6	99.6	75	4.2	98.9
85	9.3	99.7	78	4.1	98.9
88	9.2	99.7	81	4.0	98.8
91	9.6	99.6	84	3.9	98.8
94	10.3	99.6	87	3.9	98.5
97	9.8	99.7	90	3.8	98.6
100	10.3	99.6	93	3.9	98.3
103	10.2	99.5	96	3.9	98.1
106	10.2	99.4	99	4.0	98.5
109	8.8	99.2	102	4.1	98.4
112	11.9	98.6	105	4.3	98.4
115	8.9	97.7	108	4.1	98.5
118	9.9	96.7	111	4.1	98.9
			114	4.0	98.7
			117	3.6	98.9

	120	3.6	99.1

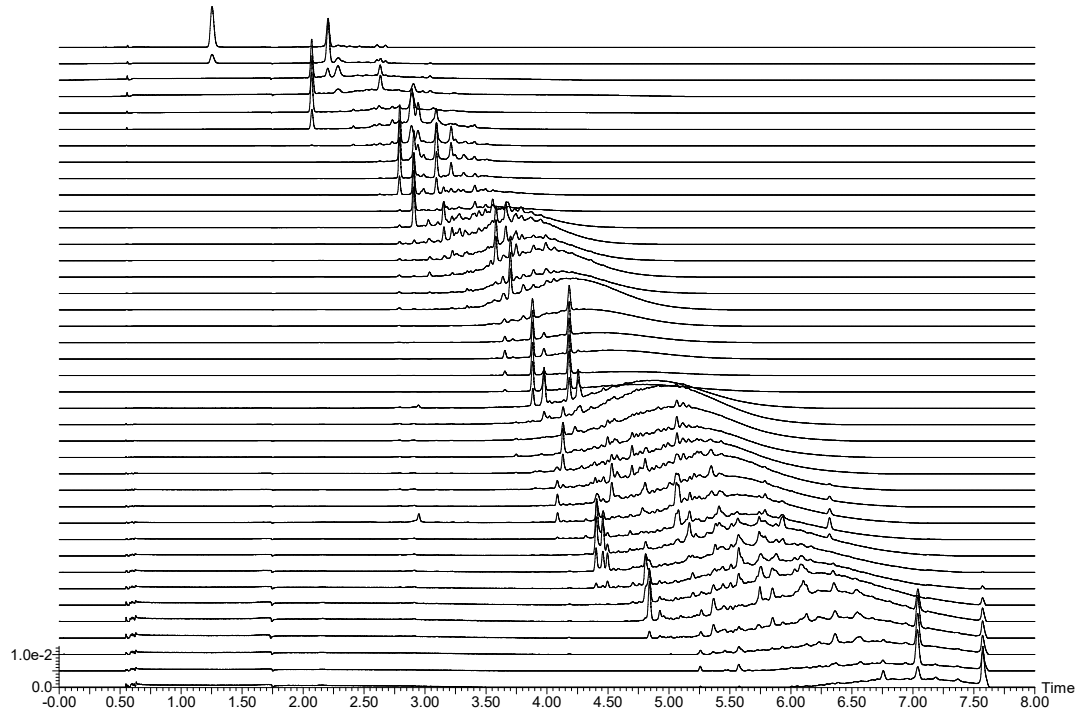

Appendix 3. Combined UV chromatograms at 280 nm of the prepMeOH fractions of pine bark procyanidins from the preparative liquid chromatography run.

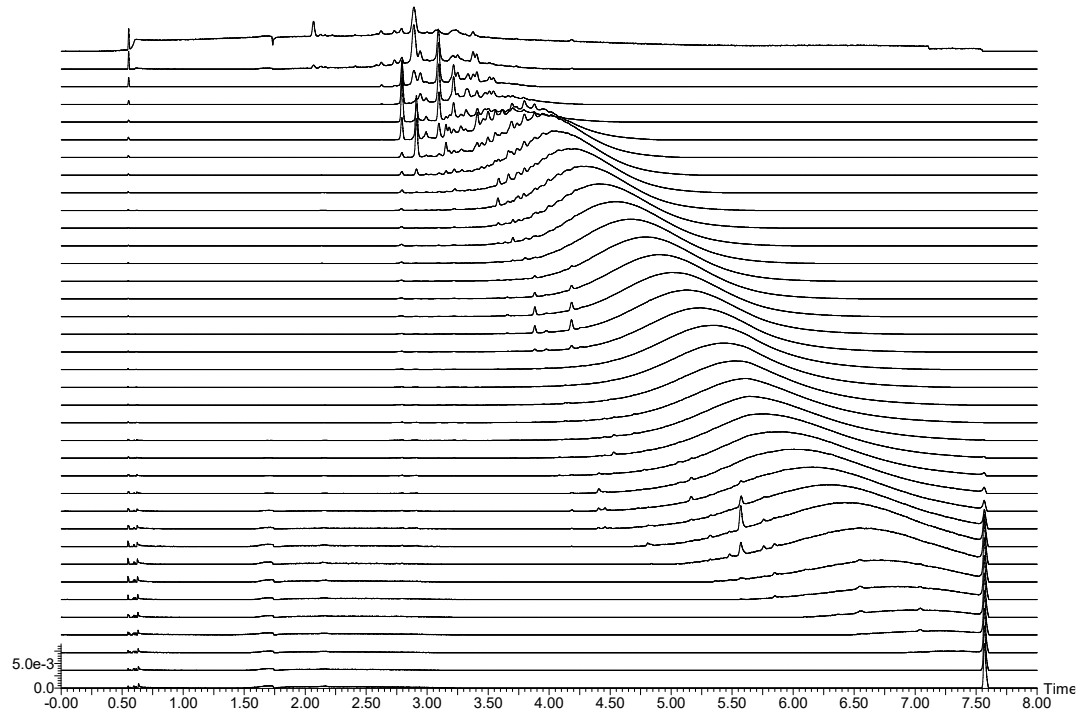

Appendix 4. Combined UV chromatograms at 280 nm of the prepAce fractions of pine bark procyanidins from the preparative liquid chromatography run. Ace = acetone.

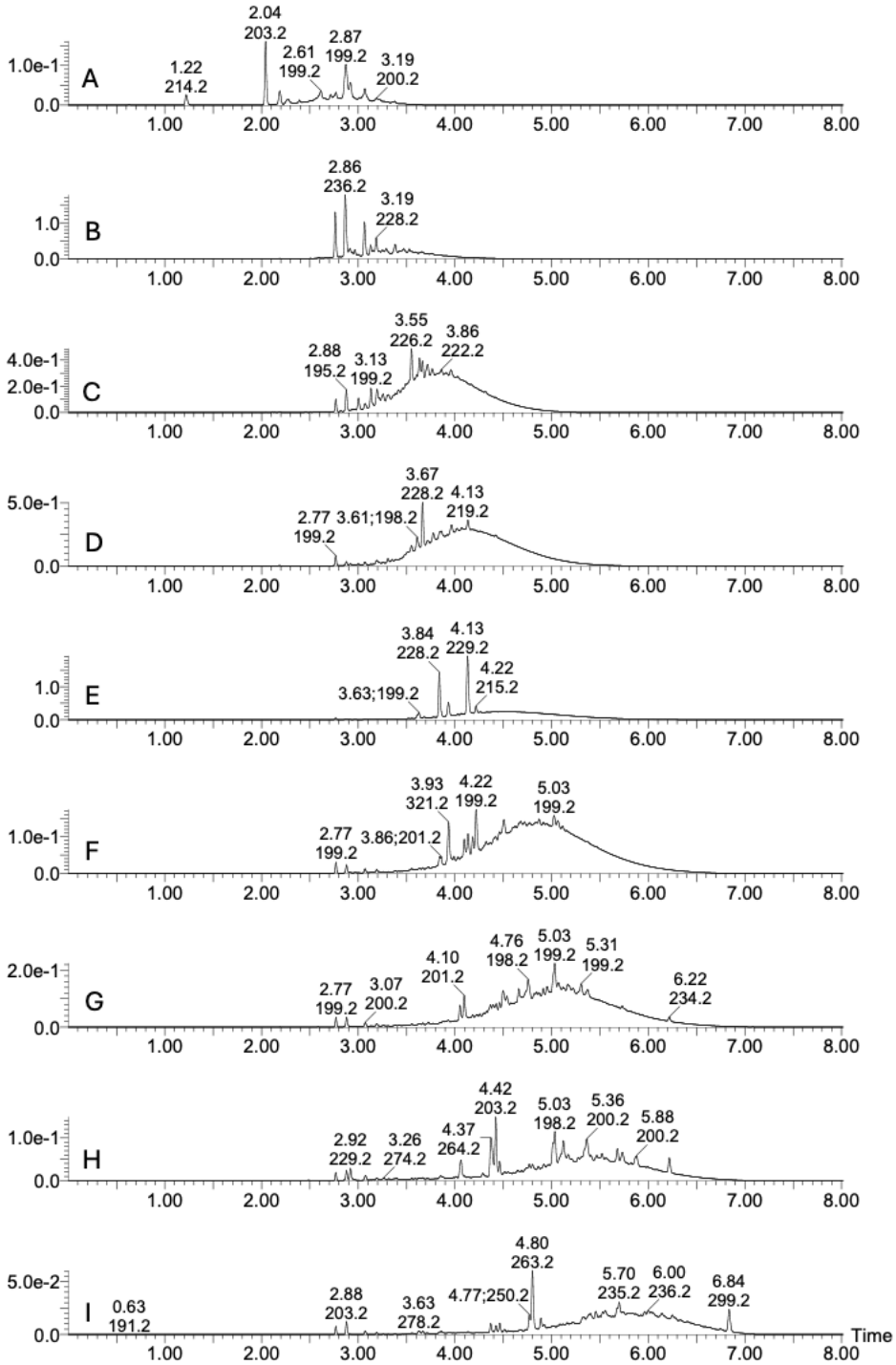

Appendix 5. UV chromatograms at 280 nm of prepMeOH 1–9 (A–I) obtained from the semisynthesis of pine bark procyanidins.

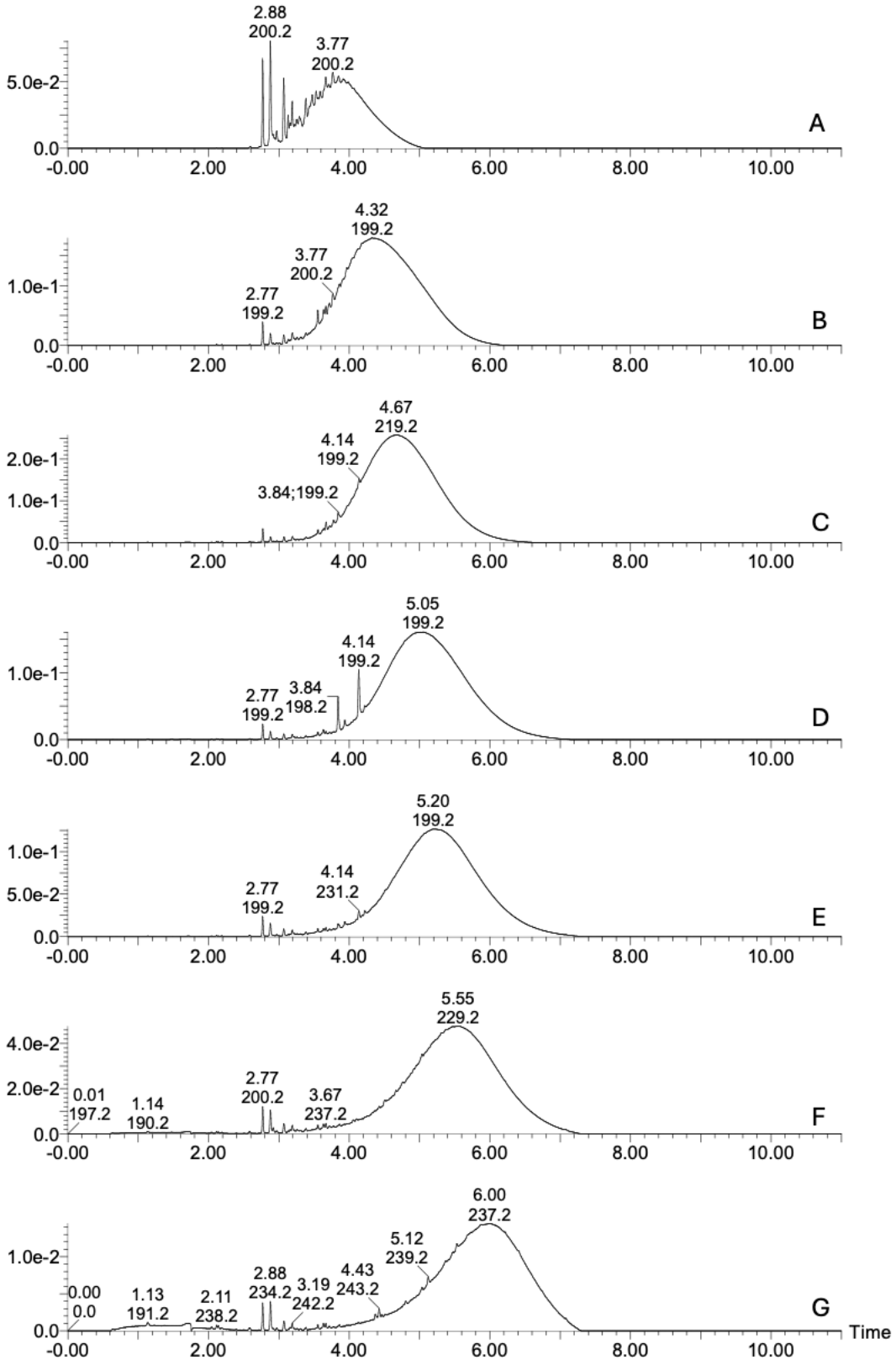

Appendix 6. UV chromatograms at 280 nm of prepAce 1–7 (A–G) obtained from the semisynthesis of pine bark procyanidins.

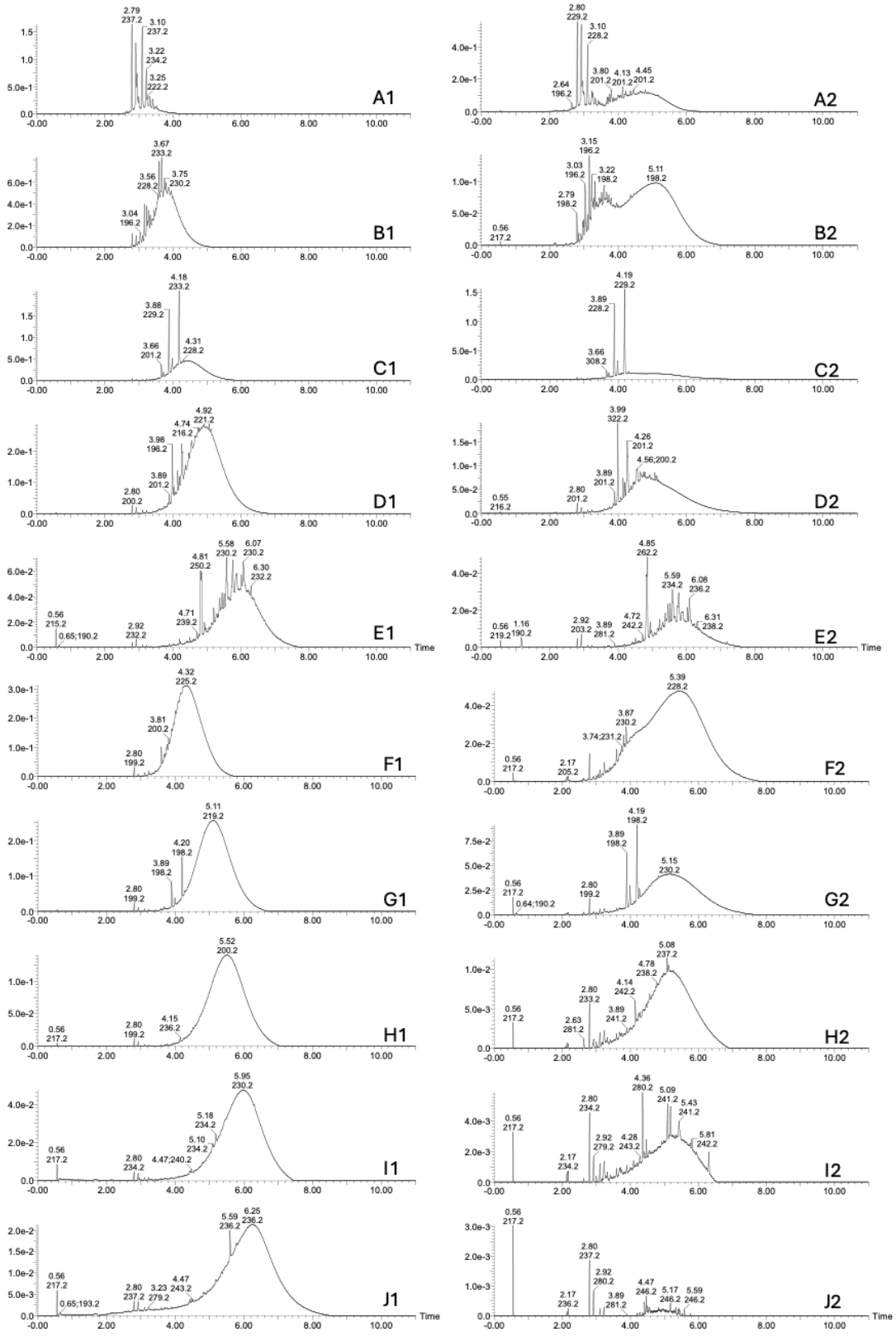

Appendix 7. UV chromatograms at 280 nm of prepMeOH fractions 24 (A), 39 (B), 57 (C), 71 (D), and 104 (E) from preparative liquid chromatography before (A1–E1) and after (A2–E2) a small-scale semisynthesis test with formaldehyde. The same information is presented for prepAce fractions 34 (F), 53 (G), 70 (H), 84 (I), and 92 (J) before (F1–J1) and after (F2–J2) the test.

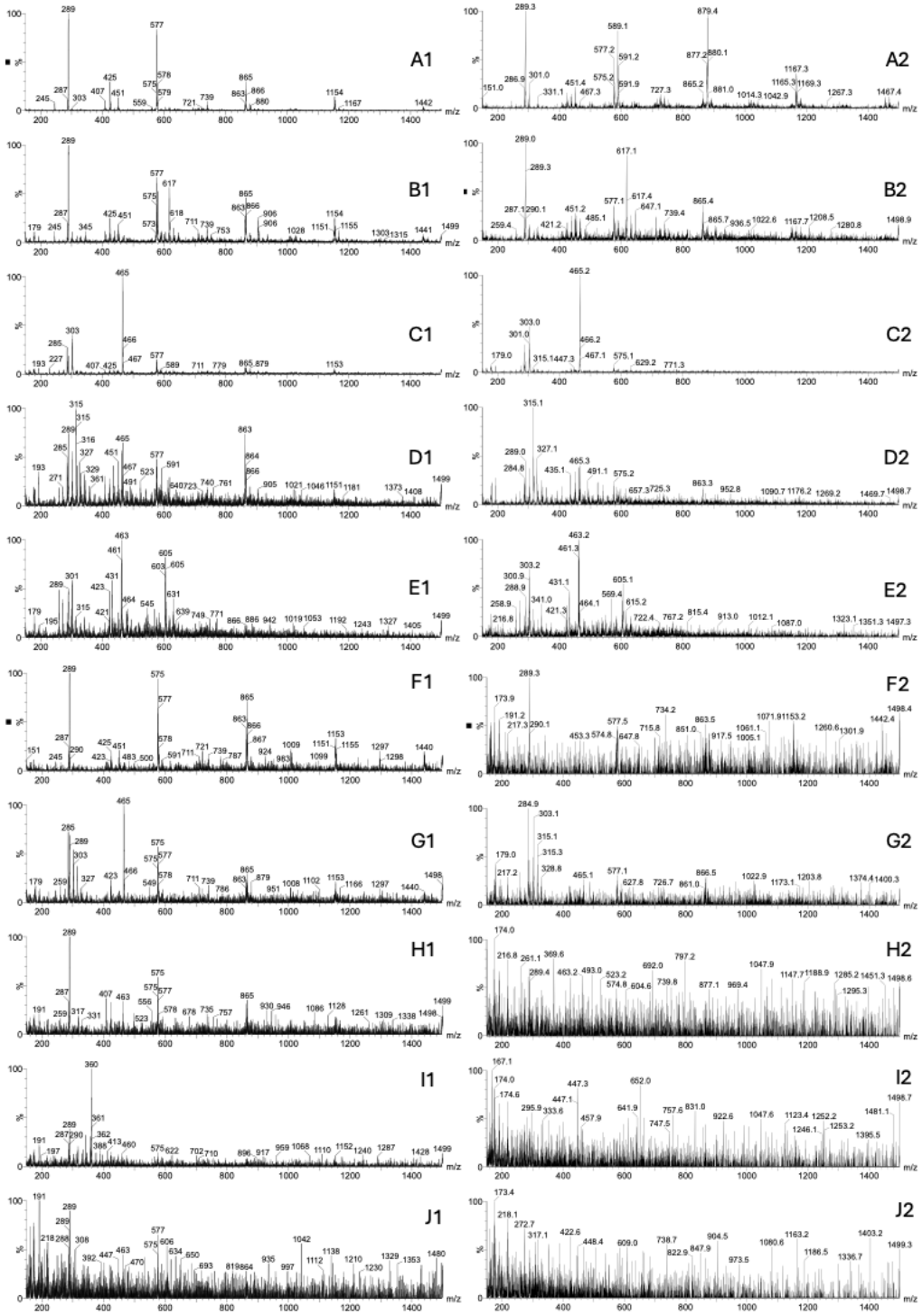

Appendix 8. Full scan MS spectra in negative electrospray ionization of prepMeOH fractions 24 (A), 39 (B), 57 (C), 71 (D), and 104 (E) from preparative liquid chromatography before (A1–E1) and after (A2–E2) a small-scale semisynthesis test with formaldehyde. The same information is presented for prepAce fractions 34 (F), 53 (G), 70 (H), 84 (I), and 92 (J) before (F1–J1) and after (F2–J2) the test.

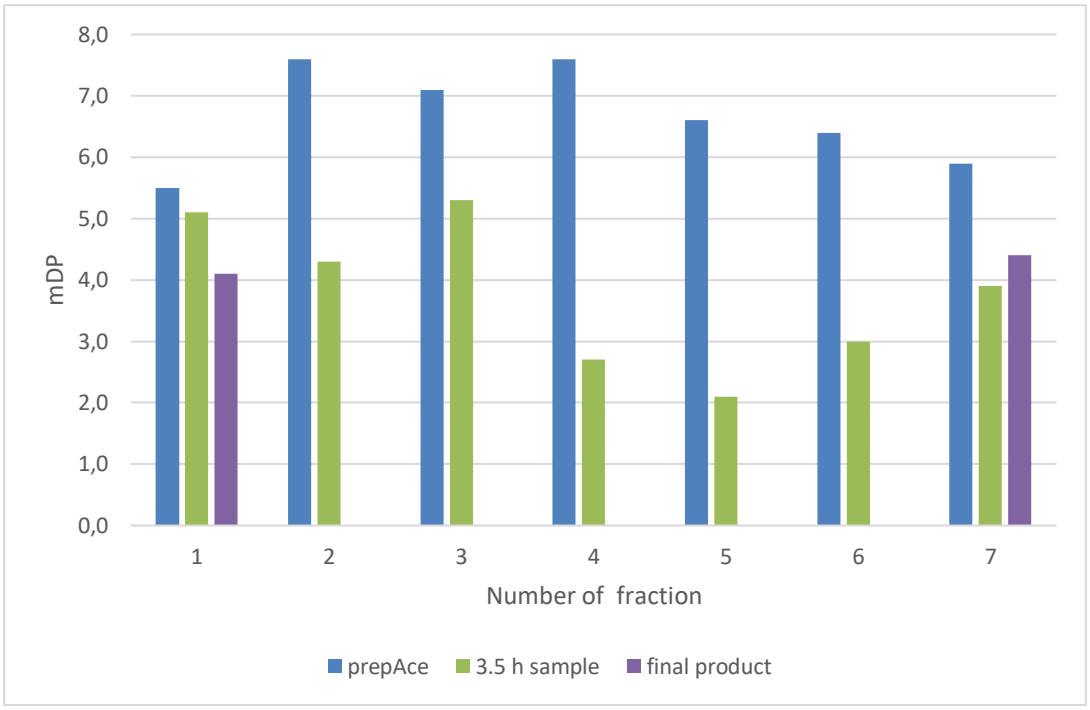

Appendix 9. Changes in the mean degrees of polymerization (mDPs) of the prepAce fractions in semisynthesis of pine bark procyanidins. The mDPs of the prepAce fractions, their 3.5 h samples, and the final product are presented.

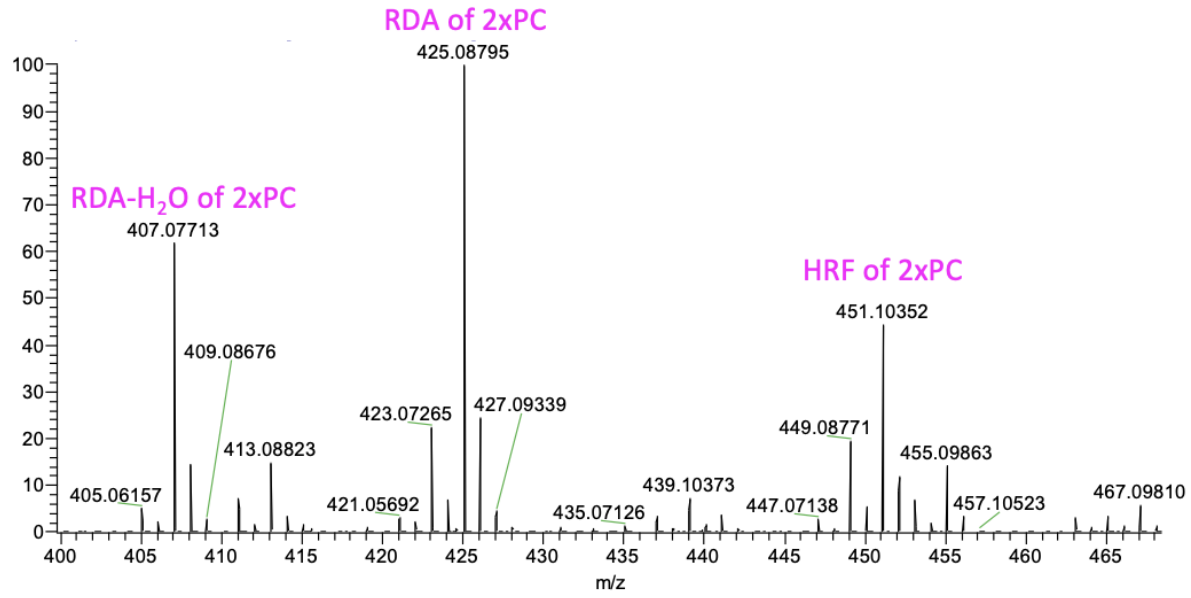

Appendix 10. Full scan MS spectrum in negative electrospray ionization presenting the fragments characteristic of B-type procyanidin (PC) dimers. Heterocyclic ring fission (HRF), Retro-Diels-Alder (RDA) fragments, and the additional RDA-H_2O fragment are found in the center of the monomer and dimer mass peaks.

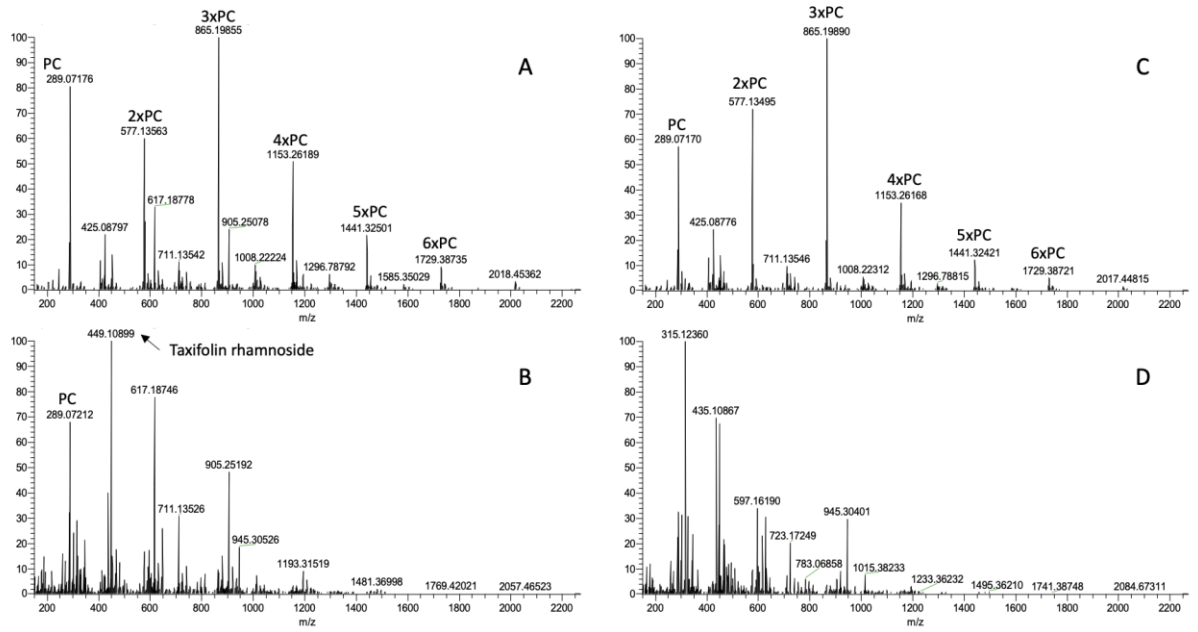

Appendix 11. Full scan MS spectra in negative electrospray ionization of prepMeOH 3 (A) and its product (B), and prepMeOH 4 (C) and its product (D) from semisynthesis of pine bark procyanidins (PCs). Tentative identifications of the most abundant compounds are presented in the spectra.

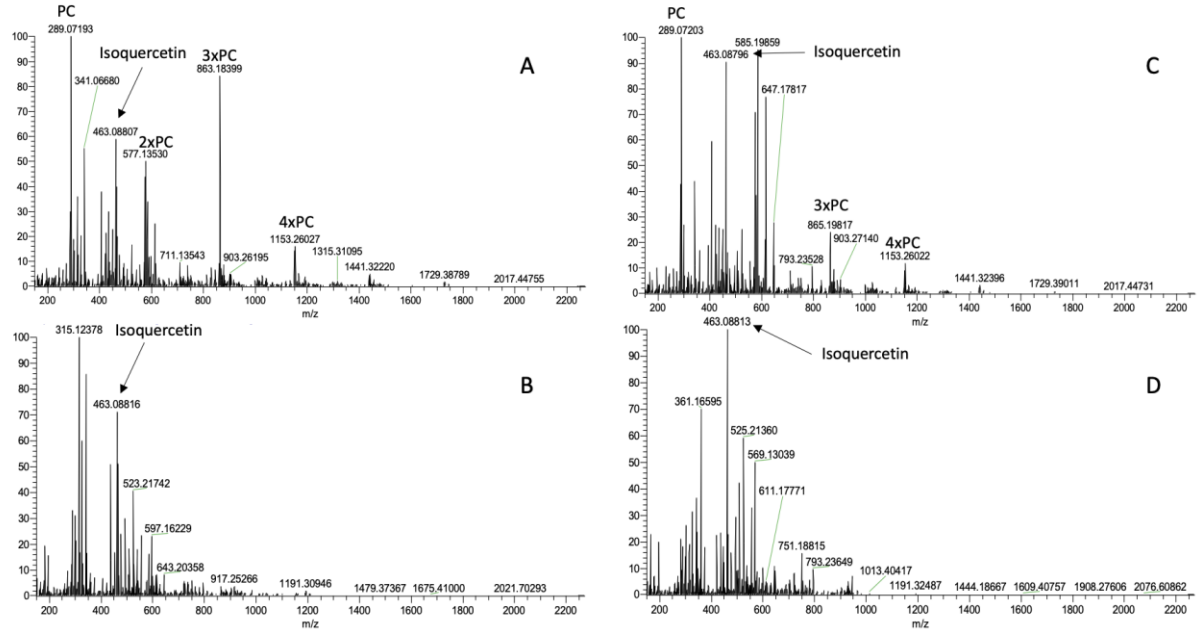

Appendix 12. Full scan MS spectra in negative electrospray ionization of prepMeOH 6 (A) and its product (B), and prepMeOH 7 (C) and its product (D) from semisynthesis of pine bark procyanidins (PCs). Tentative identifications of the most abundant compounds are presented in the spectra.

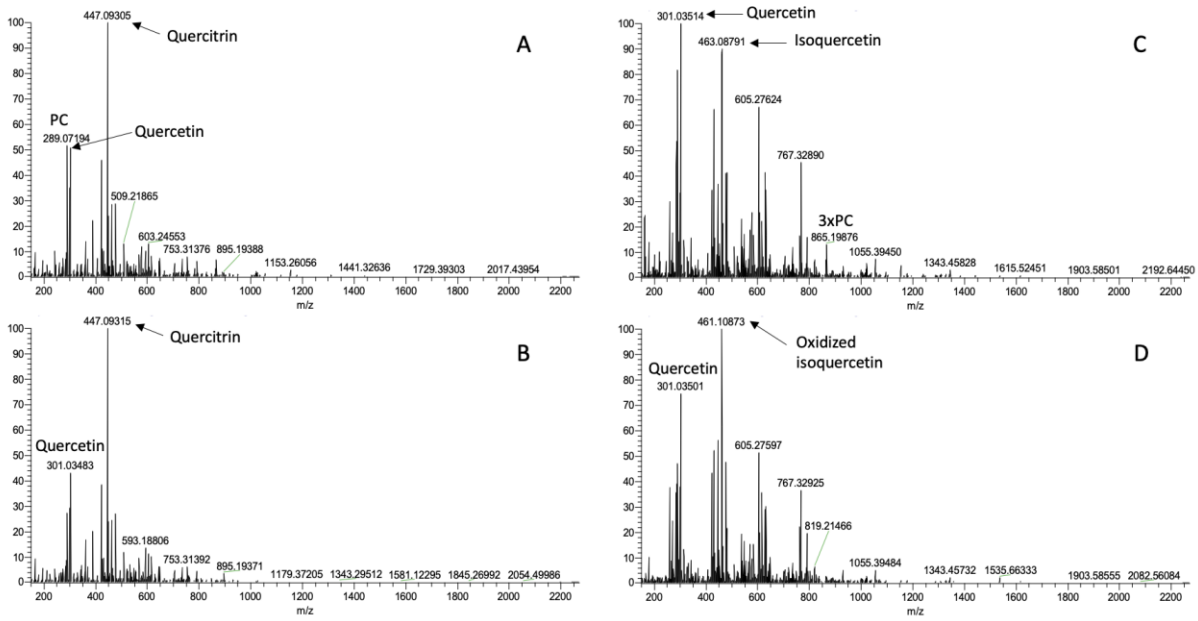

Appendix 13. Full scan MS spectra in negative electrospray ionization of prepMeOH 8 (A) and its product (B), and prepMeOH 9 (C) and its product (D) from semisynthesis of pine bark procyanidins (PCs). Tentative identifications of the most abundant compounds are presented in the spectra.

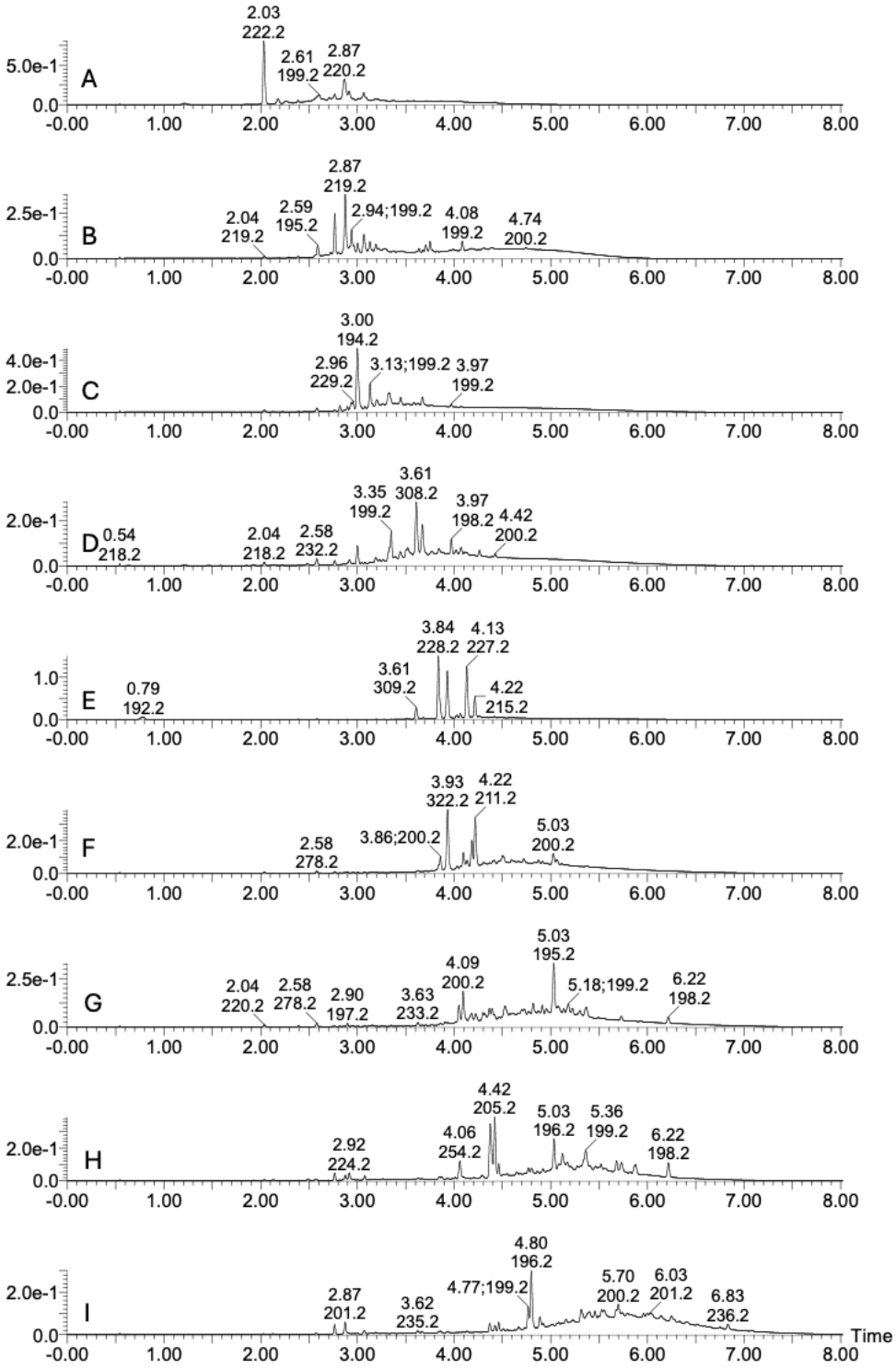

Appendix 14. UV chromatograms at 280 nm of prepMeOH 1–9 products (A–I) obtained from the semisynthesis of pine bark procyanidins.

Appendix 15. Tentative identification of the most intense abundant compounds of prepMeOH 3–5 and prepMeOH 3–5 products from the semisynthesis of pine bark procyanidins (PCs). DP = degree of polymerization.

Original PAs

prepMeOH	DP	Bond type	Molecular formula	Mcalculated	Monomeric composition	$[M-H]^-$
3	1	–	$C_{15}H_{14}O_6$	290.07904	PC	289.07176
	2	B	$C_{30}H_{26}O_{12}$	578.14243	2xPC	577.13563
	3	B	$C_{45}H_{38}O_{18}$	866.20582	3×PC	865.19855
	4	B	$C_{60}H_{50}O_{24}$	1154.26921	4×PC	1153.26189
	5	B	$C_{75}H_{62}O_{30}$	1442.33260	5×PC	1441.32501
	6	B	$C_{90}H_{74}O_{36}$	1730.39599	6xPC	1729.38735
	7	B	$C_{105}H_{86}O_{42}$	2018.45959	7xPC	2017.44583
4	1	–	$C_{15}H_{14}O_6$	290.07904	PC	289.07170
	2	B	$C_{30}H_{26}O_{12}$	578.14243	2xPC	577.13495
	3	B	$C_{45}H_{38}O_{18}$	866.20582	3×PC	865.19890
	4	B	$C_{60}H_{50}O_{24}$	1154.26921	4×PC	1153.26168
	5	B	$C_{75}H_{62}O_{30}$	1442.33260	5×PC	1441.32421
	6	B	$C_{90}H_{74}O_{36}$	1730.39599	6xPC	1729.38721
5	1	–	$C_{15}H_{14}O_6$	290.07904	PC	289.07182
	2	B	$C_{30}H_{26}O_{12}$	578.14243	2xPC	577.13524
	3	B	$C_{45}H_{38}O_{18}$	866.20582	3×PC	865.19907
	4	B	$C_{60}H_{50}O_{24}$	1154.26921	4×PC	1153.26187
	-	-	$C_{15}H_{12}O_7$	304.05834	taxifolin	303.05094
	-	-	$C_{21}H_{22}O_{12}$	466.11119	taxifolin hexoside	465.10334

FInal products

prepMeOH	DP	Bond type	Molecular formula	Mcalculated	Monomeric composition	$[M-H]^-$
3	1	-	$C_{15}H_{14}O_6$	290.07904	PC	289.07212
	-	-	$C_{21}H_{22}O_{11}$	450.11627	taxifolin rhamnoside	449.10899
4	-	-	$C_{18}H_{20}O_5$	316.13110	unidentified compound	315.12360
	-	-	$C_{24}H_{20}O_8$	436.11586	unidentified compound	435.10867
5	-	-	$C_{15}H_{12}O_7$	304.05834	taxifolin	303.05071
	-	-	$C_{21}H_{22}O_{12}$	466.11119	taxifolin hexoside	465.10293
	-	-	$C_{42}H_{44}O_{24}$	932.22238	$[2M-H]^-$ of taxifolin hexoside	931.21484

Appendix 16. Tentative identification of the most abundant compounds of prepMeOH 6–9 and the prepMeOH products 6–9 from the semisynthesis of pine bark procyanidins (PCs). DP = degree of polymerization.

Original PAs

prepMeOH	DP	Bond type	Molecular formula	Mcalculated	Monomeric composition	$[M-H]^-$
6	1	–	$C_{15}H_{14}O_6$	290.07904	PC	289.07193
	2	B	$C_{30}H_{26}O_{12}$	578.14243	2xPC	577.13530
	3	B	$C_{45}H_{38}O_{18}$	866.20582	3×PC	865.19944
	4	B	$C_{60}H_{50}O_{24}$	1154.26921	4×PC	1153.26027
	5	B	$C_{75}H_{62}O_{30}$	1442.33260	5×PC	1441.32220
	-	-	$C_{15}H_{10}O_7$	302.04269	quercetin	301.03552
	-	-	$C_{21}H_{20}O_{12}$	464.09554	isoquercetin	463.08807
	-	B	$C_{37}H_{28}O_{15}$	712.14290	RDA of 3xPC	711.13530
7	1	–	$C_{15}H_{14}O_6$	290.07904	PC	289.07203
	3	B	$C_{45}H_{38}O_{18}$	866.20582	3×PC	865.19817
	4	B	$C_{60}H_{50}O_{24}$	1154.26921	4×PC	1153.26022
	-	-	$C_{15}H_{10}O_7$	302.04269	quercetin	301.03552
	-	-	$C_{21}H_{20}O_{12}$	464.09554	isoquercetin	463.08796
8	1	–	$C_{15}H_{14}O_6$	290.07904	PC	289.07194
	2	B	$C_{30}H_{26}O_{12}$	578.14243	2xPC	577.13538
	-	-	$C_{15}H_{10}O_7$	302.04269	quercetin	301.03552
	-	-	$C_{21}H_{20}O_{11}$	448.10062	quercitrin	447.09305
	-	-	$C_{22}H_{16}O_9$	424.07948	unidentified compound	423.07187
9	1	–	$C_{15}H_{14}O_6$	290.07904	PC	289.07182
	3	B	$C_{45}H_{38}O_{18}$	866.20582	3×PC	865.19876
	-	-	$C_{15}H_{10}O_7$	302.04269	quercetin	301.03514
	-	-	$C_{21}H_{20}O_{12}$	464.09554	isoquercetin	463.08791

Final products

prepMeOH	DP	Bond type	Molecular formula	Mcalculated	Monomeric composition	$[M-H]^-$
6	-	-	$C_{18}H_{20}O_5$	316.13110	unidentified compound	315.12378
	-	-	$C_{21}H_{20}O_{12}$	464.09554	isoquercetin	463.08816
7	-	-	$C_{21}H_{20}O_{12}$	464.09554	isoquercetin	463.08813
8	-	-	$C_{15}H_{10}O_7$	302.04269	quercetin	301.03483
	-	-	$C_{21}H_{20}O_{11}$	448.10062	quercitrin	447.09315
9	-	-	$C_{15}H_{10}O_7$	302.04269	quercetin	301.03501
	-	-	$C_{21}H_{18}O_{12}$	462.07989	oxidiced isoquercetin	461.10873

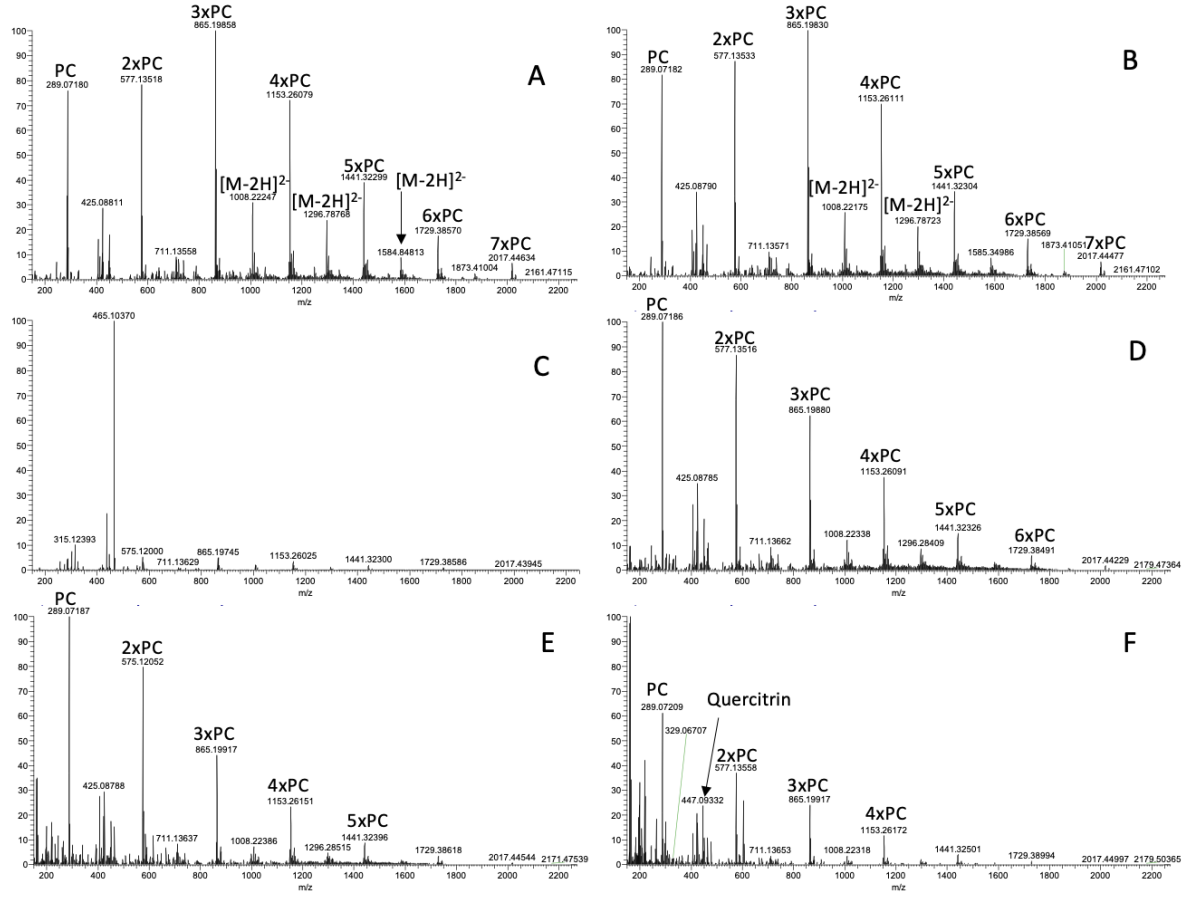

Appendix 17. Full scan MS spectra in negative electrospray ionization of prepAce 2–7 (A–F) obtained from pine bark procyanidins (PCs). Tentative identifications of the most abundant compounds are presented.

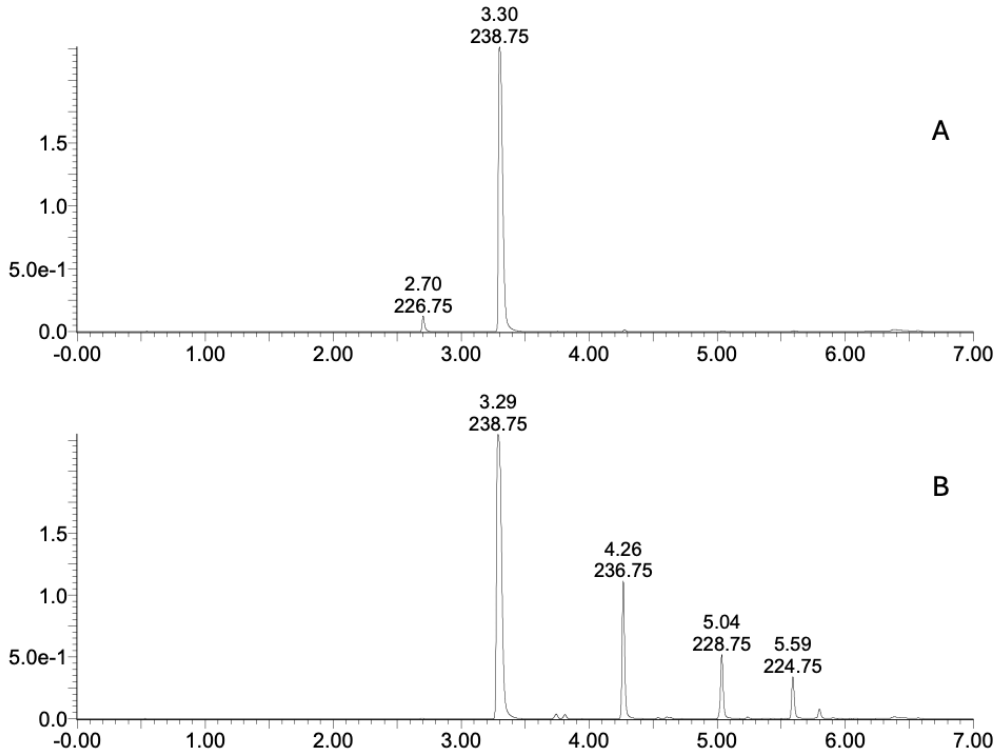

Appendix 18. UV chromatograms at 280 nm of the aldehyde condensation reaction test for solid phase extraction (SPE) zero fraction and epicatechin, which was added to the SPE zero fraction. The zero fraction (A) displays the epicatechin peak, while the one hour sample (B) exhibits four additional peaks eluting after the epicatechin peak present in the zero sample.

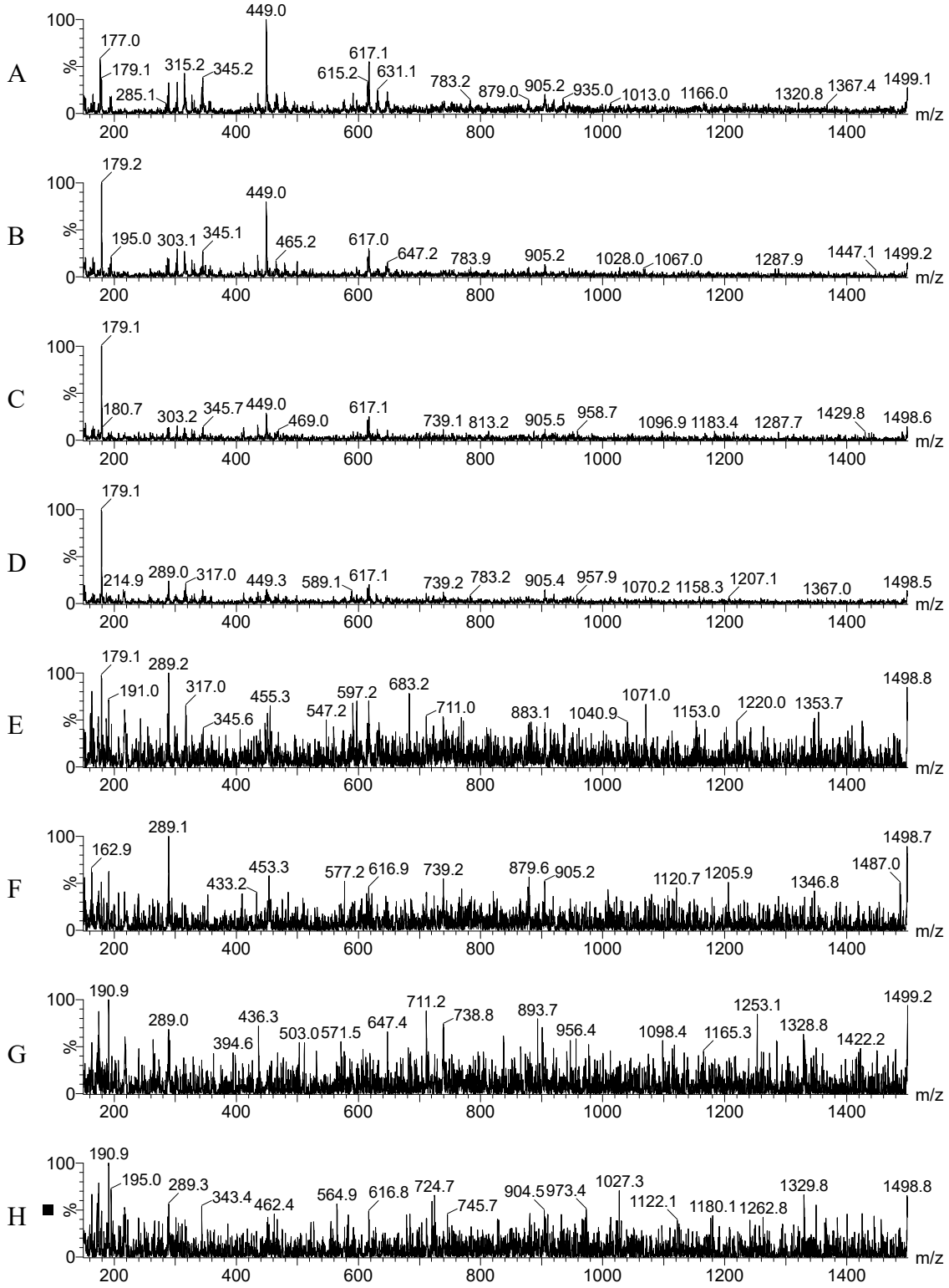

Appendix 19. Full scan MS spectra in negative electrospray ionization of solid phase extraction (SPE) fractions of prepMeOH 3 product. SPE fractions A–C are eluted with MeOH/water (50/50, v/v) and D–H with pure MeOH.

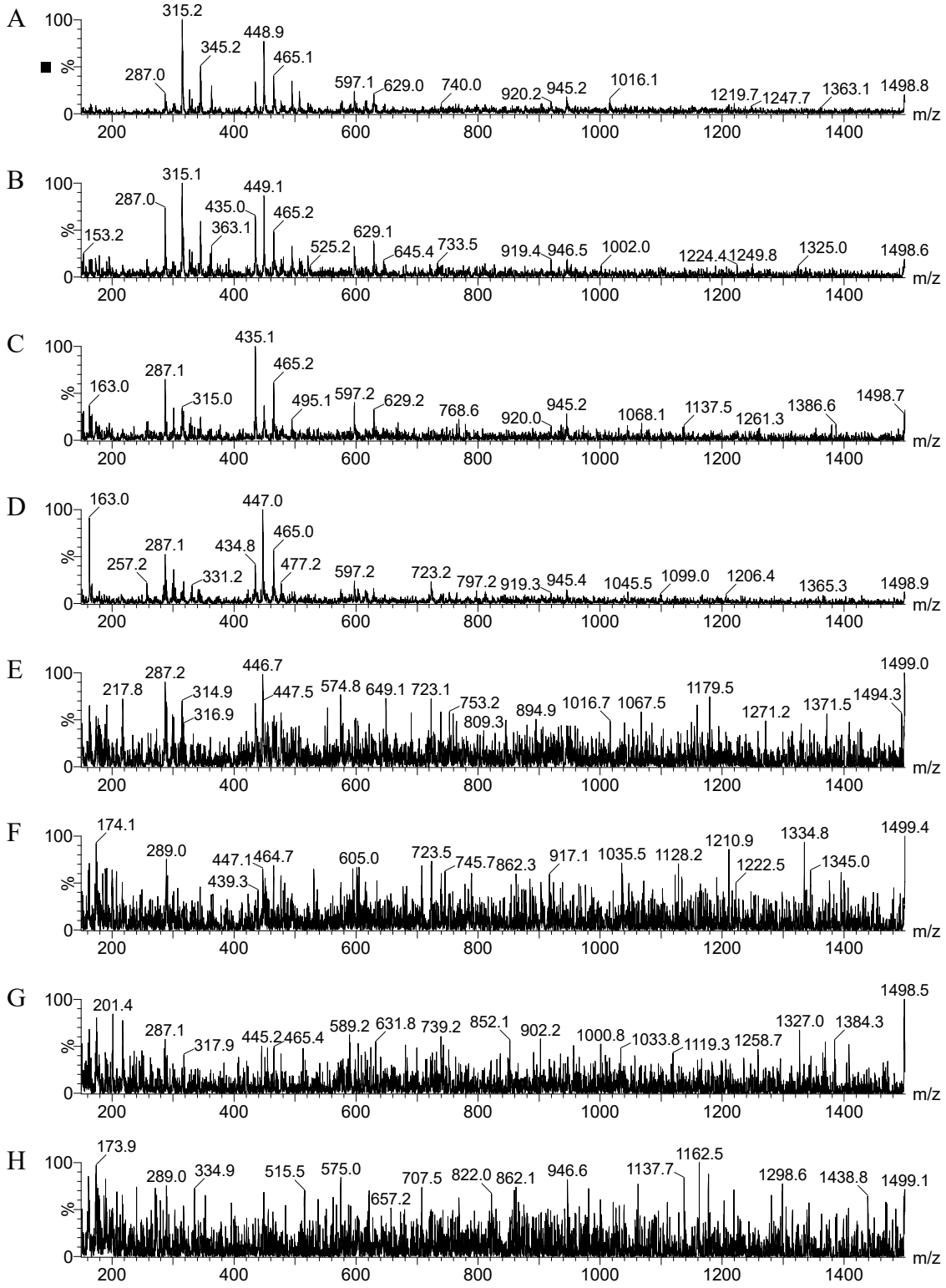

Appendix 20. Full scan MS spectra in negative electrospray ionization of solid phase extraction (SPE) fractions of prepMeOH 4 product. SPE fractions A–C are eluted with MeOH/water (50/50, v/v) and D–H with pure MeOH.